Ferry free E39 –Fjord crossings Bjørnafjorden | 304624

0	15.08.2019	Final issue	MST	PNL	SEJ	
Rev.	Publish date	Description	Made by	Checked by	Project appro.	Client appro.

Client Statens vegvesen	
Contractor AAS-JAKOBSEN COWI Multiconsult	Contract no.: 18/91094

Document name:

Preferred solution, K12 – Appendix G
Global analyses – Response

Document no.:	Rev.:	Pages:
SBJ-33-C5-AMC-90-RE-107	0	1849

CONCEPT DEVELOPMENT, FLOATING BRIDGE E39 BJØRNAFJORDEN

Preferred solution, K12

Appendix G – Global analyses - Response

CLIENT

Statens vegvesen

DATE: / REVISION: 15.08.2019 / 0

DOCUMENT CODE: SBJ-33-C5-AMC-90-RE-107

REPORT

PROJECT	Concept development, floating bridge E39 Bjørnafjorden	DOCUMENT CODE	SBJ-33-C5-AMC-90-RE-107
SUBJECT	Appendix G – Global analyses – Response – K12	ACCESSIBILITY	Restricted
CLIENT	Statens vegvesen	PROJECT MANAGER	Svein Erik Jakobsen
CONTACT	Øyvind Kongsvik Nedrebø	PREPARED BY	Martin Storheim
		RESPONSIBLE UNIT	AMC

SUMMARY

This report describes load modelling, methods and response evaluations performed in the concept development work of a floating bridge over Bjørnafjorden.

Permanent, temperature, traffic, tidal, current, wind and wave loads are simulated based on input from the design basis. A thorough screening of selected response variables was performed to select key environmental conditions. Wind responses are simulated using 10 seeds from a set of directions and used to select the worst seed for further load combination.

Ultimate limit state combinations were performed based on separate simulations of each load component (uncoupled approach) and combined with individual load-, correlation- and combination factors. These results were used in design development, and several design iterations have been performed. Two methods were used for load combinations; a direct method based on combination of time series of the individual loads or a factorized method in which design forces are established individually and then combined. The former is used for all design evaluations, but the latter gives an easier overview of the contributions of the individual load components. Both are included as enclosures to this appendix.

Coupled environmental load simulations were also performed in time-domain in which all environmental loads were included simultaneously. Ten seeds were run for each environmental condition and the extreme values were estimated using the AUR method at defined percentile levels. Comparison of the coupled and uncoupled approach revealed that using the observed maximum sectional response in the uncoupled was conservative (with some few exceptions) and coupled response with extreme value estimation gave a response reduction. The only exception was axial force and torsional moment response close to the high bridge, in which coupled simulations gave a slightly worse response than uncoupled. The uncoupled method is generally conservative for the calculated Von Mises stress.

A comfort evaluation was performed using the overall vibration total value (OVTV), in which a weighted sum of RMS accelerations was evaluated. The evaluation was conducted along the 1-year contour with waves and wind run separately in frequency domain and local wind on the vehicle based on a time series. The forward speed of the vehicle was accounted for when evaluating the encountered acceleration response from dynamic bridge response and the local wind time series was generated based on the instantaneous vehicle heading as it drives over the bridge. The results show that wind and waves utilize about 15% each of the OVTV criterion, whereas local wind on the vehicle utilize 300% of the criterion. Aerodynamic damping is important for the local vehicle response to wind. Hence, the OVTV criterion would not be satisfied even for a rigid bridge. The dynamic bridge motion is around 10% of the discomfort.

0	15.08.2019	Final issue	M. Storheim	P. N. Larsen	S. E. Jakobsen
REV.	DATE	DESCRIPTION	PREPARED BY	CHECKED BY	APPROVED BY

Check of dynamic response to environmental conditions with 10 000-year return periods showed that the sectional forces could be higher for 10 000-year than ULS, but that the stresses were lower for 10 000-year response. Accidental limit state capacity was checked for damaged conditions of the bridge, with flooding, damaged bridge girder due to ship collision and loss of mooring clusters (up to four anchors). Only loss of a mooring cluster gave a significant increase in the dynamic response from a 100-year environmental condition, but the increase in responses were lower than the load factors applied for ULS. The bridge was thus found to be robust against the global effect of accidental events.

Sensitivity studies for a few parameters were performed. Response from wind-waves is not sensitive to variation in wave spectrum parameters, whereas swell waves are moderately sensitive. Swell waves are extremely sensitive to period. Mooring line damping is dependent on the line pretension and thereby the static transverse offset of the bridge girder, but the overall effect on the bridge is small. Variations of abutment stiffness in a reasonable range does not affect global bridge behavior. If the effect of traffic is included for ULS2 (increased mass, aerodynamic drag and hydrodynamic excitation) the strong-axis bridge response increases somewhat (but is still lower than ULS3). Weak-axis moment are worse for the conventional ULS2 check. Second order wave drift forces affect the mean bending moment about strong axis but not the dynamic values and is not considered to have a significant effect on the bridge response. Inverse methods revealed uncertainty in the metocean contour lines which may increases bridge girder response somewhat.

TABLE OF CONTENTS

1 Introduction

This report describes load modelling, methods and response evaluations performed in the concept development work of a floating bridge over Bjørnafjorden. In the initial round four concepts were evaluated:

- K11 : End-anchored arch-type floating bridge
- K12 : End-anchored arch-type floating bridge with side moorings
- K13 : Straight floating bridge with side moorings
- K14 : Curved floating bridge with side moorings

K12 was selected as the preferred concept and is the primary focus of this report. For details regarding concept development and design considerations, see [1, 2], and for details on modelling and assumptions see [3].

A uncertainty assessment was performed for known uncertainties related to design basis, hydrodynamic behavior, analysis and methodology and parametric excitation. This is shown in Enclosure 16 to this report.

2 Load modelling and assumptions

This section describes the load modelling and related assumptions as they are used for static and dynamic simulations of the global bridge response.

2.1 Static

2.1.1 Permanent loads

The permanent loads and the tension of stay cables are defined in [3].

The permanent loads are applied on the structures at different stages prescribed in Table 2-1 and are defined in Table 2-2. The final permanent situation is dependent on the chosen construction order and construction method. Hence, the following construction sequence is assumed to account for the main effects on the construction phase. The axis numbering is presented for the K11-concept, but this is similar to the discretization of the K12 concept.

Table 2-1 Permanent loads and construction stages

Stage	Description
MainBridge	The stay cable bridge from axis A1 to A3 is activated and all permanent loads associated with this part is calculated. Here the pretension of the cables and additional self-weight is included
FloatingBridge	The floating bridge from A3 to A41 is activated and all permanent loads associated with this part is calculated on fictitious rigid supports (vertical and roll degrees is locked). The floating bridge is not connected to the stay cable bridge at this stage.
ActPontoons	At this stage the rigid supports are replaced with linear springs representing the properties of the pontoons. The rigid supports are deactivated without applying their forces back on the structure. This is to have the correct ballasted situation, i.e. ballast for having correct vertical and roll angle of the pontoon.
CloseJoint	At this stage the connection between the stay cable bridge and the floating bridge is established.

The permanent loads applied are:

Table 2-2 Permanent loads applied in the RM-Bridge analyses

	K11 - Beam elements			Permanent loads	
	Start	End	Step	g-w [kN/m]	g-w-add [kN/m]
Bridge girder					
High Bridge	101	192	1		
- (Concrete)	101	138	1	726.9	49.1
- (Steel)	139	192	1	137.3	49.1
Floating bridge	251	858	1		
- (Span sections)				137.3	49.1
- (Support sections)				137.3	49.1
Pier, viaduct					
- Pier A1-A	2101	2104	1	312.0	
- Pier A1-B	2201	2204	1	312.0	
- Pier A1-C	2301	2304	1	312.0	
- Pier A1-D	2401	2404	1	312.0	
- Pier A1-E	2501	2504	1	312.0	
Pier, floating bridge					
- Pier A3	4031	4034	1	88.1	
- Pier A4	4041	4044	1	88.1	
- Pier A5	4051	4054	1	88.1	
- Pier A6	4061	4064	1	88.1	
- Pier A7	4071	4074	1	88.1	
- Pier A8	4081	4084	1	88.1	
- Pier A9	4091	4094	1	63.0	
- Pier A10	4101	4102	1	63.0	
- Pier A11	4111	4112	1	63.0	
- Pier A12	4121	4122	1	63.0	
- Pier A13	4131	4132	1	63.0	
- Pier A14	4141	4142	1	63.0	
- Pier A15	4151	4152	1	63.0	
- Pier A16	4161	4162	1	63.0	
- Pier A17	4171	4172	1	63.0	
- Pier A18	4181	4182	1	63.0	
- Pier A19	4191	4192	1	63.0	
- Pier A20	4201	4202	1	63.0	
- Pier A21	4211	4212	1	63.0	
- Pier A22	4221	4222	1	63.0	
- Pier A23	4231	4232	1	63.0	
- Pier A24	4241	4242	1	63.0	
- Pier A25	4251	4252	1	63.0	
- Pier A26	4261	4262	1	63.0	
- Pier A27	4271	4272	1	63.0	
- Pier A28	4281	4282	1	63.0	
- Pier A29	4291	4292	1	63.0	
- Pier A30	4301	4302	1	63.0	
- Pier A31	4311	4312	1	63.0	
- Pier A32	4321	4322	1	63.0	
- Pier A33	4331	4332	1	63.0	
- Pier A34	4341	4342	1	63.0	
- Pier A35	4351	4352	1	63.0	
- Pier A36	4361	4362	1	63.0	
- Pier A37	4371	4372	1	63.0	
- Pier A38	4381	4382	1	63.0	
- Pier A39	4391	4392	1	63.0	
- Pier A40	4401	4402	1	63.0	
Pylon, A2					
- Lower Leg, right	3101	3108	1	750.0 - 1131.6	
- Upper Leg, right	3110	3125	1	278.4 - 459.7	
- Lower Leg, left	3201	3208	1	750.0 - 1131.6	
- Upper Leg, Left	3210	3225	1	278.4 - 459.7	
- Spire	3301	3308	1	196.9 - 410.4	
- Cross-beam	3401	3402	1	349.4 - 349.9	
Cables					
- Back span, right	21011	21181	10	0.299 - 0.795	
- Back span, left	22011	22181	10	0.299 - 0.795	
- Main span, right	23011	23181	10	0.299 - 0.795	
- Main span, left	24011	24181	10	0.299 - 0.795	

2.1.2 *Temperature*

The thermal loading on the bridge is described in ref [4].

2.1.3 *Traffic*

The traffic loading on the bridge is described in ref [4].

2.1.4 *Tide*

Tidal variation around the mean water lever (+0.77m) was taken as +1.33 and -0.97 m for 100 year high and low tide respectively.

2.1.5 *Current*

The vertical current profiles have for simplicity been applied as defined phase 3, as this was considered more conservative than the current profile in ref [5]. Horizontal variation of the current has been accounted for by examining horizontal profiles as listed in Table 2-3. The profile function *f* is defined as a function of normalized position *x*, where *x* is 0 at the tower axis, and 1 at the North abutment axis. The total current field is hence $U(x,z) = U(z) \cdot f(x)$

Table 2-3 Horizontal current variation

Case	Type	Definition
1	Constant	$f(x) = 1$
2	Linear	$f(x) = \frac{x+1}{2}$
3	Crossflow	$f(x) = \begin{cases} 2/3, & x < 0.5 \\ -2/3, & \text{else} \end{cases}$
4	Center weighted	$f(x) = \begin{cases} 1, & 0.25 < x < 0.75 \\ 0.5, & \text{else} \end{cases}$

Note that an error in the current application was discovered late in the project execution. The peak current velocity was applied in the wrong direction (East vs. West), and only current from the Eastern direction was included in the load combination. Hence, compressive force in the bridge is overestimated and the maximum tension of the bridge is somewhat underestimated. However, the current is a small part of the total utilization (see section 4.2.1), and as such this error is not of consequence from design. See Enclosure 17 for details.

2.2 Screening of wave conditions

As stated in the metocean design basis [5] waves in Bjørnafjorden are a combination of local wind generated waves and swell coming in from the ocean. When wind is blowing from the west, local wind generated waves are to be combined with swell. When the weather is coming from the east it is assumed that there is no swell. The direction and magnitude of the waves are as stated in [5].

The main objective of the screening is to identify a limited amount of sea states that cover the expected maximum wave responses of the bridge structure subjected to the wave conditions given in [5]. In the design phase it is necessary to break the response in the girder down into its separate load components, since optimization of response ultimately boils down to making design decisions that minimize load components. A direct stress screening is not considered, as the relationship between load and response is difficult to extract based on stresses, as stated in DNV-RP-C103 chapter 4.1 [6] :

"For structural design evaluation, engineering judgement and knowledge of structural behaviour is vital for designing a sound and safe unit. For this purpose, stochastic stress results are not well suited, as simultaneity of force and stress distribution is lost, making it difficult to judge the most effective ways of improving the structure. Application of "design wave" approach or regular wave analyses are effective methods for design evaluation and engineering judgement."

The max stress occurs when the combined effect of bending moment about strong axis, bending moment about weak axis and torsion has a maximum, and consequently the selected wave cases are the ones that maximize all of these load components. In addition, the selected wave cases maximize other important effects:

- Mooring forces, based on maximum horizontal displacement.
- Axial load in bridge girder, to evaluate buckling
- Bridge motions
- Displacement and rotations at bearings

During phase 3 of the Bjørnafjorden floating bridge project, all the individual responses was checked in a screening, and the responses for the cable loads and tower loads were also presented. Primarily, the focus was to look for outliers in sea states with regards to response, but it was not seen as necessary to add any individual sea states other than those with maximum moments and axial force. This is assumed to hold for the bridge concept in the current project phase.

When establishing wave conditions, there is made no differentiation between time domain results and frequency domain results. Especially in cases where non-linear effects due to waves become significant, a time domain screening might yield different results from a frequency domain screening. Herein, time domain design waves are assumed to be the design waves found in the frequency domain screening.

2.2.1 Results

The results are given in the following tables where the 1-hour expected maximum load and motion is listed for each extreme return period. The maximum response and the corresponding bridge axis are listed for the whole bridge girder, for only the low part of the bridge, and for the abutments. The low bridge is here the part of the bridge girder with a constant height.

2.2.1.1 Wind waves

In addition to summarizing results given in tables, for each response the 1-hour maxima for all waves are given in plots, see Enclosures to this report. In Figure 2-1 is an example plot where the maximum bending moment about weak axis is shown. The maximum response occurs for a peak period of 5.5s, a significant wave height of 2.1m and a direction of 75deg. The color bar on the right shows that the 1-hour maximum weak axis bending moment for the whole bridge is 229.6MNm. The top plot shows the vertical layout of the bridge together with the envelope of the response. The red marker indicates that the plot is for axis 3, on the tower side. In the rose-plots are indicated the horizontal layout of the bridge and a red dot to indicate the location of the responses showed in the rose-plots.

Note that the bridge profile is shown in the polar diagrams, and the red dot along the profile indicate the location for which cross-sectional results are extracted.

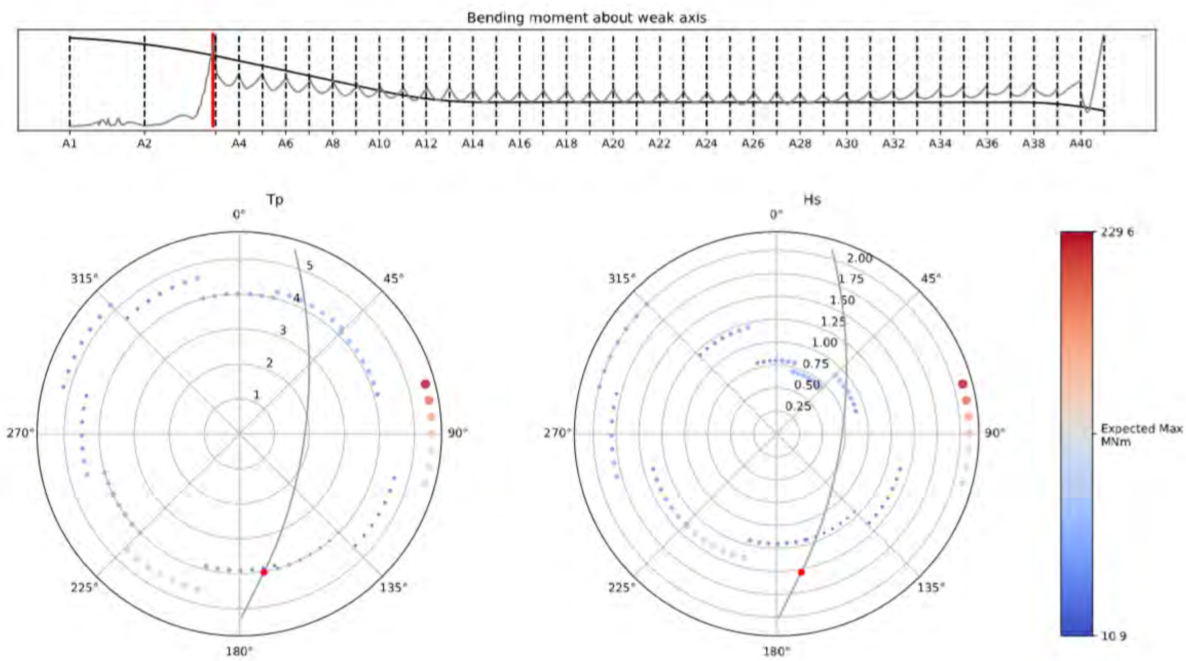

Figure 2-1: 100 year return period wind sea, 1 hour maximum bending moment about weak axis

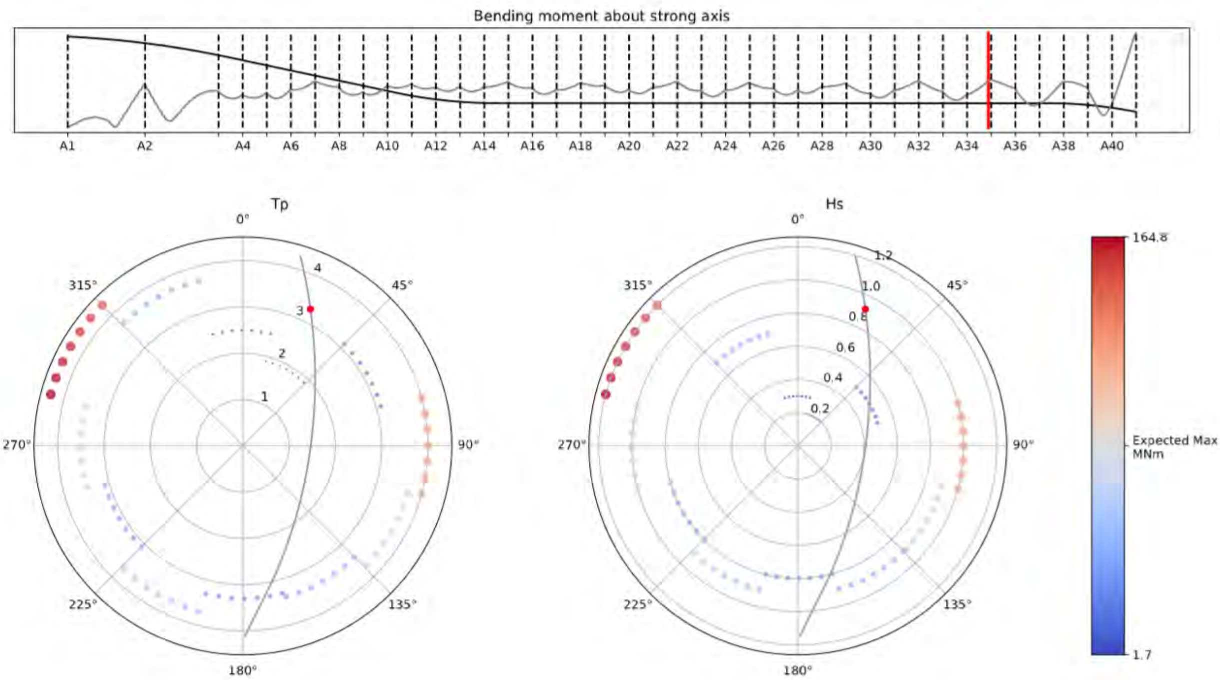

Figure 2-2: 1 year return period wind sea, 1 hour maximum bending moment about strong axis

Summary of screening 1 year wind waves

Table 2-4: Summary of 1 hour expected maxima for 1-year return period waves for the bridge girder

Where	Response	Hs [m]	Tp [sec]	Heading [deg]	Value	Unit
tower	Axial force	0.9	3.7	200	9.2	MN
	Bending moment about strong axis	1.2	4.3	300	150.7	MNm
	Bending moment about weak axis	0.9	3.7	200	0.5	MNm
	Torsional moment	1.2	4.3	295	5.1	MNm
axis 3	Axial force	0.9	3.7	195	8.5	MN
	Bending moment about strong axis	1.2	4.3	300	124.1	MNm
	Bending moment about weak axis	0.9	3.7	215	80.3	MNm
	Torsional moment	1.2	4.3	295	58.8	MNm
axis 35	Axial force	0.9	3.7	195	8.1	MN
	Bending moment about strong axis	1.2	4.3	285	164.8	MNm
	Bending moment about weak axis	1.2	4.3	315	46.5	MNm
	Torsional moment	1.2	4.3	315	27.4	MNm
axis 38	Axial force	0.9	3.7	195	8.9	MN
	Bending moment about strong axis	1.2	4.3	290	157.7	MNm
	Bending moment about weak axis	1.2	4.3	315	43.7	MNm
	Torsional moment	1.2	4.3	285	16.7	MNm
axis 40	Axial force	0.9	3.7	195	9.0	MN
	Bending moment about strong axis	1.2	4.3	290	78.5	MNm
	Bending moment about weak axis	1.2	4.3	315	56.0	MNm
	Torsional moment	1.2	4.3	305	25.5	MNm
abutment north	Axial force	0.9	3.7	195	9.1	MN
	Bending moment about strong axis	1.2	4.3	285	324.8	MNm
	Bending moment about weak axis	1.2	4.3	315	99.7	MNm
	Torsional moment	1.2	4.3	305	33.1	MNm

Summary of screening 100 year wind waves

Table 2-5: Summary of 1 hour expected maxima for 100-year return period waves for the bridge girder

Where	Response	Hs [m]	Tp [sec]	Heading [deg]	Value	Unit
tower	Axial force	2.1	5.5	75	18.3	MN
	Bending moment about strong axis	2.1	5.5	105	465.0	MNm
	Bending moment about weak axis	1.4	4.6	200	0.9	MNm
	Torsional moment	2.1	5.5	105	17.5	MNm
axis 3	Axial force	2.1	5.5	75	17.3	MN
	Bending moment about strong axis	2.1	5.5	105	393.6	MNm
	Bending moment about weak axis	2.1	5.5	75	229.7	MNm
	Torsional moment	2.1	5.5	105	122.4	MNm
axis 16	Axial force	2.1	5.5	75	9.9	MN
	Bending moment about strong axis	2.1	5.5	75	302.8	MNm
	Bending moment about weak axis	1.4	4.6	195	93.9	MNm
	Torsional moment	2.1	5.5	105	58.2	MNm
axis 38	Axial force	1.4	4.6	195	16.6	MN
	Bending moment about strong axis	2.1	5.5	75	416.4	MNm
	Bending moment about weak axis	2.0	5.2	315	94.0	MNm
	Torsional moment	2.1	5.5	75	54.4	MNm
abutment north	Axial force	1.4	4.6	195	17.1	MN
	Bending moment about strong axis	2.1	5.5	75	790.3	MNm
	Bending moment about weak axis	2.0	5.2	315	227.3	MNm
	Torsional moment	2.1	5.5	75	82.8	MNm

Summary of screening 10.000-year wind waves

Table 2-6: Summary of 1 hour expected maxima for 10.000-year return period waves for the bridge girder

Where	Response	Hs [m]	Tp [sec]	Heading [deg]	Value	Unit
tower	Axial force	3.1	6.5	75	38.9	MN
	Bending moment about strong axis	3.1	6.5	105	898.9	MNm
	Bending moment about weak axis	3.1	6.5	75	1.8	MNm
	Torsional moment	3.1	6.5	105	38.2	MNm
axis 3	Axial force	3.1	6.5	75	40.0	MN
	Bending moment about strong axis	3.1	6.5	105	768.5	MNm
	Bending moment about weak axis	3.1	6.5	75	416.7	MNm
	Torsional moment	3.1	6.5	105	197.2	MNm
axis 16	Axial force	3.1	6.5	75	26.4	MN
	Bending moment about strong axis	3.1	6.5	75	621.5	MNm
	Bending moment about weak axis	1.8	5.2	195	131.6	MNm
	Torsional moment	3.1	6.5	95	99.7	MNm
axis 38	Axial force	3.1	6.5	105	30.2	MN
	Bending moment about strong axis	3.1	6.5	75	848.2	MNm
	Bending moment about weak axis	2.7	5.9	315	128.3	MNm
	Torsional moment	3.1	6.5	80	103.8	MNm
abutment north	Axial force	3.1	6.5	105	30.8	MN
	Bending moment about strong axis	3.1	6.5	75	1589.6	MNm
	Bending moment about weak axis	2.7	5.9	315	326.5	MNm
	Torsional moment	3.1	6.5	80	141.5	MNm

2.2.1.2 Swell

When selecting wave states from swell the 1-hour maxima is evaluated at the tower only. The response in the tower is assumed to be representative of the response of the whole bridge because of the shape of the modes triggered by swell. See example plots of the response evaluated at the tower in Figure 2-3 and Figure 2-4.

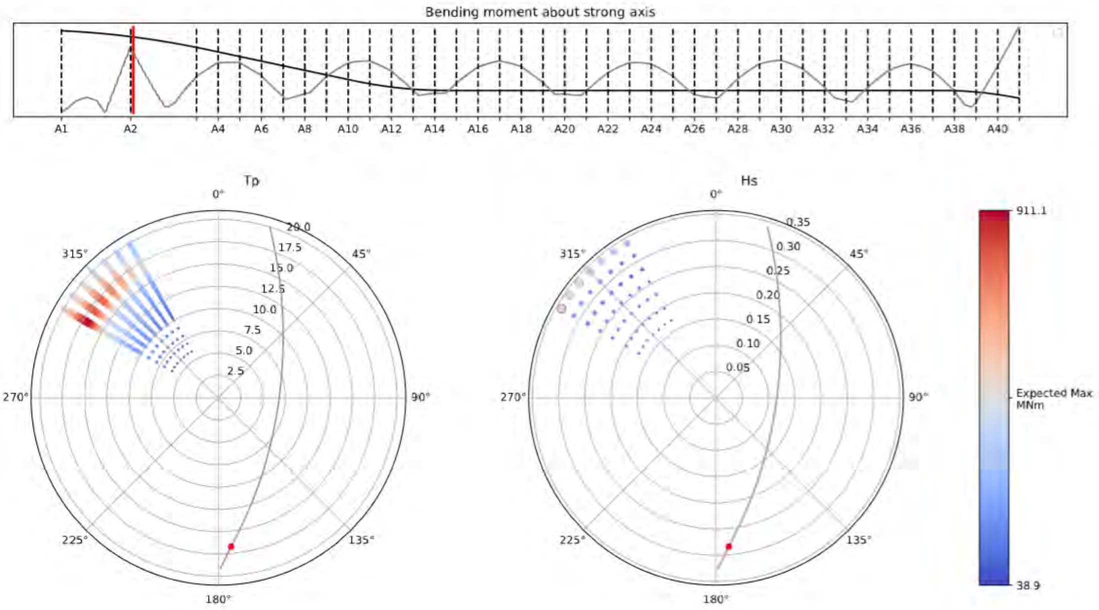

Figure 2-3: Bending moment about strong axis in the bridge girder at the tower for 100-year return period swell sea states.

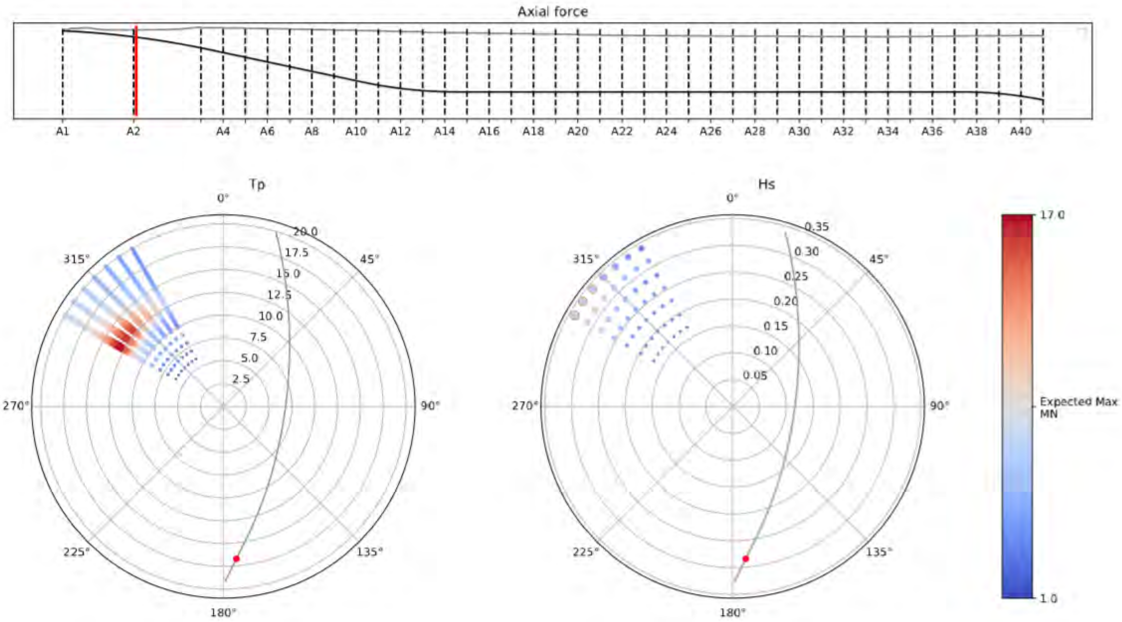

Figure 2-4: Axial force in the bridge girder at the tower for 100-year return period swell sea states.

Summary of screening 1-year swell

Table 2-7: Summary of 1 hour expected maxima for 1-year return period swell

	At	Axis	Heading [deg]	Hs [m]	Tp [sec]	Unit	Value
Axial force	Whole bridge	2	300	0.22	13.25	MN	12.2
Bending moment about strong axis	Whole bridge	2	300	0.22	17.25	MNm	630.5

Summary of screening 100-year swell

Table 2-8: Summary of 1 hour expected maxima for 100-year return period swell

	At	Axis	Heading [deg]	Hs [m]	Tp [sec]	Unit	Value
Axial force	Whole bridge	2	300	0.34	13.25	MN	17.1
Bending moment about strong axis	Whole bridge	2	300	0.34	17.25	MNm	911.2

Summary of screening 10.000-year swell

Table 2-9: Summary of 1 hour expected maxima for 10.000-year return period swell

	At	Axis	Heading [deg]	Hs [m]	Tp [sec]	Unit	Value
Axial force	Whole bridge	2	300	0.46	13.25	MN	21.6
Bending moment about strong axis	Whole bridge	2	300	0.46	17.25	MNm	1171.5

2.2.2 Selected design wave cases

2.2.2.1 1-year design load cases

Wind waves

Table 2-10: Selected design load cases for the 1-year wind waves

	Design case 1	Design case 2	Design case 3	Design case 4
Hs [m]	0.9	1.2	1.2	1.0
Tp [s]	3.7	4.3	4.3	4.0
Wave Direction [deg]	195	285	315	75

Swell

Table 2-11: Selected design load case for the 1-year swell

	Design case 1	Design case 2
Hs [m]	0.22	0.22
Tp [s]	17.25	13.25
Wave Direction [deg]	300	300

2.2.2.2 100-year design load cases

Wind waves

Table 2-12: Selected design load cases for the 100-year wind waves

	Design case 1	Design case 2	Design case 3	Design case 4
Hs [m]	2.1	2.1	1.4	2.0
Tp [s]	5.5	5.5	4.6	5.2
Wave Direction [deg]	75	105	195	315

Swell

Table 2-13: Selected design load case for the 100-year swell

	Design case 1	Design case 2
Hs [m]	0.34	0.34
Tp [s]	17.25	13.25
Wave Direction [deg]	300	300

2.2.2.3 10.000-year design load cases

Wind waves

Table 2-14: Selected design load cases for the 10.000-year wind waves

	Design case 1	Design case 2	Design case 3	Design case 4
Hs [m]	3.1	3.1	1.8	2.7
Tp [s]	6.5	6.5	5.2	5.9
Wave Direction [deg]	75	105	195	315

Swell

Table 2-15: Selected design load case for the 1-year swell

	Design case 1	Design case 2
Hs [m]	0.46	0.46
Tp [s]	17.25	13.25
Wave Direction [deg]	300	300

2.3 Wind conditions

2.3.1 Wind input

See [3] for a description of wind modelling in Orcaflex and Novaframe.

The following wind conditions are considered for ULS assessments. 10 seeds of 1-hour simulation were used for each condition.

$$V(z) = C_r(z) \cdot V_b$$

$$C_r(z) = k_T \cdot \ln\frac{z}{z_0}$$

$$V_b = C_{dir} \cdot C_{prob} \cdot V_{b0}$$

$$V_{b0} = 24.3\ m/s \quad k_T = 0.17 \quad z_0 = 0.01\ m$$

Return period	C_{prob}
1 year	0.75
100 year	1.04
10 000 year	1.26

Direction	C_{dir}
280	1.00
100	0.85

Return period	Direction [deg]	Vb [m/s]	V @ 2m [m/s]
1 year	280.00	18.2	16.3
1 year	100.00	15.5	13.8
100 year	280.00	25.2	22.5
100 year	100.00	21.4	19.2
10.000 year	280.00	30.7	27.4
10.000 year	100.00	26.1	23.3

2.3.2 Screening of wind directions

A simplified screening of wind directions was performed for K12_06 and K14_07 concepts, in which time-domain simulations of wind was simulated with 30-degree intervals. The corresponding wind velocity to each direction was selected from the metocean design basis. Two seeds were simulated for each direction, and the results are presented as the maximum response of these two seeds pr. direction.

Figure 2-5 and Figure 2-6 show the strong-axis and torsional moments from the time-domain wind screening with varying wind direction compared to the characteristic values from two directions that are used for design (both for 100-year wind conditions).

The strong-axis moment has a slight exceedance above design values towards the Northern abutment for positive moment, but the amplitude is less than the negative moment and hence not dimensioning. For torsional response K12 is captured well.

Note that the effects of skew wind are not considered in the current simulations, rather the wind is decomposed into parallel and perpendicular components and only the perpendicular component contributes to the loading. More refined methods are recommended for detailed design.

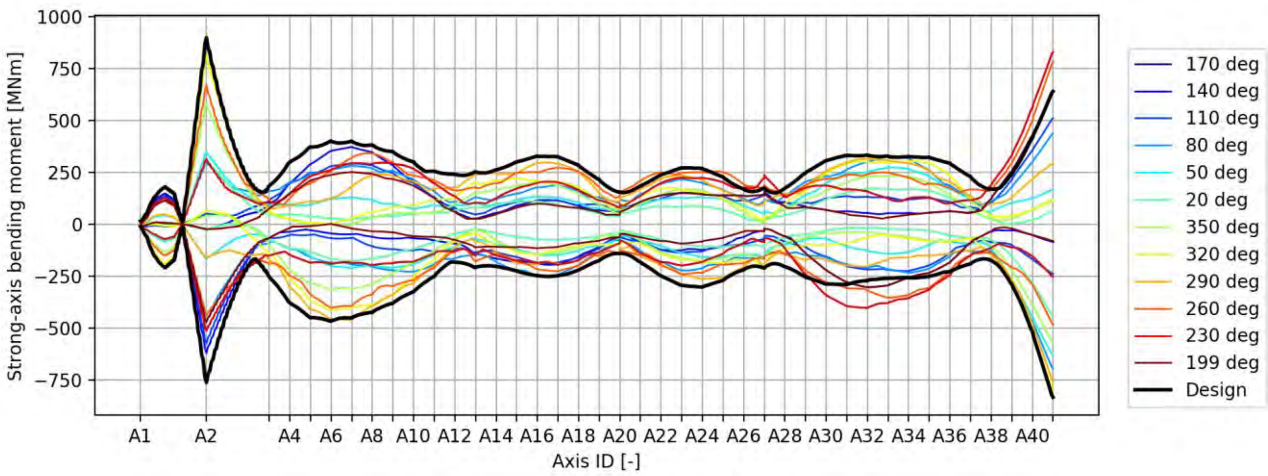

Figure 2-5 Wind-screening, strong-axis bending moment for K12_06

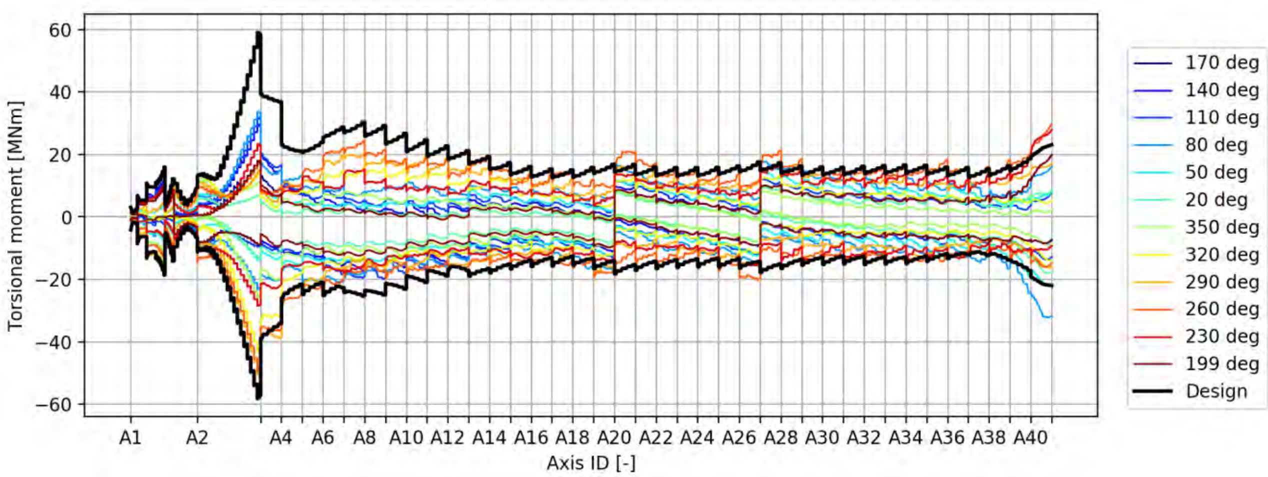

Figure 2-6 Wind-screening, torsional moment for K12_06

2.4 1 year combined wave/wind/current

The following environmental conditions were simulated in time-domain with coupled wind- and wave response, each with 10 seeds for an ULS verification. Simulations were as part of a sensitivity study on the effect of traffic loads effects on the bridge response, see section 8.5.

Table 2-16: 1-year return period combined wave/wind/current design load cases

Concept	Combi-nation	Hs [m] ww/sw	Tp [sec] ww/sw	Direction [deg] ww/sw	Basis Wind Speed [m/s]	Wind Direction [deg]	Current Speed [m/s]	Current Direction [deg]
K12_07	0	0.9/0.22	3.7/17.25	195/300	18.2	280	1.7	280
K12_07	1	0.9/0.22	3.7/13.25	195/300	18.2	280	1.7	280
K12_07	2	1.2/0.22	4.3/17.25	285/300	18.2	280	1.7	280
K12_07	3	1.2/0.22	4.3/13.25	285/300	18.2	280	1.7	280
K12_07	4	1.2/0.22	4.3/17.25	315/300	18.2	280	1.7	280
K12_07	5	1.2/0.22	4.3/13.25	315/300	18.2	280	1.7	280
K12_07	6	1.0	4.0	75	15.5	100	1.7	100

2.5 100 year combined wave/wind/current

The following environmental conditions were simulated in time-domain with coupled wind- and wave response, each with 10 seeds for an ULS verification (see Section 0). For ALS checks of post-damage capacity, the worst seed was selected and used for checking.

Table 2-17: 100-year return period combined wave/wind/current design load cases

Concept	Combi-nation	Hs [m] ww/sw	Tp [sec] ww/sw	Direction [deg] ww/sw	Basis Wind Speed [m/s]	Wind Direction [deg]	Current Speed [m/s]	Current Direction [deg]
K12_07	0	1.4/0.34	4.6/17.25	195/300	25.2	280	1.7	280
K12_07	1	1.4/0.34	4.6/13.25	195/300	25.2	280	1.7	280
K12_07	2	2.0/0.34	5.2/17.25	315/300	25.2	280	1.7	280
K12_07	3	2.0/0.34	5.2/13.25	315/300	25.2	280	1.7	280
K12_07	4	2.1	5.5	75	21.5	100	1.7	100
K12_07	5	2.1	5.5	105	21.5	100	1.7	100

2.6 10 000 year combined wave/wind/current

The following environmental conditions were simulated in time-domain with coupled wind- and wave response, each with 10 seeds for an ALS verification.

Table 2-18: 10 000-year return period combined wave/wind/current design load cases

Concept	Combi-nation	Hs [m] ww/sw	Tp [sec] ww/sw	Direction [deg] ww/sw	Basis Wind Speed [m/s]	Wind Direction [deg]	Current Speed [m/s]	Current Direction [deg]
K12_07	0	1.8/0.46	5.2/17.25	195/300	30.7	280	1.7	280
K12_07	1	1.8/0.46	5.2/13.25	195/300	30.7	280	1.7	280
K12_07	2	2.7/0.46	5.9/17.25	315/300	30.7	280	1.7	280
K12_07	3	2.7/0.46	5.9/13.25	315/300	30.7	280	1.7	280
K12_07	4	3.1	6.5	75	26.2	100	1.7	100
K12_07	5	3.1	6.5	105	26.2	100	1.7	100

2.7 Load combination and correlation

The following briefly describes the load combination and correlation considerations used for the results given in this report. Details can be found in the relevant enclosures to the report.

2.7.1 Direct method

With the direct method, all dynamic load groups are combined directly in the time domain. This can either be done by coupled time domain analysis where wind-waves, swell and wind loads are applied simultaneously, or by combining force time series from each load group analysed separately (un-coupled). The

When time series of the total dynamic forces (wind-waves, swell and wind) have been established these can be further processed in the following ways:

- Extreme value estimation of individual dynamic force components and subsequent combination with static loads to arrive at total design forces for ULS/ALS.
- Combination with static loads to establish total design force time series. These time series can be further used for the following purposes:
    - Find min/max and associated values for different response variables. This is typically used for structural capacity checks.
    - Generate Von Mises stress time series. This allows for an accurate prediction of the stress response in the bridge, and extreme value estimation can be performed directly on the stress processes.
    - Similarly, cross section capacity checks can also be performed directly on the force time series.

2.7.2 Factor method

With the factor method, design force values are established for all individual load groups and combination factors are used to account for the correlation between dynamic load groups and individual force components. This method is only applied for the bridge girder and is used primarily as a tool in the design process to better understand the contribution from individual load groups.

2.7.3 Extreme value estimation

Two different methods are used for extreme value estimation of the dynamic response processes.

1. Peak factor method. Based on zero up-crossing frequency under assumption of a Gaussian process (Rayleigh-distributed peaks). This is typically used for single seed realizations.
2. AUR method (average upcrossing rate). Used when multiple seeds are run per environmental condition and for non-Gaussian processes. This method can e.g. be used directly on the von mises stress processes that is non-gaussian in nature. See ref. [7] for a discussion of the methodology.

3 Static response

3.1 Permanent loads

3.1.1 Typical results, bridge girder

Typical results are presented for the K12_07 concept. More results are included in the benchmark of softwares in Appendix F [3].. Stay-cable tension cause axial compression in the high-bridge. Weak-axis shear force and moment are dominated by gravity loading.

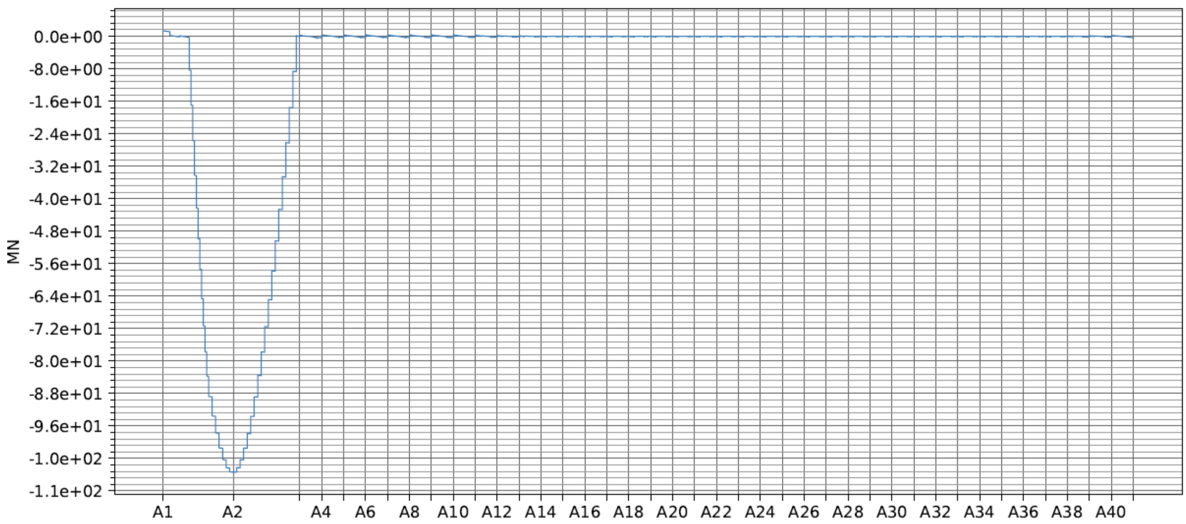

Figure 3-1 Permanent loads – Axial force in bridge girder [MN]

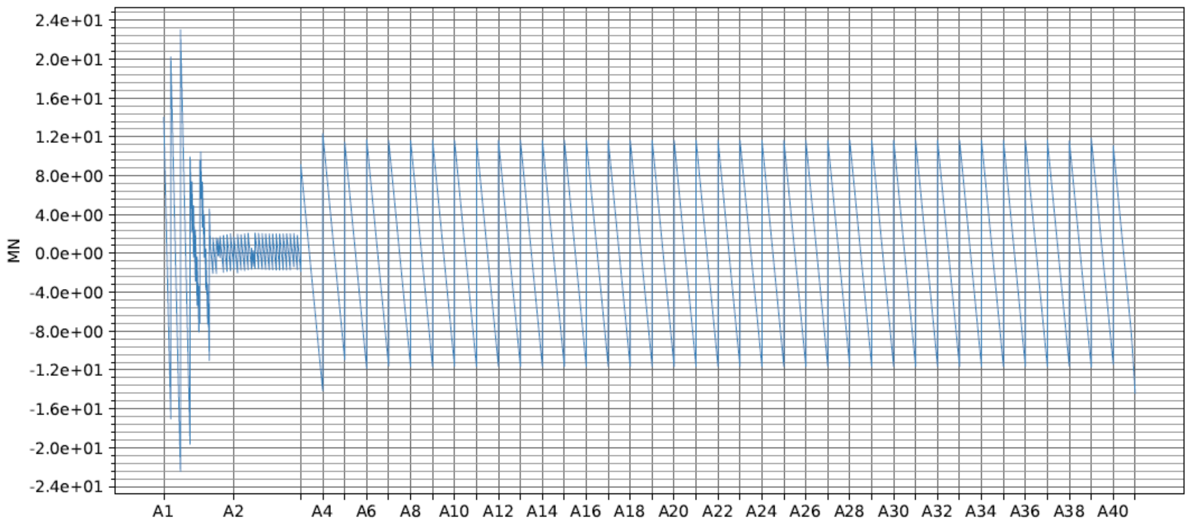

Figure 3-2 Permanent loads – vertical shear force in bridge girder [MN]

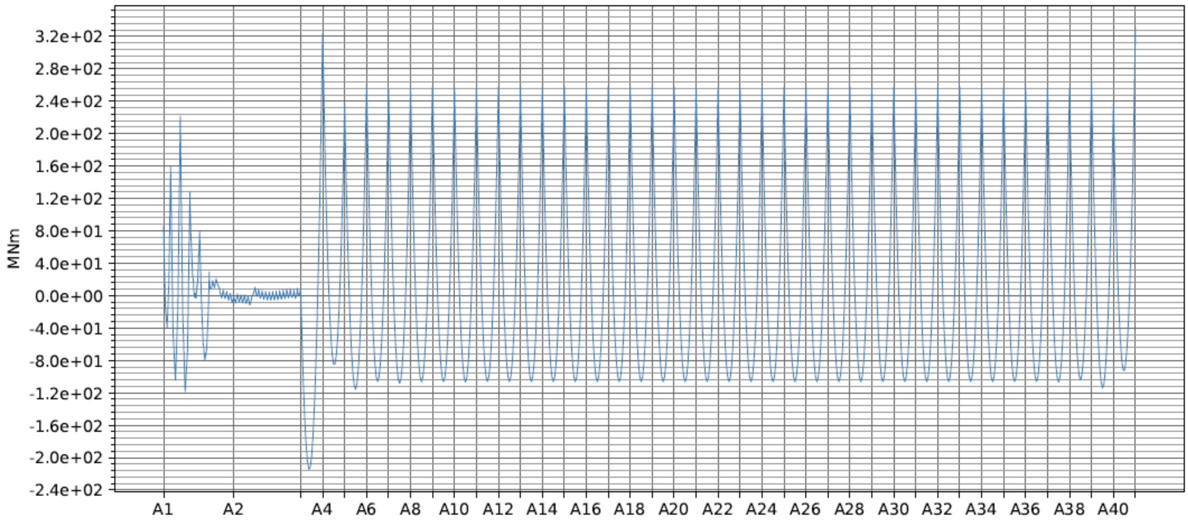

Figure 3-3 Permanent loads – Weak axis bending moment in bridge girder for K11_07 [MNm]

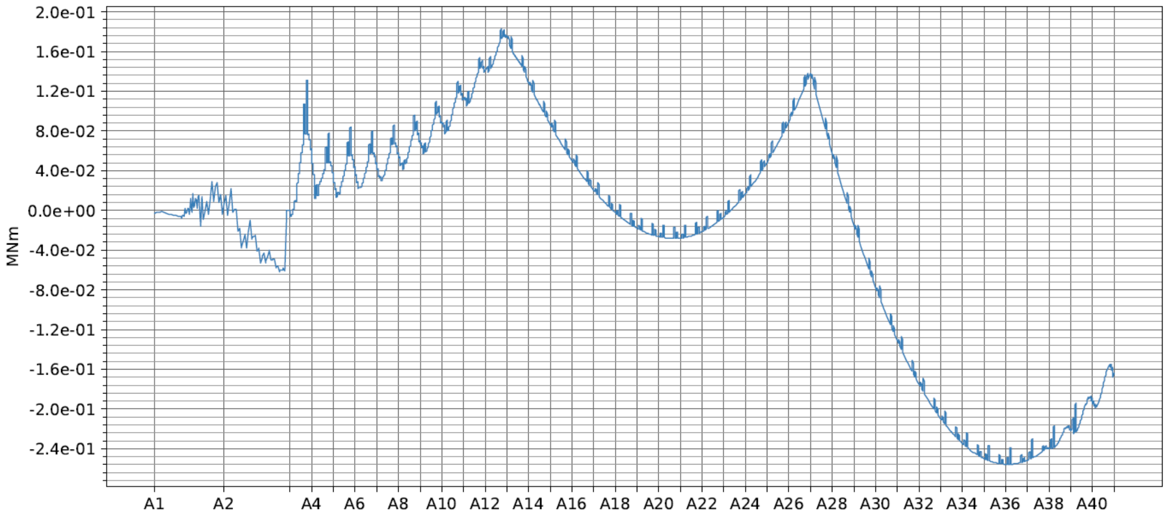

Figure 3-4 Permanent loads - Strong-axis bending moment in bridge girder for K12_07 [MNm]

3.1.2 Verification, hand calculations

The moment distribution in the floating bridge part of concept K12_07 is verified below:

Bjørnafjorden - phase 5
Permanent loading
HT, 2019.06.27

Permanent load

Construction weigth and asphalt $q := (137.2 + 49.1)\ \frac{kN}{m} = 186.3\ \frac{kN}{m}$

Beam parameteres

Span length in flooting bridge $L := 125\ m$

Elastic modulus steel $E := 210\ GPa$

2nd moment of area, weak axis

$$I_z(x) := \left(\begin{array}{l} \text{if } 0\ m \le x < \frac{2}{16} L \\ \quad \| 3.668\ m^4 \\ \text{else if } \frac{2}{16} L \le x < \frac{4}{16} L \\ \quad \| 3.311\ m^4 \\ \text{else if } \frac{4}{16} L \le x \le \frac{12}{16} L \\ \quad \| 2.569\ m^4 \\ \text{else if } \frac{12}{16} L \le x \le \frac{14}{16} L \\ \quad \| 3.311\ m^4 \\ \text{else if } \frac{14}{16} L \le x \le \frac{16}{16} L \\ \quad \| 3.668\ m^4 \end{array} \right)$$

Moment distribution

Assume support moments until zero rotation at supports $\theta_A = 0$ (calculated below):

$M_{sup.1} := 257.7645\ MN \cdot m$

$M_{sup.2} := M_{sup.1} = 257.765\ MN \cdot m$

Support reaction 1 $R_{sup.1} := \frac{q \cdot L}{2} + \frac{M_{sup.1}}{L} - \frac{M_{sup.2}}{L} = 11.644\ MN$

Support reaction 2 $R_{sup.2} := \frac{q \cdot L}{2} - \frac{M_{sup.1}}{L} + \frac{M_{sup.2}}{L} = 11.644\ MN$

Moment distribution $M(x) := R_{sup.1} \cdot x - M_{sup.1} - \frac{q \cdot x^2}{2}$

Curvature $\kappa(x) := \frac{M(x)}{E \cdot I_z(x)}$

Support rotation (iterated on support moment to have $\theta_{sup.1} = 0$):

$$\theta_{sup.1} := \frac{\int_0^L \kappa(x)\, x\, \mathrm{d}x}{L} = 3.365 \cdot 10^{-8}$$

Span moment

$$M_{span} := M\left(\frac{L}{2}\right) = 106.103\ \boldsymbol{MN \cdot m}$$

Compared to RM-Analyses

$$\left(\frac{257.865\ \boldsymbol{MN \cdot m}}{M_{sup.1}}\right) = 1$$

(Typical support moment in floating bridge - value chosen for axis 24)

$$\left(\frac{106.200\ \boldsymbol{MN \cdot m}}{M_{span}}\right) = 1.001$$

(Typical span moment in floating bridge - value chosen for span between axis 23-24)

Plot, curvature and moment distribution

$x := 0\ \boldsymbol{m}, 0.1\ \boldsymbol{m} .. L$

Curvature distribution:

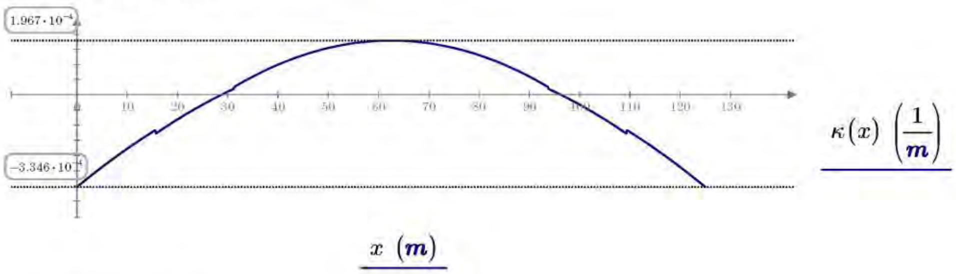

Moment distribution:

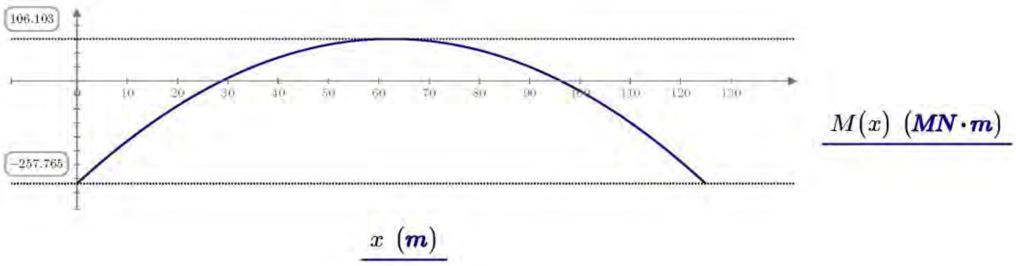

The stay cable forces in K12_07 are verified by hand-calculations based on that each stay cable in front span have a vertical component corresponding to $\frac{137.3+49.1}{2}\frac{kN}{m} \cdot 20m = 1864kN$ plus half the cable weight. The back span stay cables are determined by horizontal equilibrium about the pylon. The results and comparison are presented below:

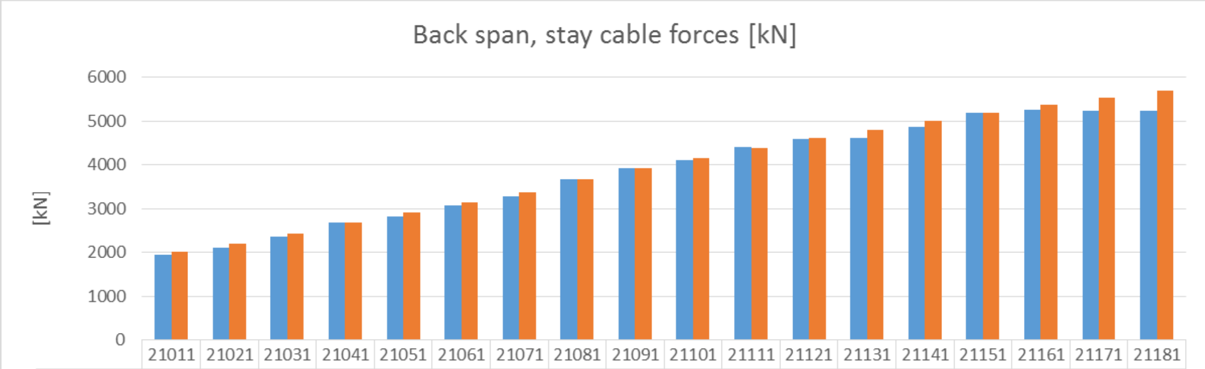

	21011	21021	21031	21041	21051	21061	21071	21081	21091	21101	21111	21121	21131	21141	21151	21161	21171	21181
RM	1949	2111	2373	2677	2823	3085	3277	3674	3923	4110	4417	4596	4613	4880	5189	5269	5228	5227
Hand calc.	2029	2205	2433	2677	2921	3155	3385	3664	3925	4168	4396	4611	4804	4999	5193	5371	5534	5690

Figure 3-5 Permanent loads, back span stay cable forces – comparison RM Bridge to hand calculations [kN]

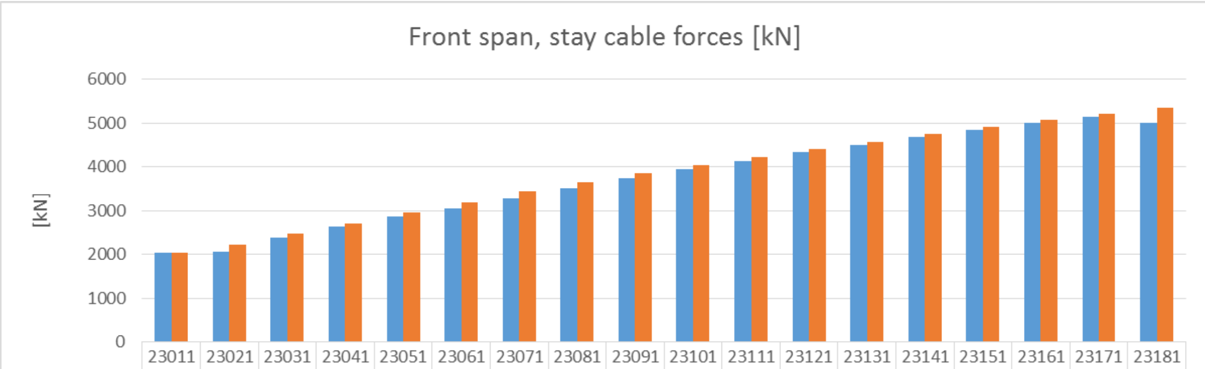

	23011	23021	23031	23041	23051	23061	23071	23081	23091	23101	23111	23121	23131	23141	23151	23161	23171	23181
RM	2053	2076	2391	2639	2874	3059	3292	3518	3737	3945	4144	4334	4506	4681	4855	5012	5145	4999
Hand calc.	2047	2235	2470	2719	2966	3202	3434	3646	3852	4048	4236	4417	4580	4749	4918	5074	5217	5355

Figure 3-6 Permanent loads, front span stay cable forces – comparison RM Bridge to hand calculations [kN]

3.2 Temperature

3.2.1 Typical results, bridge girder

Typical characteristic temperature results are presented for the K12_07 concept.

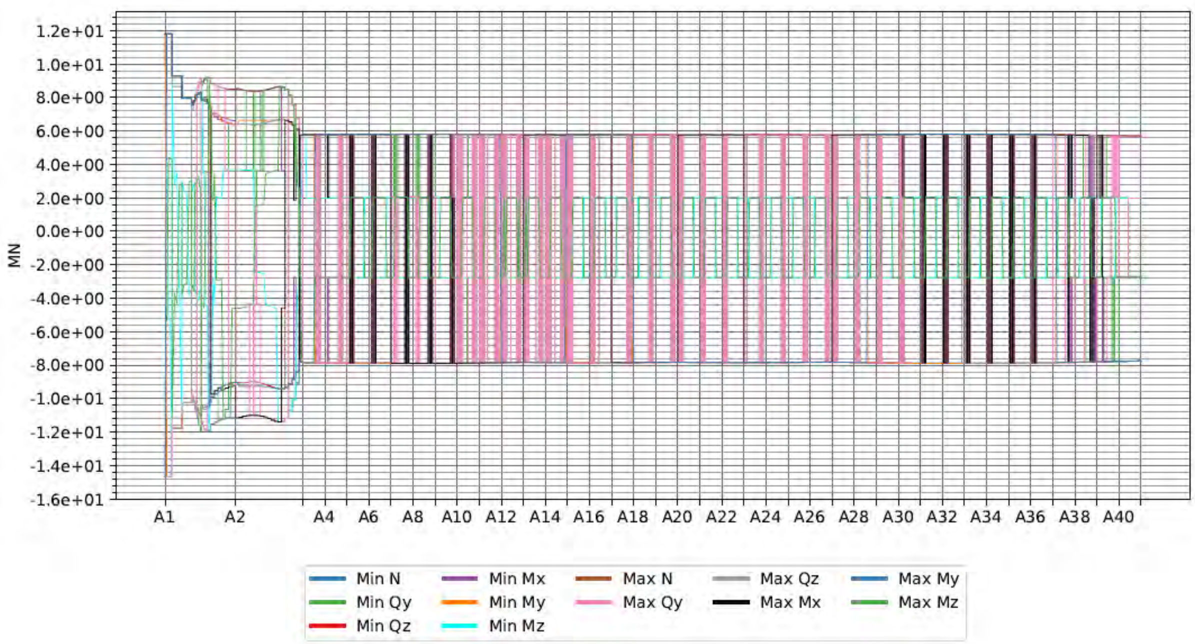

Figure 3-7 Temperature loads – Axial force in bridge girder (envelope values) [kN]

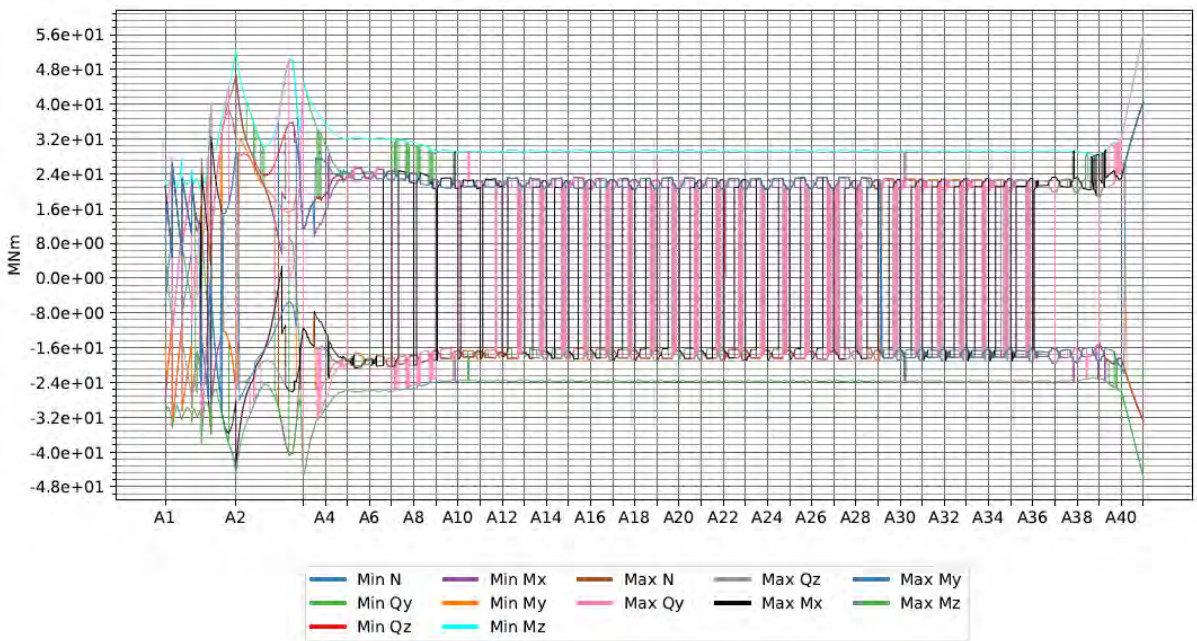

Figure 3-8 Temperature loads - Weak axis bending moment in bridge girder (envelope values) [kNm]

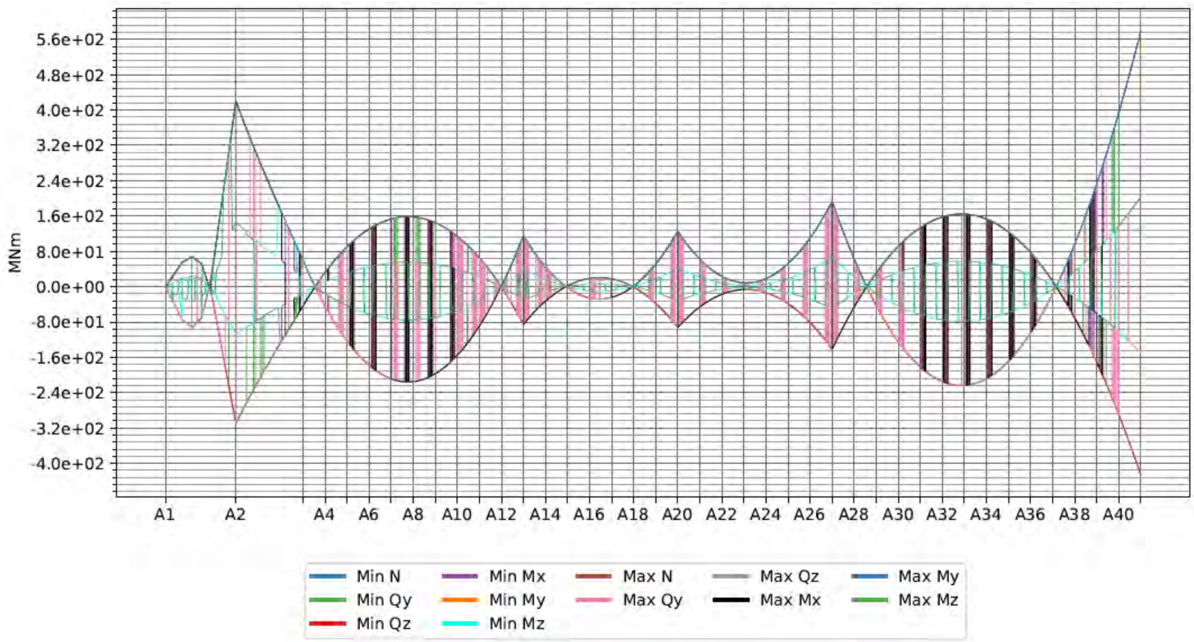

Figure 3-9 Temperature loads – Strong axis bending moment in bridge girder (envelope values) [kNm]

3.2.2 Verification, hand calculations

The load effect on the floating bridge part of concept K12 is verified below for the temperature gradient:

Bjørnafjorden - phase 5
Temperature loading
HT, 2019.06.28

Thermal loads (Designbasis MetOcean, rev1)

$$T_{max} := 33$$
$$T_{min} := -17$$

Design thermal loads (Steel cross-section - Type 1)

$$\Delta T_{M.heat} := 0.7 \cdot 18 = 12.6$$ [NS-EN 1991-1-5, table NA.6.1 adn NA.6.2]

$$\Delta T_{M.cool} := -(1.2 \cdot 13) = -15.6$$ [NS-EN 1991-1-5, table NA.6.1 adn NA.6.2]

Bridge girder properties

$$h := 4\ \mathbf{m}$$ Bridge girder, cross-section height

$$I_z := \frac{(4 \cdot 3.668\ \mathbf{m}^4 + 4 \cdot 3.311\ \mathbf{m}^4 + 8 \cdot 2.569\ \mathbf{m}^4)}{16} = 3.029\ \mathbf{m}^4$$ Average Second moment of inertia, bridge girder - weak axis

Material properties

$$E := 210\ \mathbf{GPa}$$

$$\alpha := 1.2 \cdot 10^{-5}$$

Temperature gradient - warmer top side $\Delta T_{M.heat} = 12.6$

$$\kappa := \frac{\Delta T_{M.heat} \cdot \alpha}{h} = (3.78 \cdot 10^{-5})\ \frac{1}{\mathbf{m}}$$

$$M_z := \kappa \cdot E \cdot I_z = 24.046\ \mathbf{MN \cdot m}$$

$$\left(\frac{23.851\ \mathbf{MN \cdot m}}{M_z}\right) = 0.992$$ (Compared to RM-Bridge analyses)

Temperature gradient - warmer bottom side $\Delta T_{M.cool} = -15.6$

$$\kappa := \frac{\Delta T_{M.cool} \cdot \alpha}{h} = -4.68 \cdot 10^{-5}\ \frac{1}{\mathbf{m}}$$

$$M_z := \kappa \cdot E \cdot I_z = -29.771\ \mathbf{MN \cdot m}$$

$$\left(\frac{-29.479\ \mathbf{MN \cdot m}}{M_z}\right) = 0.99$$ (Compared to RM-Bridge analyses)

3.3 Traffic

3.3.1 Typical results, bridge girder

Typical characteristic traffic results are presented for the K12_07 concept.

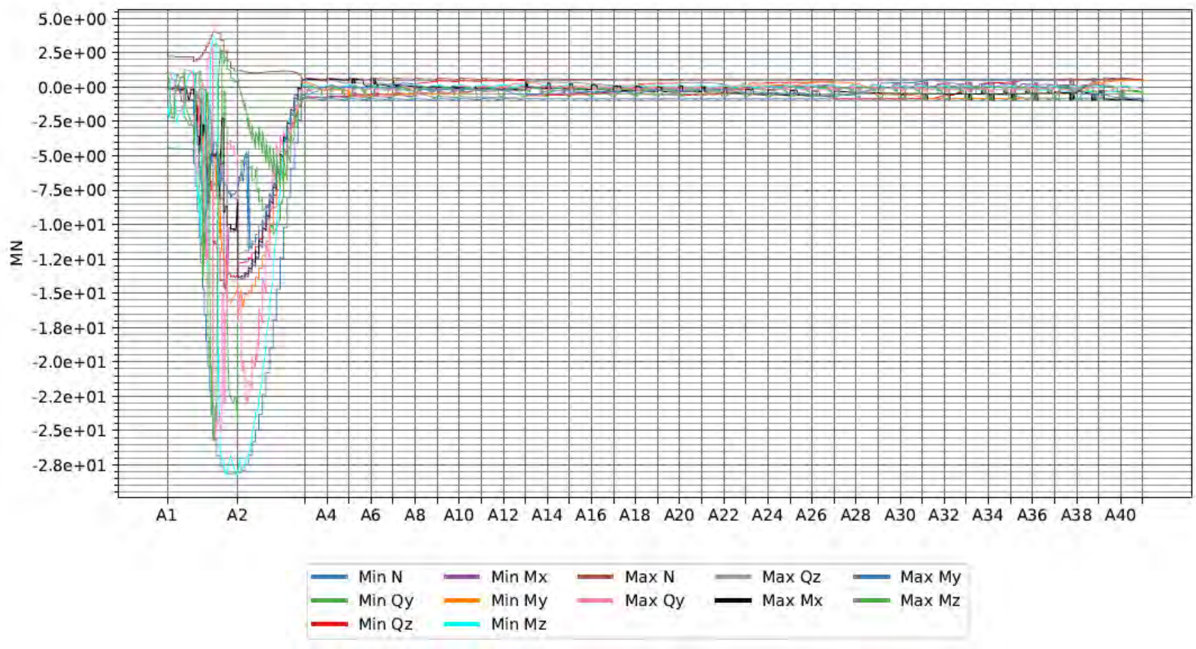

Figure 3-10 Traffic loads – Axial force in bridge girder (envelope values) [MN]

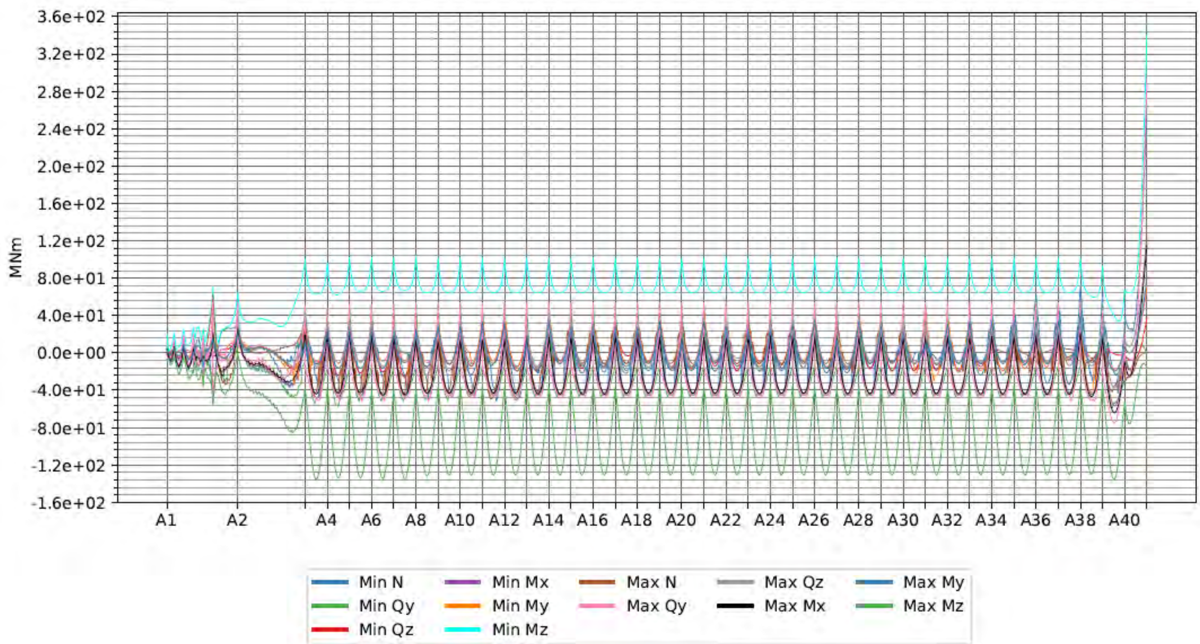

Figure 3-11 Traffic loads - Weak axis bending moment in bridge girder (envelope values) [MNm]

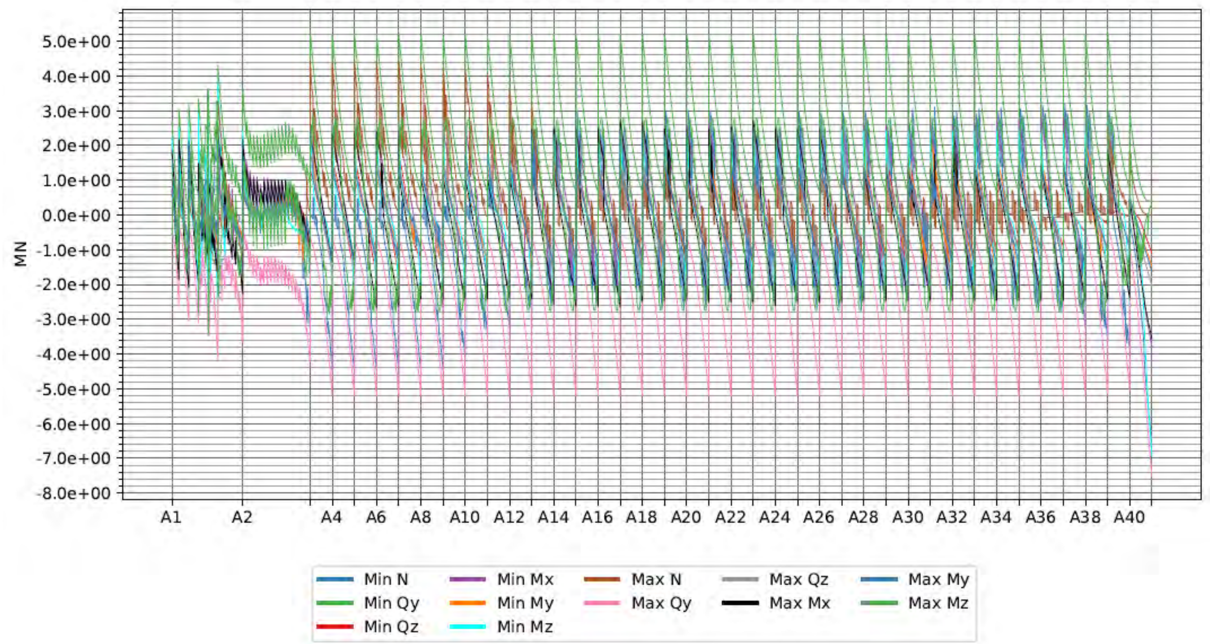

Figure 3-12 Traffic loads – vertical shear force in bridge girder (envelope values) [MN]

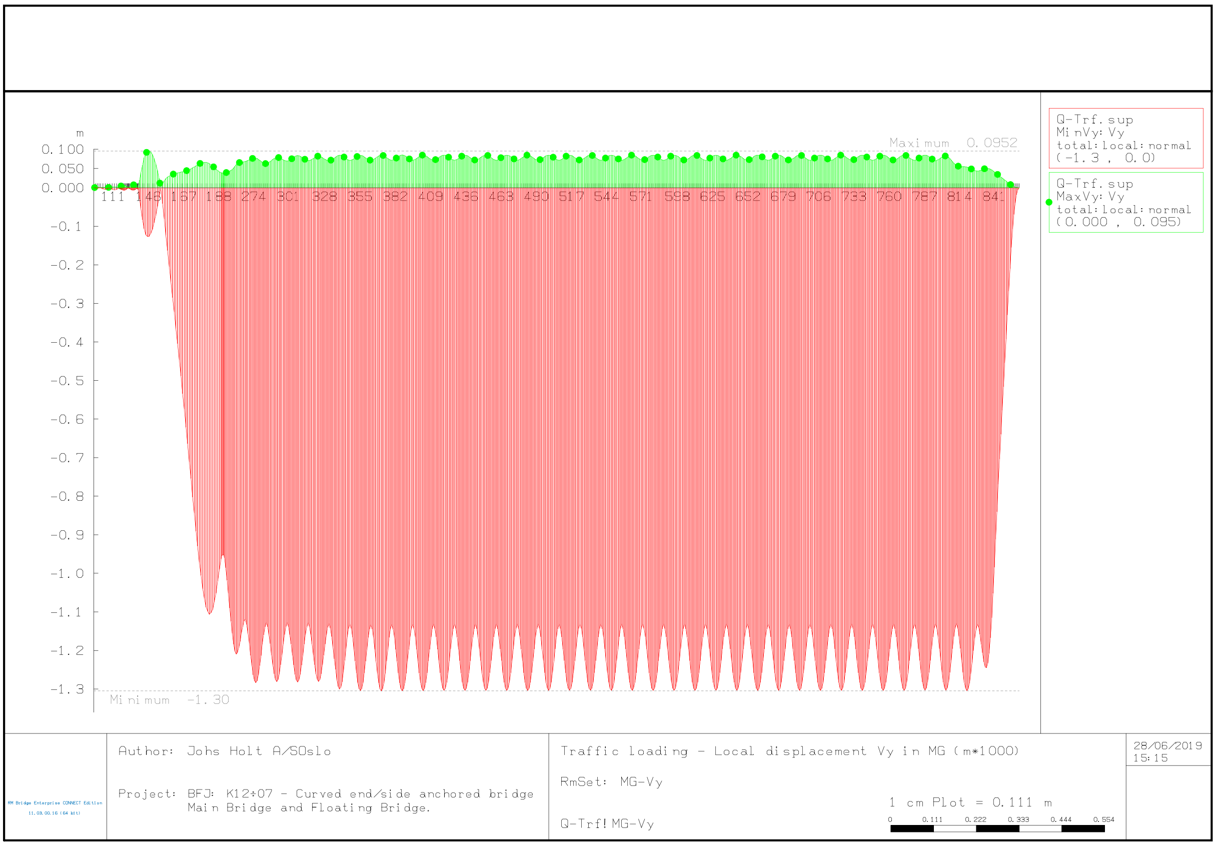

Figure 3-13 Traffic loading – vertical displacements in bridge girder (envelope values) [m]

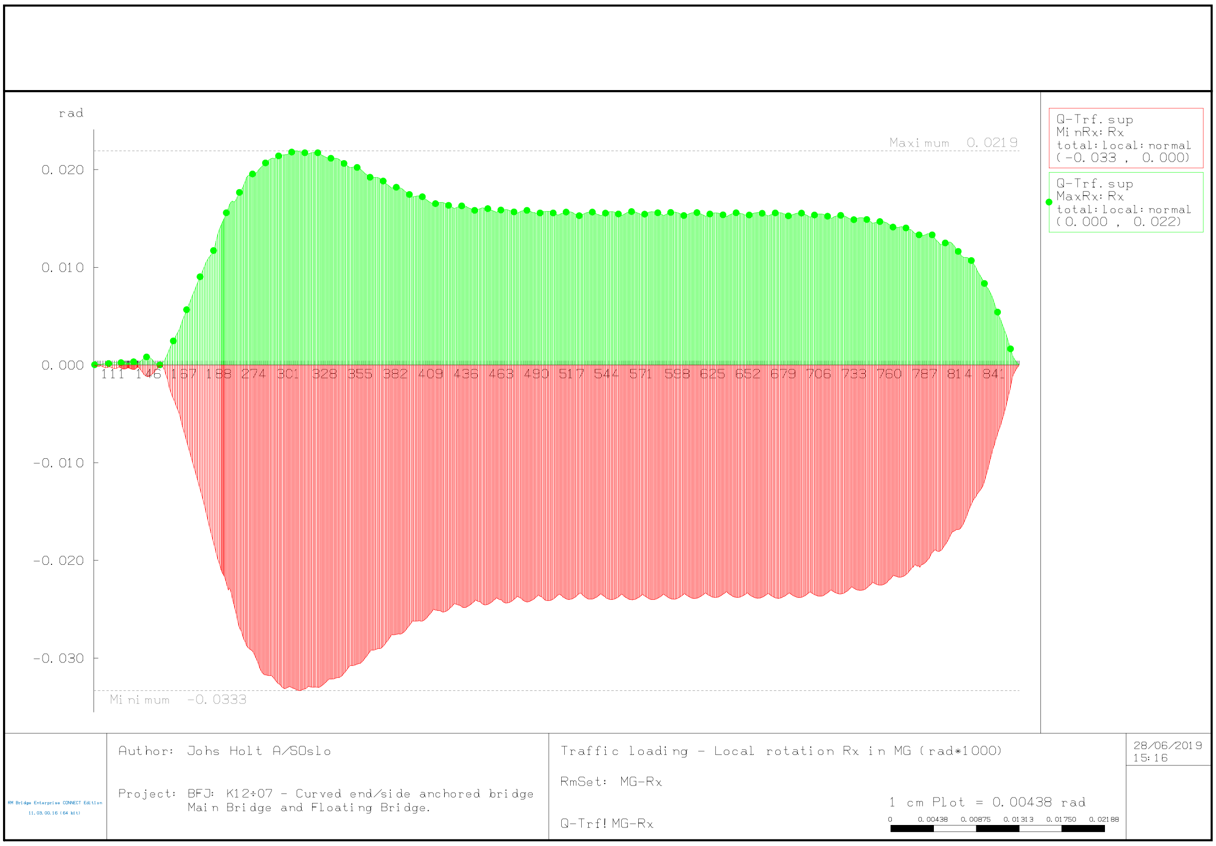

Figure 3-14 Traffic loading – rotation (roll) in bridge girder (envelope values) [rad]

3.3.2 Verification, hand calculations

The load effect on the floating bridge part of concept K12_07 is verified below:

Bjørnafjorden - phase 5
Traffic loading
HT, 2019.06.28

Eurocode loads (LM1), loaded length $L < 200\ m$

$$q := 3\ \mathbf{m} \cdot (5.4+2.5+2.5+2.5+2.5+2.5+2.5)\ \frac{\mathbf{kN}}{\mathbf{m}^2} = 61.2\ \frac{\mathbf{kN}}{\mathbf{m}}$$

$$Q := 2 \cdot (300+200+100)\ \mathbf{kN} = 1200\ \mathbf{kN}$$

Pontoon stiffness (typical in the floating bridge part)

$$C_{33} := 7459\ \frac{\mathbf{kN}}{\mathbf{m}}$$

$$C_{44} := 1.11971 \cdot 10^6\ \frac{\mathbf{kN} \cdot \mathbf{m}}{\mathbf{rad}}$$

Spanlength, girder

$$L := 125\ \mathbf{m}$$

$$I := \frac{(4 \cdot 3.668\ \mathbf{m}^4 + 4 \cdot 3.311\ \mathbf{m}^4 + 8 \cdot 2.569\ \mathbf{m}^4)}{16} = 3.029\ \mathbf{m}^4$$ (Average Second moment of inertia)

$$E := 210\ \mathbf{GPa}$$

Load intensity pr. lane as function of loaded length $200\ m < L < 1000\ m$

$$q_1(qlen) := 5.4\ \frac{\mathbf{kN}}{\mathbf{m}^2} + \frac{(4.5-5.4)}{1000\ \mathbf{m} - 200\ \mathbf{m}}\ \frac{\mathbf{kN}}{\mathbf{m}^2} \cdot (qlen - 200\ \mathbf{m})$$

$$q_2(qlen) := 2.5\ \frac{\mathbf{kN}}{\mathbf{m}^2} + \frac{(2.5-2.5)}{1000\ \mathbf{m} - 200\ \mathbf{m}}\ \frac{\mathbf{kN}}{\mathbf{m}^2} \cdot (qlen - 200\ \mathbf{m})$$

$$q_3(qlen) := 2.5\ \frac{\mathbf{kN}}{\mathbf{m}^2} + \frac{(0-2.5)}{1000\ \mathbf{m} - 200\ \mathbf{m}}\ \frac{\mathbf{kN}}{\mathbf{m}^2} \cdot (qlen - 200\ \mathbf{m})$$

$$q_4(qlen) := 2.5\ \frac{\mathbf{kN}}{\mathbf{m}^2} + \frac{(2.5-2.5)}{1000\ \mathbf{m} - 200\ \mathbf{m}}\ \frac{\mathbf{kN}}{\mathbf{m}^2} \cdot (qlen - 200\ \mathbf{m})$$

$$q_5(qlen) := 2.5\ \frac{\mathbf{kN}}{\mathbf{m}^2} + \frac{(2.5-2.5)}{1000\ \mathbf{m} - 200\ \mathbf{m}}\ \frac{\mathbf{kN}}{\mathbf{m}^2} \cdot (qlen - 200\ \mathbf{m})$$

$$q_6(qlen) := 2.5\ \frac{\mathbf{kN}}{\mathbf{m}^2} + \frac{(0-2.5)}{1000\ \mathbf{m} - 200\ \mathbf{m}}\ \frac{\mathbf{kN}}{\mathbf{m}^2} \cdot (qlen - 200\ \mathbf{m})$$

$$q_f(qlen) := 2.5\ \frac{\mathbf{kN}}{\mathbf{m}^2} + \frac{(0.625-2.5)}{1000\ \mathbf{m} - 200\ \mathbf{m}}\ \frac{\mathbf{kN}}{\mathbf{m}^2} \cdot (qlen - 200\ \mathbf{m})$$

$$q(qlen) := 3\ \mathbf{m}\ (q_1(qlen) + q_2(qlen) + q_3(qlen) + q_4(qlen) + q_5(qlen) + q_6(qlen) + q_f(qlen))$$

Plot, load intensity as function of loaded length

$$qlen := 200\ \boldsymbol{m}, 201\ \boldsymbol{m} .. 1000\ \boldsymbol{m}$$

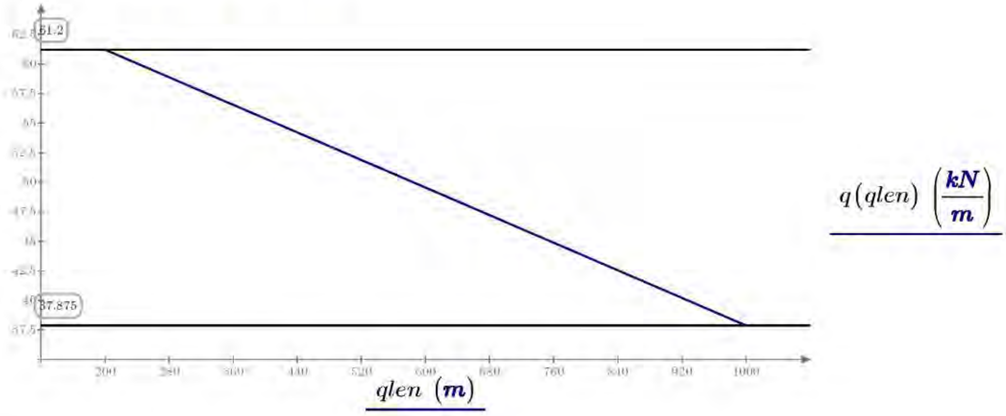

Beam on elastic bed (three equal spans) - [Handboken Bygg - Byggtabeller]

Span moment

$$qlen := 200\ \boldsymbol{m} \qquad q(qlen) = 61.2\ \frac{\boldsymbol{kN}}{\boldsymbol{m}}$$ (Loaded length and load intensity)

$$\mu := \frac{48 \cdot E \cdot I}{L^3 \cdot C_{33}} = 2.096$$

$$f_A := -0.0357 + \frac{(-0.0109 - -0.0357)}{(3-1)} \cdot (\mu - 1) = -0.022$$

$$f_B := 0.5357 + \frac{(0.5109 - 0.5357)}{(3-1)} \cdot (\mu - 1) = 0.522$$

(Assume linear variation between $\mu = 1$ and $\mu = 3$)

$$R_{A.q} := f_A \cdot q(qlen) \cdot L = -169.141\ \boldsymbol{kN}$$

$$R_{B.q} := f_B \cdot q(qlen) \cdot L = 3.994\ \boldsymbol{MN}$$

$$R_{A.Q} := f_A \cdot Q = -26.532\ \boldsymbol{kN}$$

$$R_{B.Q} := f_B \cdot Q = 0.627\ \boldsymbol{MN}$$

$$M_{span.q} := \frac{-q(qlen) \cdot L^2}{8} + \frac{R_{B.q} \cdot L}{2} + \frac{R_{A.q} \cdot 3\ L}{2} = 98.389\ \boldsymbol{MN \cdot m} \qquad \frac{q(qlen) \cdot L^2}{M_{span.q}} = 9.719$$

$$M_{span.Q} := \frac{R_{B.Q} \cdot L}{2} + \frac{R_{A.Q} \cdot 3\ L}{2} = 34.184\ \boldsymbol{MN \cdot m} \qquad \frac{Q \cdot L}{M_{span.Q}} = 4.388$$

$$M_{span} := M_{span.q} + M_{span.Q} = 132.572\ \boldsymbol{MN \cdot m}$$

$$\left(\frac{133.615\ \boldsymbol{MN \cdot m}}{M_{span}}\right) = 1.008$$ (Compared to RM-Bridge analyses)

Bridge girder deflection

$qlen := 369\ \boldsymbol{m}$ $q(qlen) = 56.273\ \frac{\boldsymbol{kN}}{\boldsymbol{m}}$ (Loaded length and load intensity)

$$\delta_{sup} := \frac{q(qlen) \cdot L + Q}{C_{33}} = 1103.911\ \boldsymbol{mm}$$

$$\left(\frac{1132\ \boldsymbol{mm}}{\delta_{sup}}\right) = 1.025$$ (Compared to RM-Bridge analyses)

$$\delta_{span} := q(qlen) \cdot \left(\frac{L}{C_{33}} + \frac{5\ L^4}{384 \cdot E \cdot I}\right) + Q\ \frac{L^3}{48 \cdot E \cdot I} = 1300.992\ \boldsymbol{mm}$$

$$\left(\frac{1303\ \boldsymbol{mm}}{\delta_{span}}\right) = 1.002$$ (Compared to RM-Bridge analyses)

Bridge girder rotations

$qlen := 1000\ \boldsymbol{m}$ $q(qlen) = 37.875\ \frac{\boldsymbol{kN}}{\boldsymbol{m}}$ (Loaded length and load intensity)

$$M_t := 3\ \boldsymbol{m} \cdot L \cdot \left(q_1(qlen) \cdot (10.25\ \boldsymbol{m}) + q_2(qlen) \cdot 7.25\ \boldsymbol{m} + q_3(qlen) \cdot 4.25\ \boldsymbol{m}\right) + \frac{(600\ \boldsymbol{kN} \cdot 10.25\ \boldsymbol{m} + 400\ \boldsymbol{kN} \cdot 7.25\ \boldsymbol{m} + 200\ \boldsymbol{kN} \cdot 4.25\ \boldsymbol{m})}{4} = 26568.75\ \boldsymbol{kN \cdot m}$$

$\theta := \frac{M_t}{C_{44}} = 0.024\ \boldsymbol{rad}$ $\theta = 1.36\ \boldsymbol{deg}$ $0.7\ \theta = 0.952\ \boldsymbol{deg}$

$$\left(\frac{0.024\ \boldsymbol{rad}}{\theta}\right) = 1.011$$ (Compared to RM-Bridge analyses)

3.4 Lateral buckling of bridge girder

Linear buckling analyses is performed for a uniformly distributed line load of 1kN/m in radial bridge direction. The first three buckling modes are shown in Figure 3-15. The corresponding buckling factors and the calculated buckling length is presented in Table 3-1.

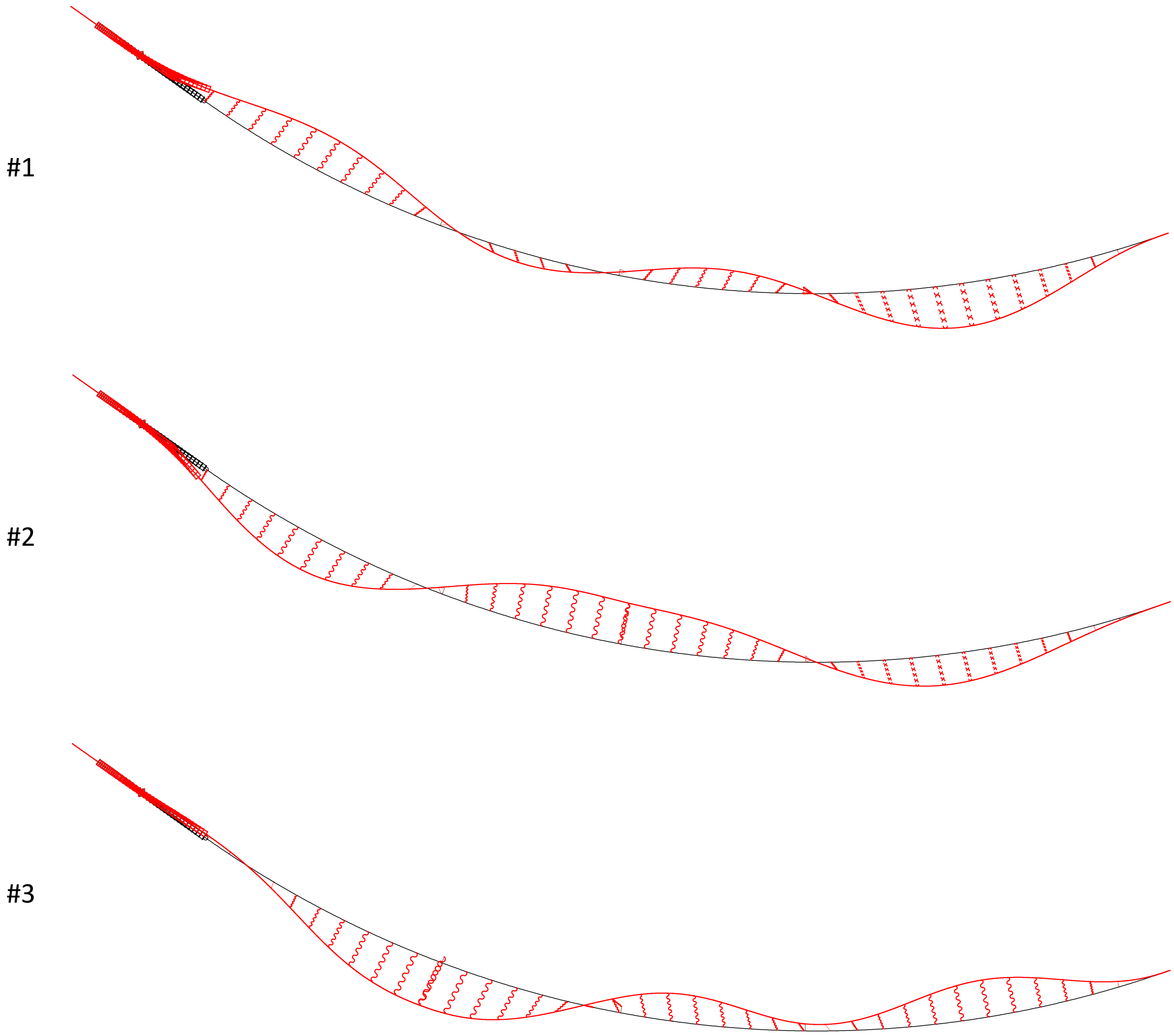

Figure 3-15 First three buckling modes of K12

The critical buckling length is calculated as $L_{cr} = k \cdot L = \sqrt{\frac{\pi^2 \cdot E \cdot I_y}{\lambda \cdot N_x}}$ where L is the bridge length from Pylon in axis A2 to the North bridge end, $E \cdot I_y$ is the cross-sectional stiffness, λ is the buckling factor calculated by RM Bridge and N_x is the beam axial force due to the line load.

Table 3-1 Critical linear buckling load and buckling lengths for the first three buckling modes

From RM BRIDGE: Linear buckling					q1 load		Crit. Buckl load			Acr
NUMBER	LAMBDA	NODE	DOF	LOADCASE	Nx [kN]	Lamda	lambda*q1	Lcr=k*L	k=Lcr/L	[MN]
1	38.08	726	Vz	Buckl#1	4805	38.08	182974	1085	0.21	7.3
2	43.878	497	Vz	Buckl#2	4805	43.878	210834	1011	0.20	8.4
3	64.83	410	Vz	Buckl#3	4805	64.83	311508	832	0.16	12.5

4 Dynamic response

See enclosures to this report for details of the dynamic response for the individual loads for each concept and eigenmodes. The calculated modal damping and decay test of the longest eigenperiod are presented in the accompanying Appendix F [3].

4.1 Eigenmodes

The first 10 eigenmodes are shown in Figure 4-1. A full set of modes are given in Enclosure 1, and a comparison of modes between Orcaflex and Novaframe is shown in Appendix F [3].

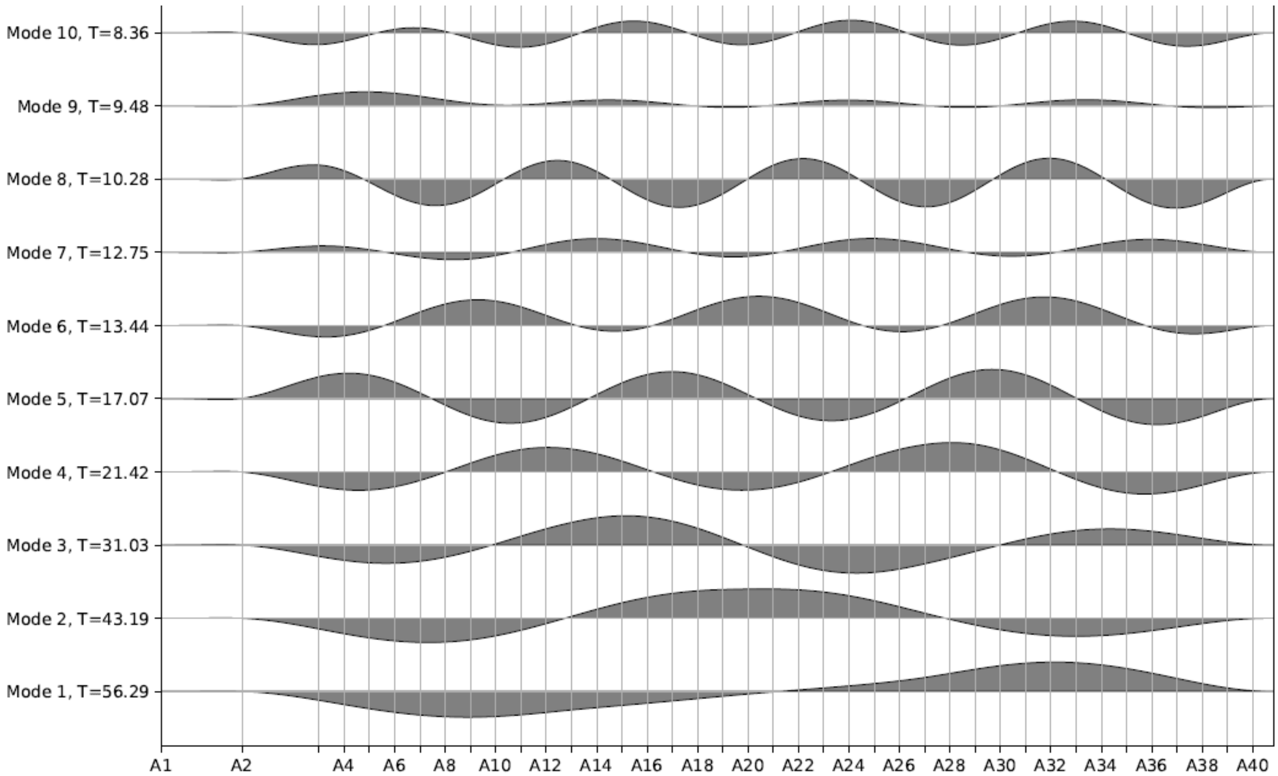

Figure 4-1 Orcaflex transverse eigenmodes for K12_07

4.2 Overview

4.2.1 Sectional forces and moments

The bridge girder response for various load components are shown in Figure 4-2 to Figure 4-7.

Strong-axis bending moments are governed by temperature, wind and swell, whereas weak-axis and torsional moments are governed by permanent loads, traffic and wind sea waves.

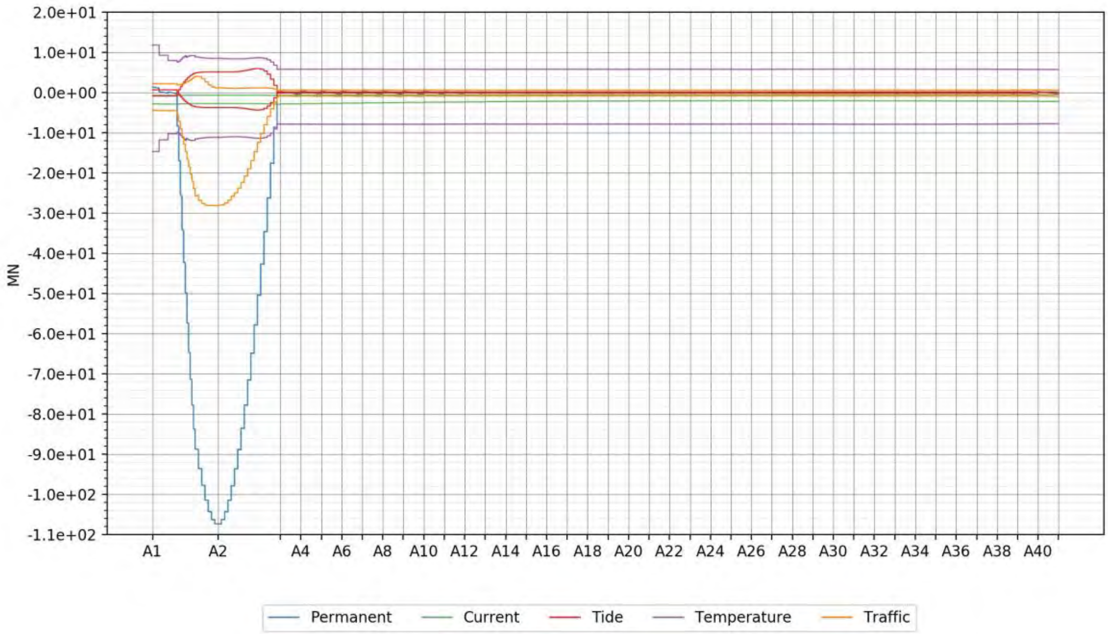

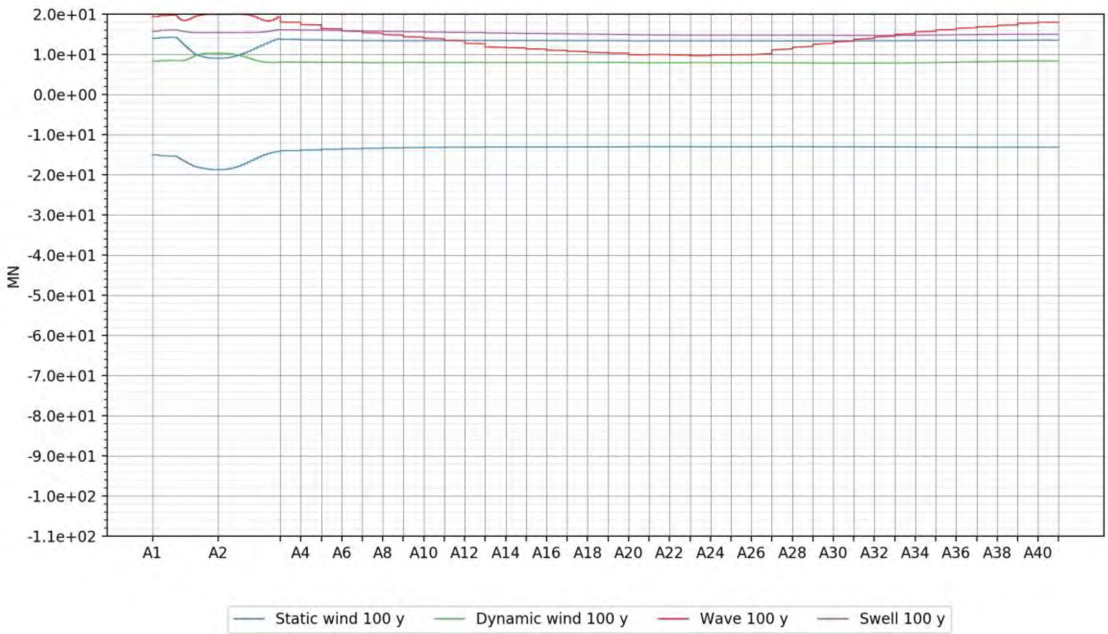

Figure 4-2 Overview of axial force contribution from slowly varying loads (top) and wave and wind loading (bottom) for the K12_07 concept.

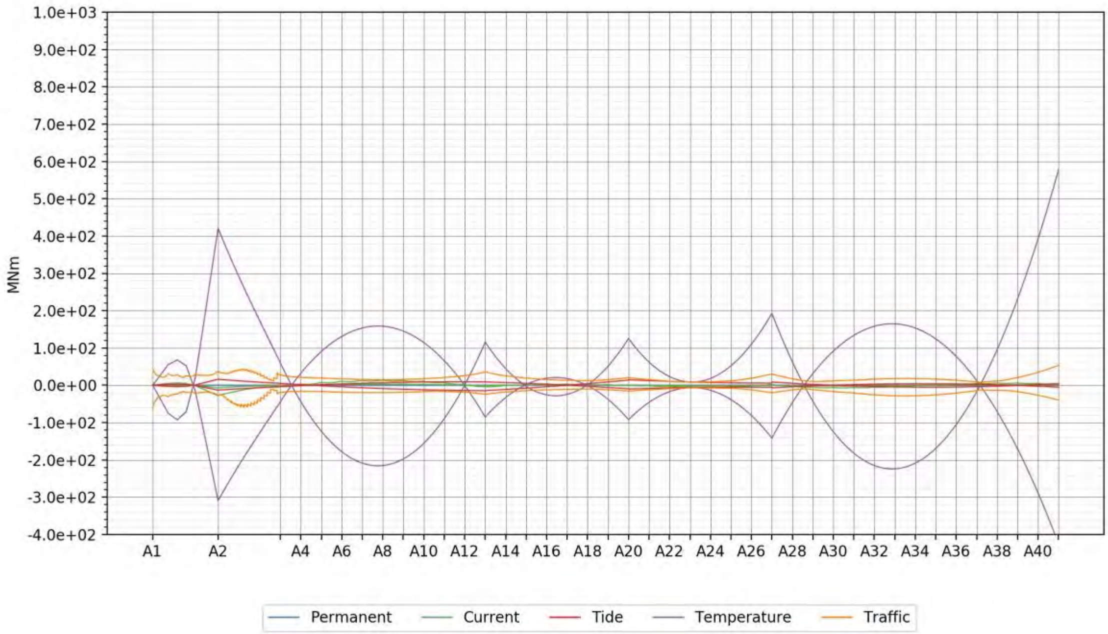

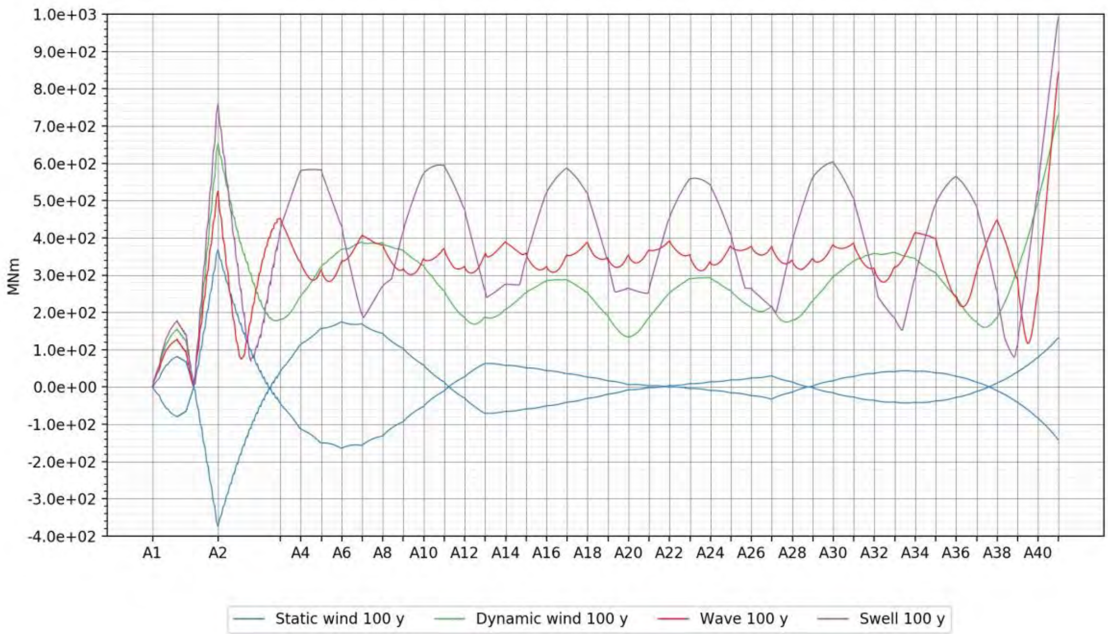

Figure 4-3 Overview of strong-axis bending moment contribution from slowly varying loads (top) and wave and wind loading (bottom) for the K12_07 concept.

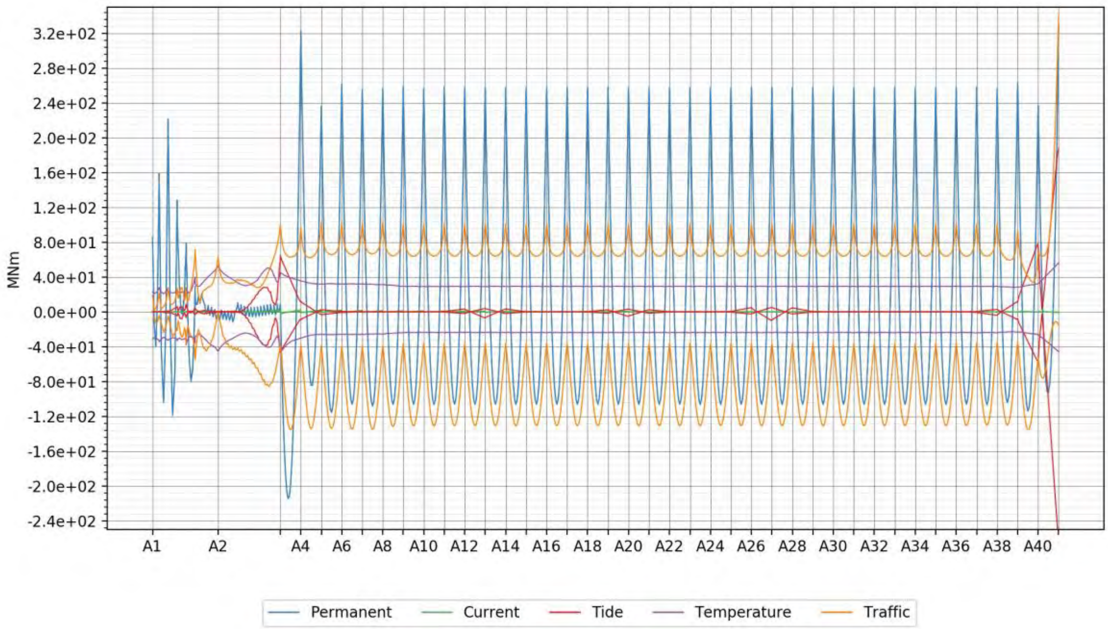

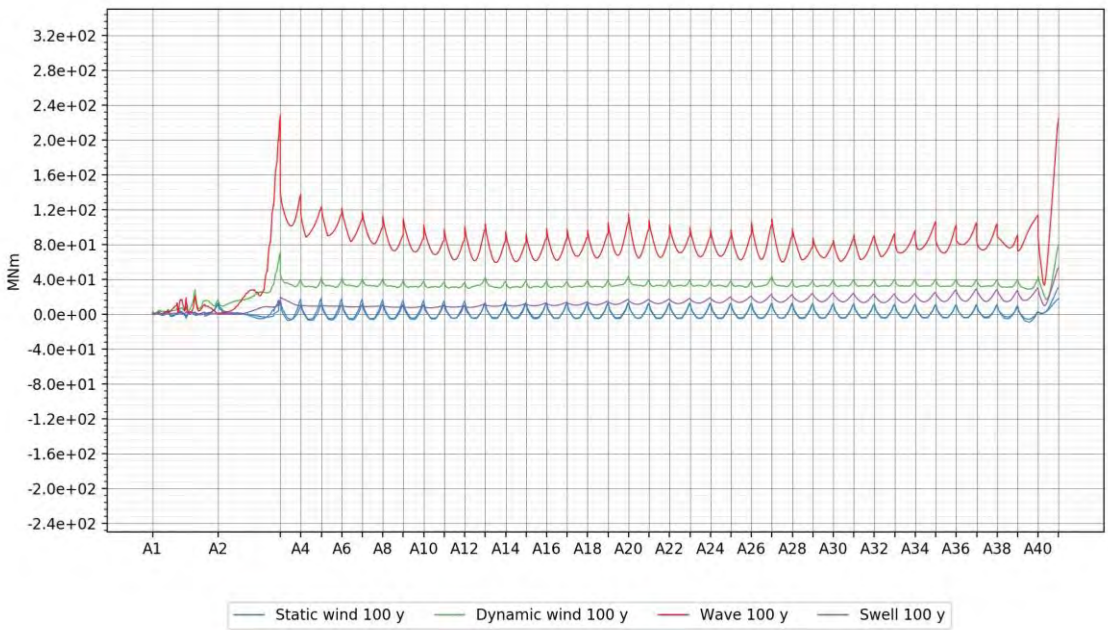

Figure 4-4 Overview of weak-axis bending moment contribution from slowly varying loads (top) and wave and wind loading (bottom) for the K12_07 concept.

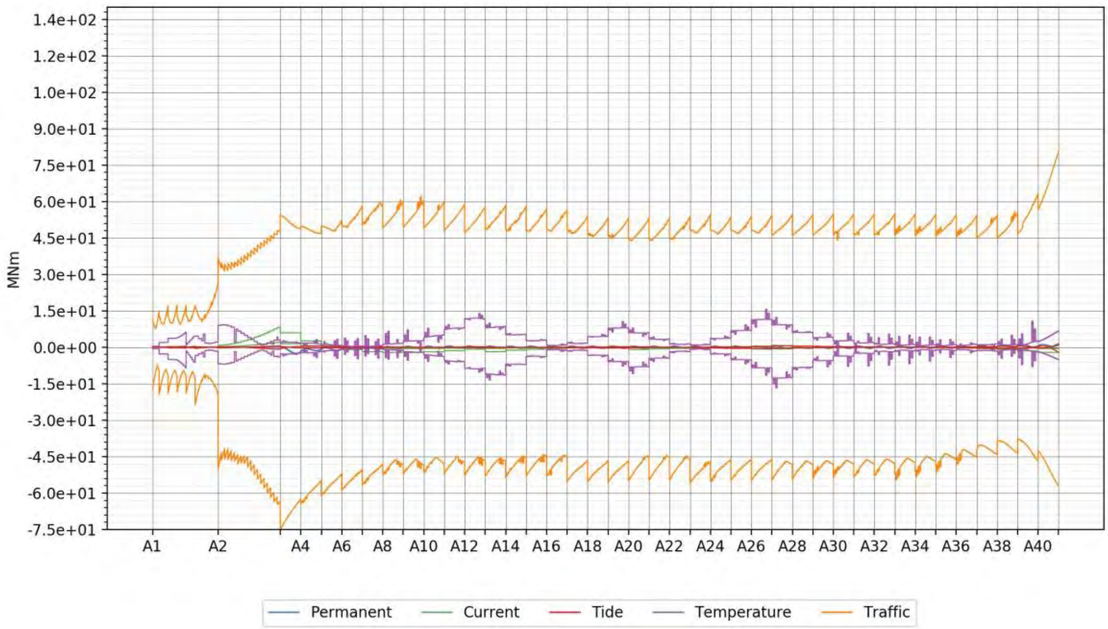

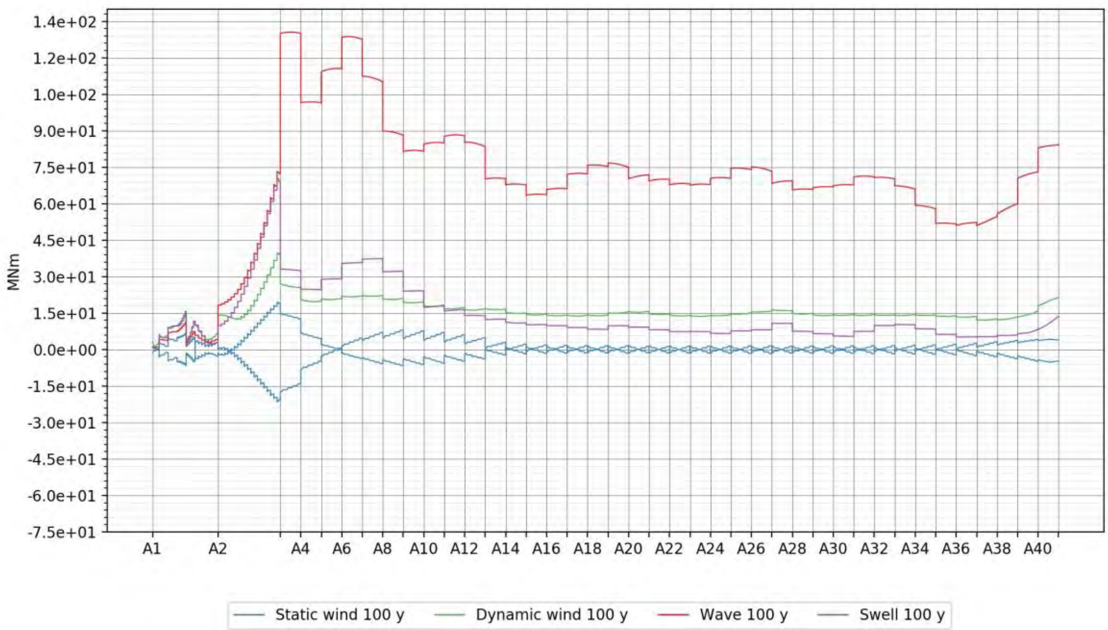

Figure 4-5 Overview of torsional moment contribution from slowly varying loads (top) and wave and wind loading (bottom) for the K12_07 concept.

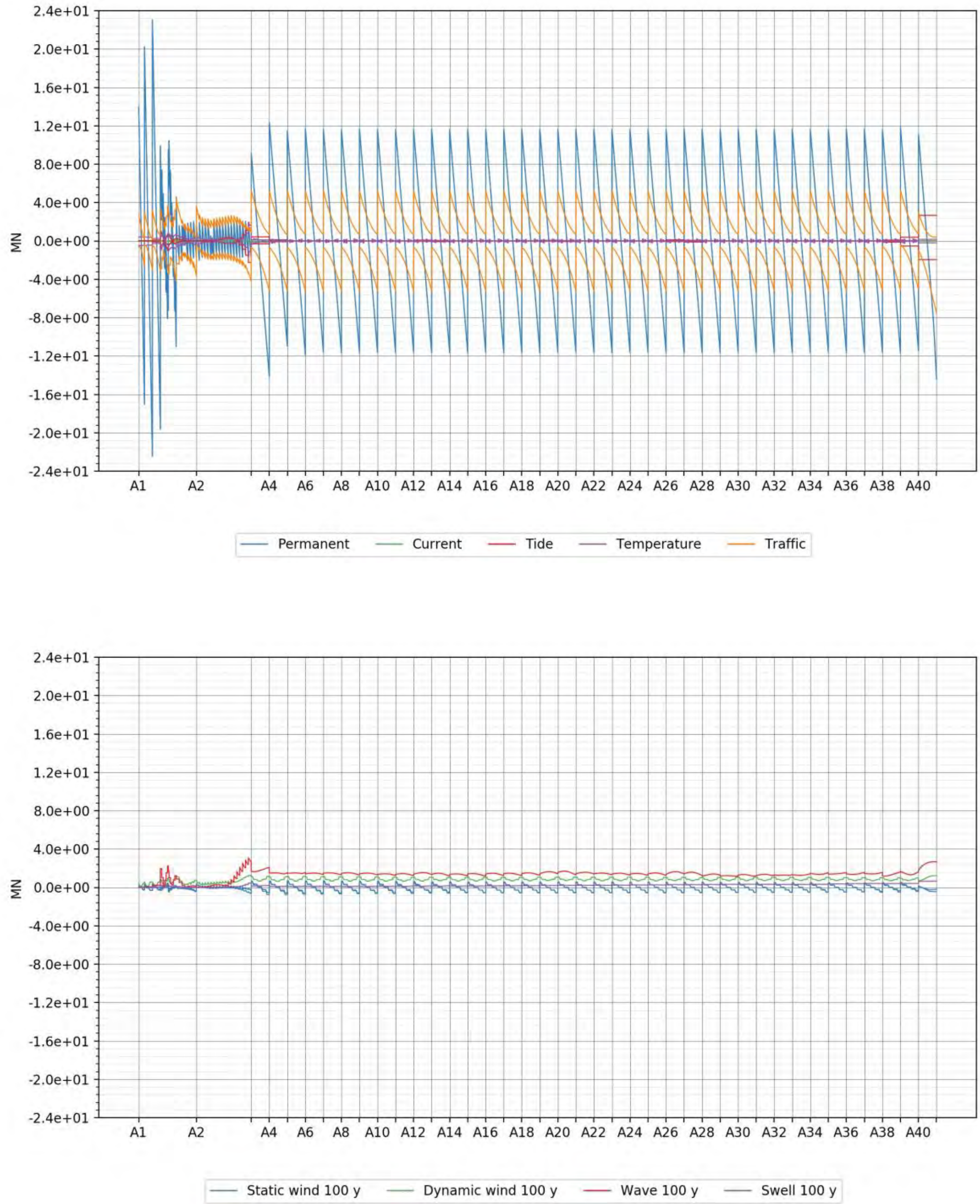

Figure 4-6 Overview of vertical shear force contribution from slowly varying loads (top) and wave and wind loading (bottom) for the K12_07 concept.

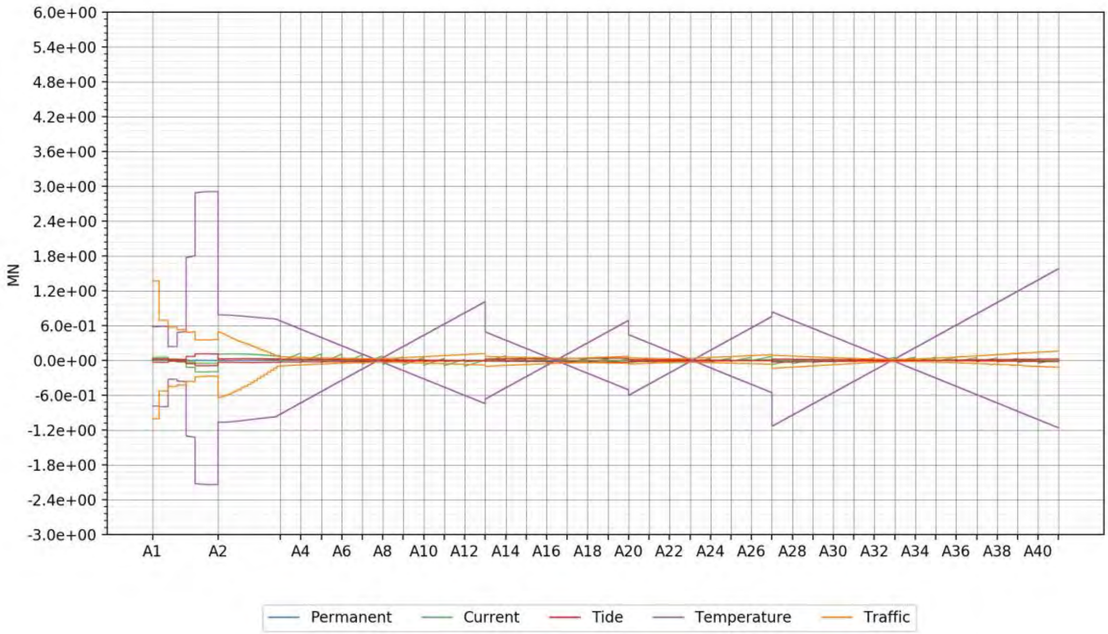

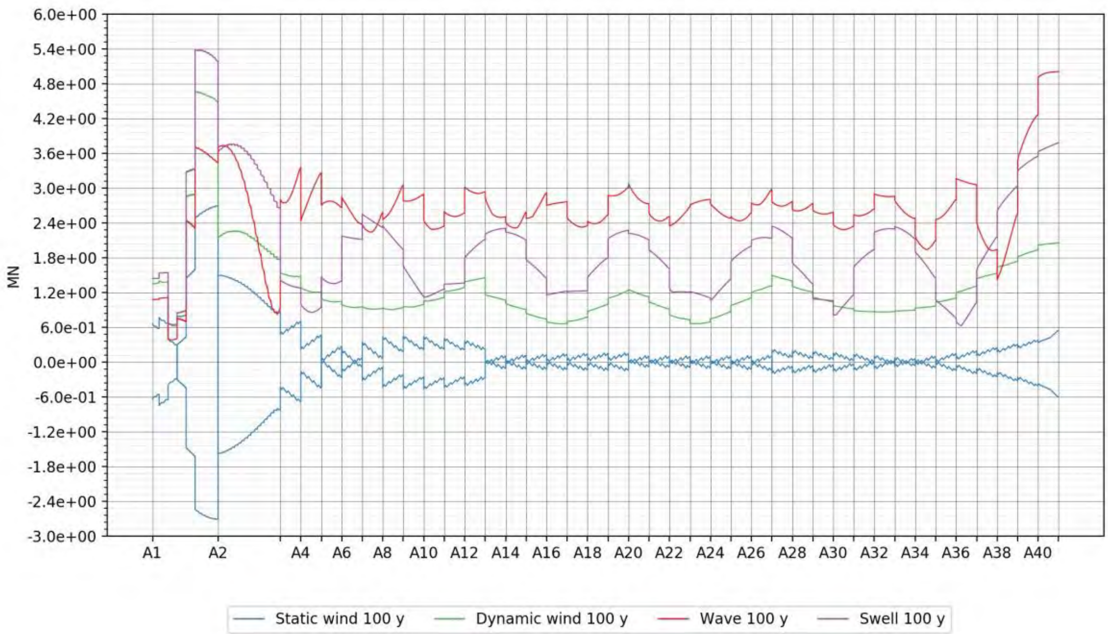

Figure 4-7 Overview of transverse shear force contribution from slowly varying loads (top) and wave and wind loading (bottom) for the K12_07 concept.

4.2.2 Displacements, rotations and accelerations for 100-year return period

Displacements, rotations and accelerations are given in the following for various load components with a 100-year return period.

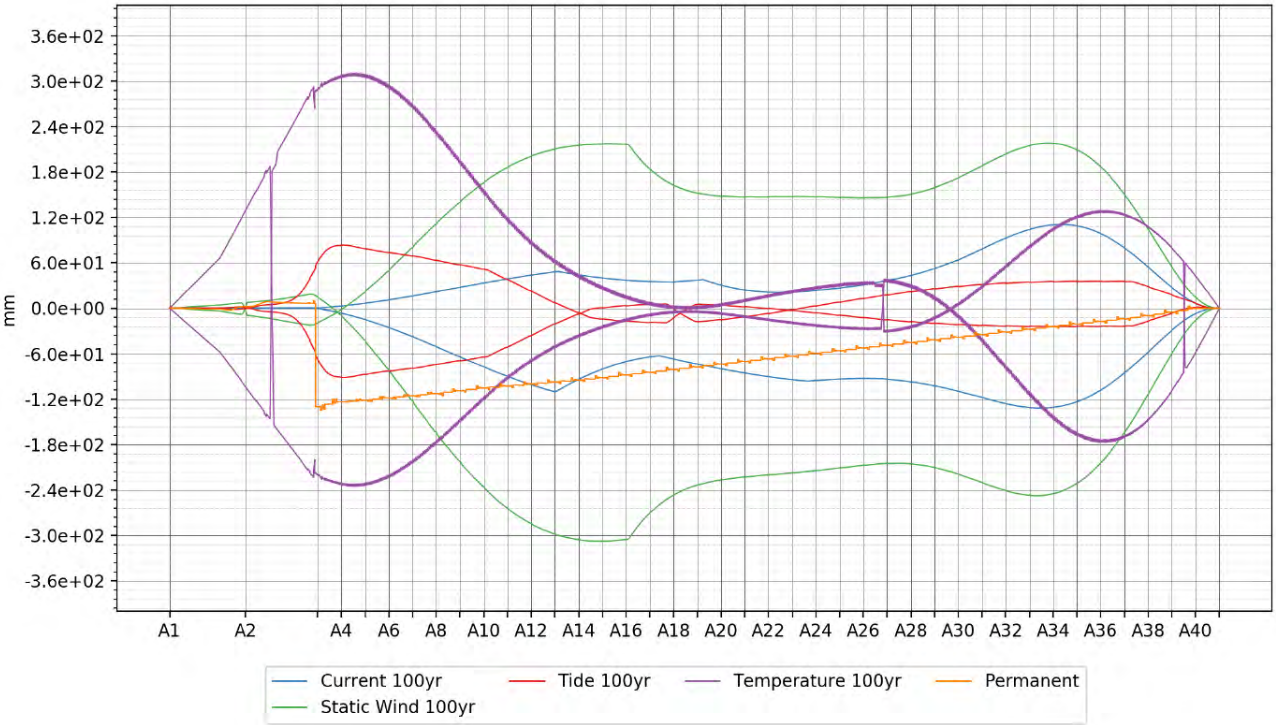

Figure 4-8 Overview of contributions to longitudinal displacements from various load components for the K12_07 concept, 100 year return period.

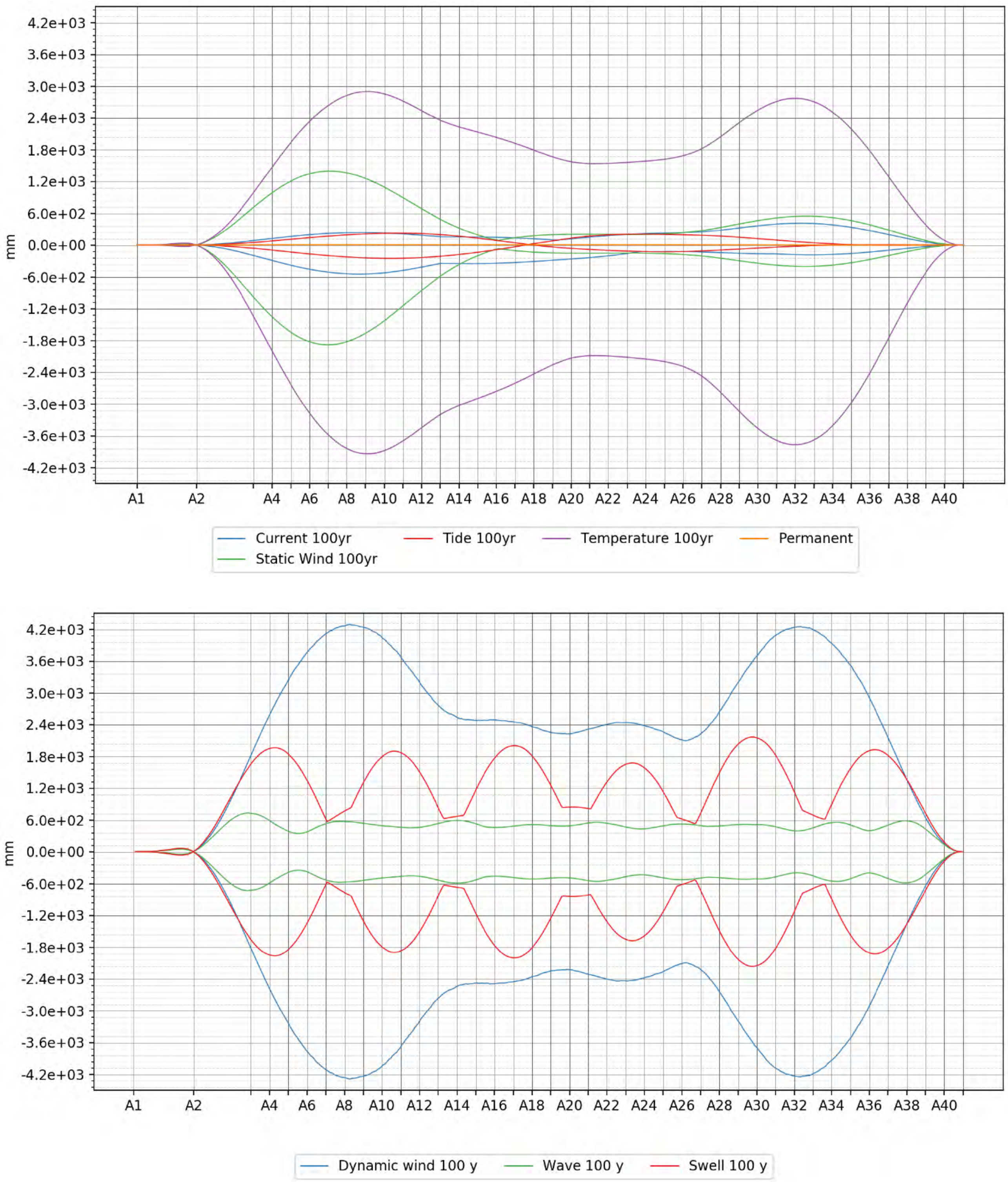

Figure 4-9 Overview of contributions to transverse displacements from slowly varying (top) and wave and wind (bottom) load components for the K12_07 concept, 100 year return period.

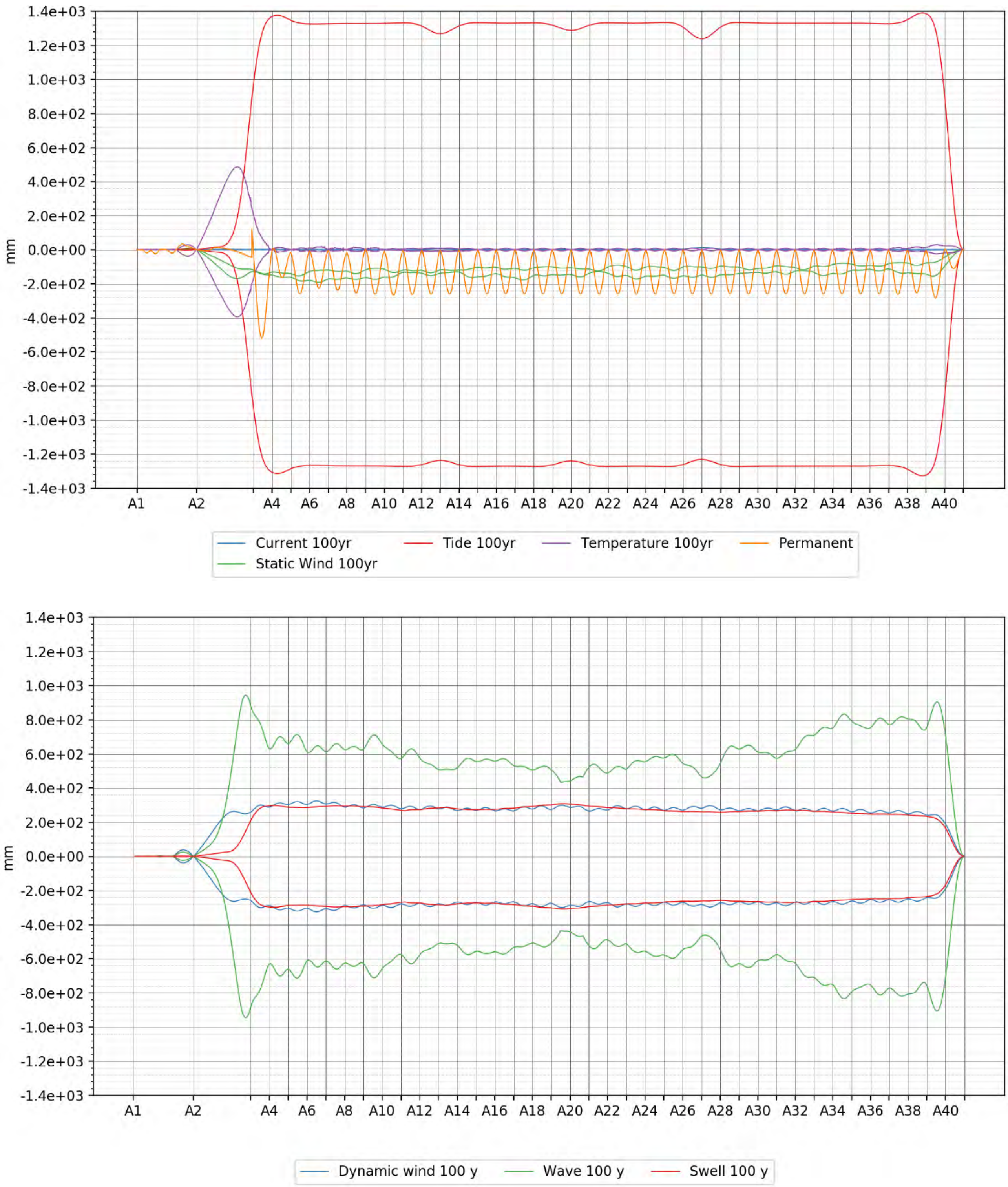

Figure 4-10 Overview of contributions to vertical displacements from slowly varying (top) and wave and wind (bottom) load components for the K12_07 concept, 100 year return period.

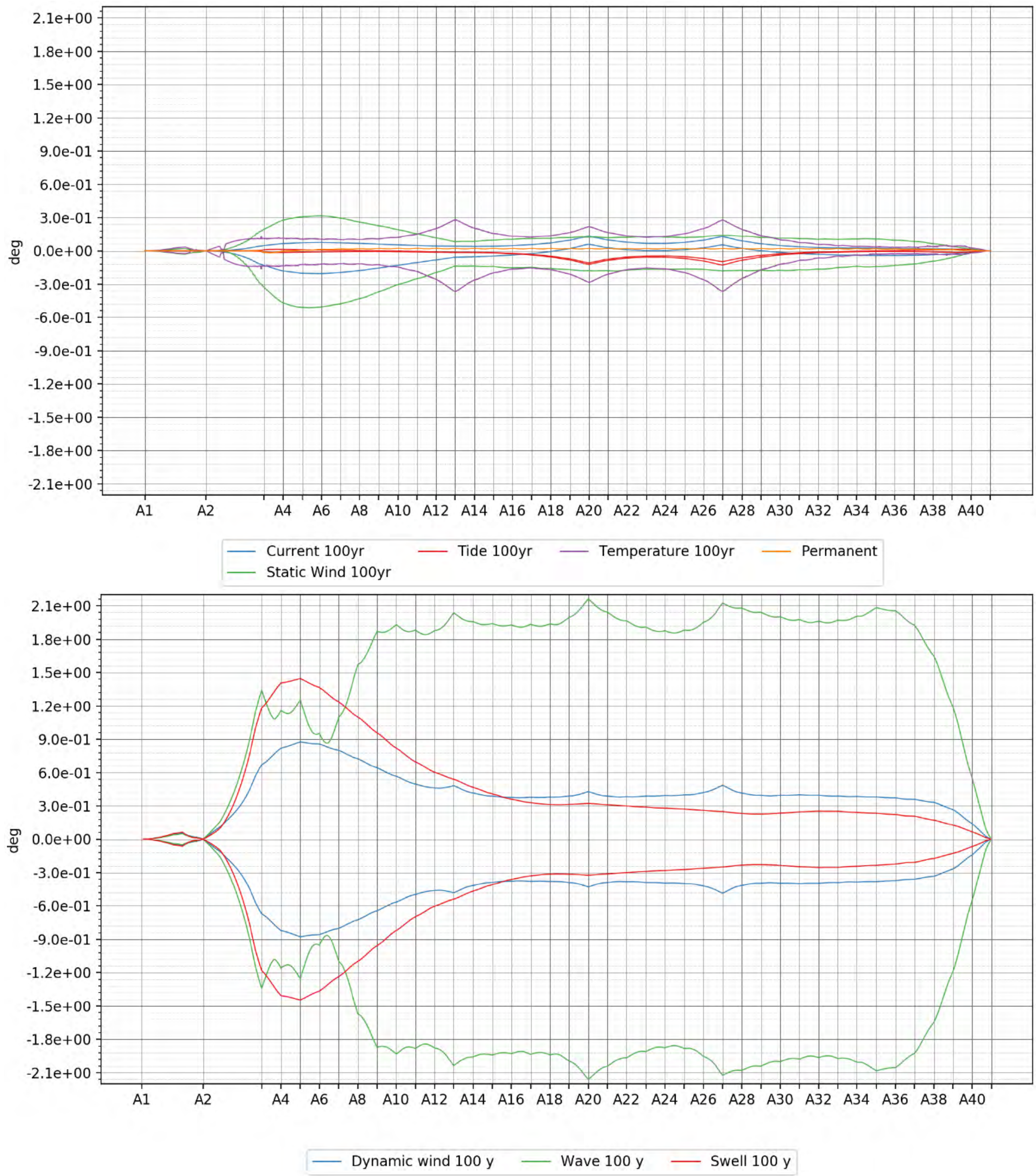

Figure 4-11 Overview of contributions to rotation about the longitudinal bridge axis from slowly varying (top) and wave and wind (bottom) load components for the K12_07 concept, 100 year return period.

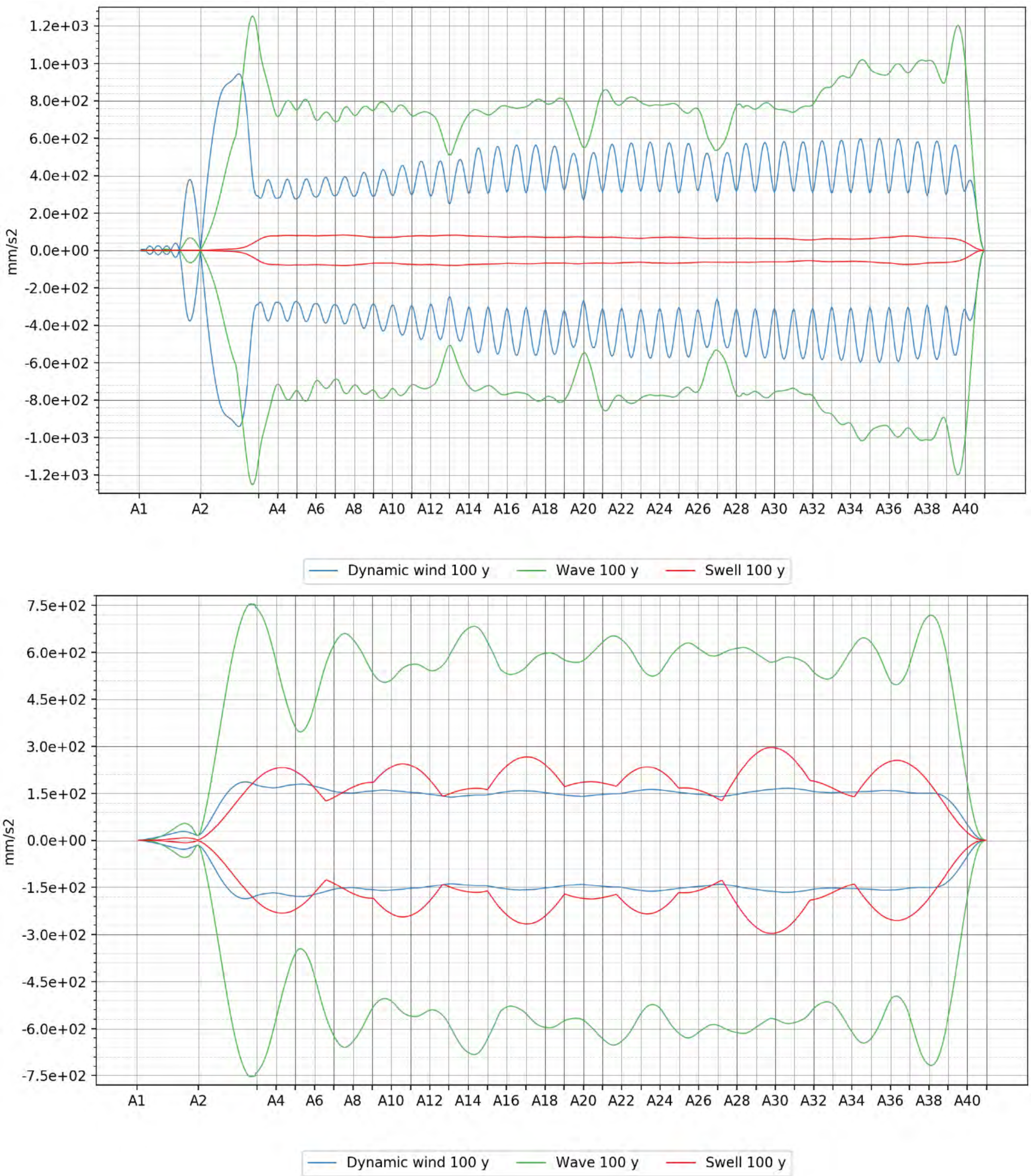

Figure 4-12 Overview of contributions to vertical (top) and transverse (bottom) acceleration from wave and wind load components for the K12_07 concept, 100 year return period.

4.2.3 Displacements, rotations and accelerations for 1 year return period

Displacements, rotations and accelerations are given in the following for various load components with a 1-year return period.

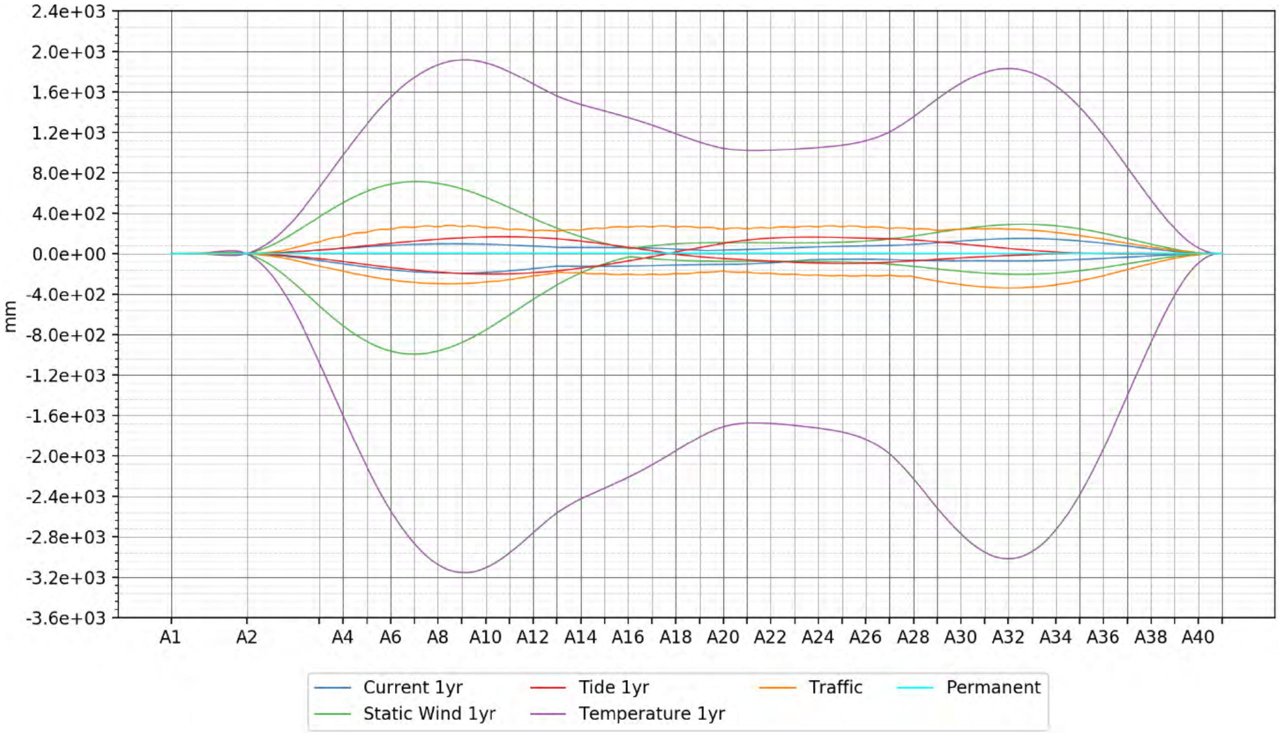

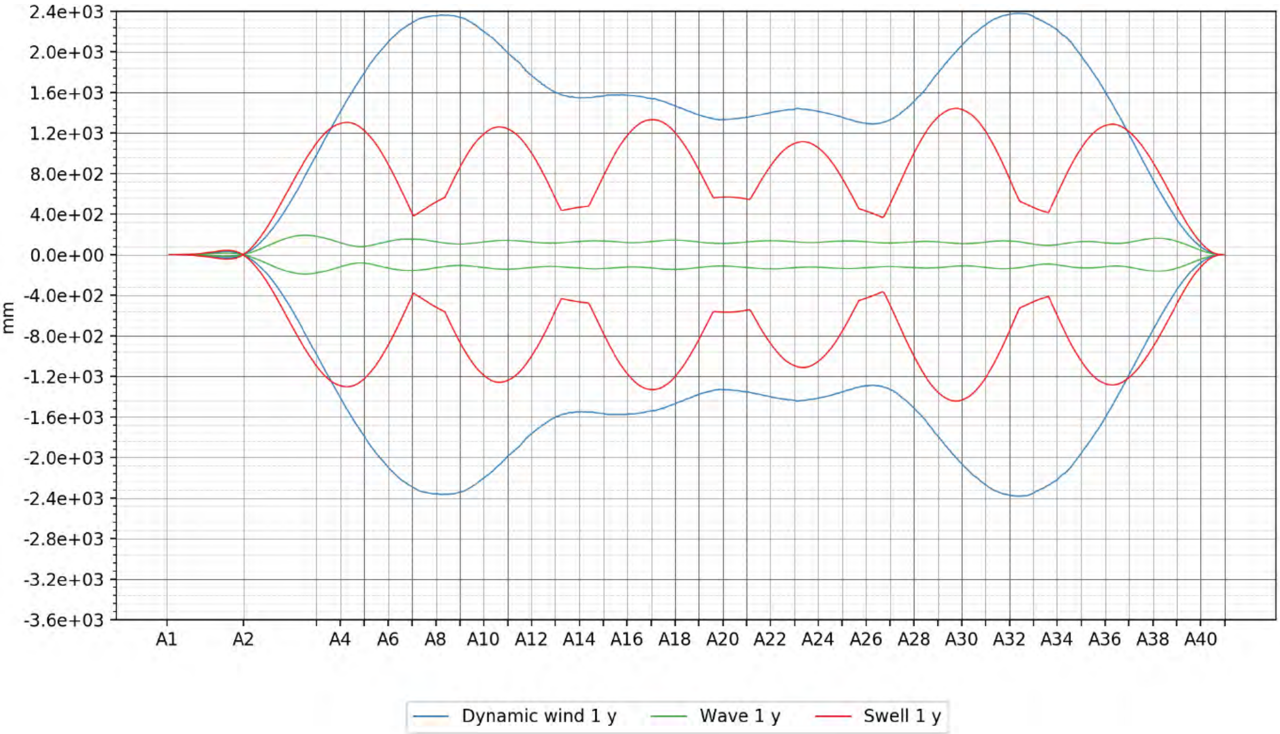

Figure 4-13 Overview of contributions to transverse displacements from slowly varying (top) and wave and wind (bottom) load components for the K12_07 concept, 1 year return period.

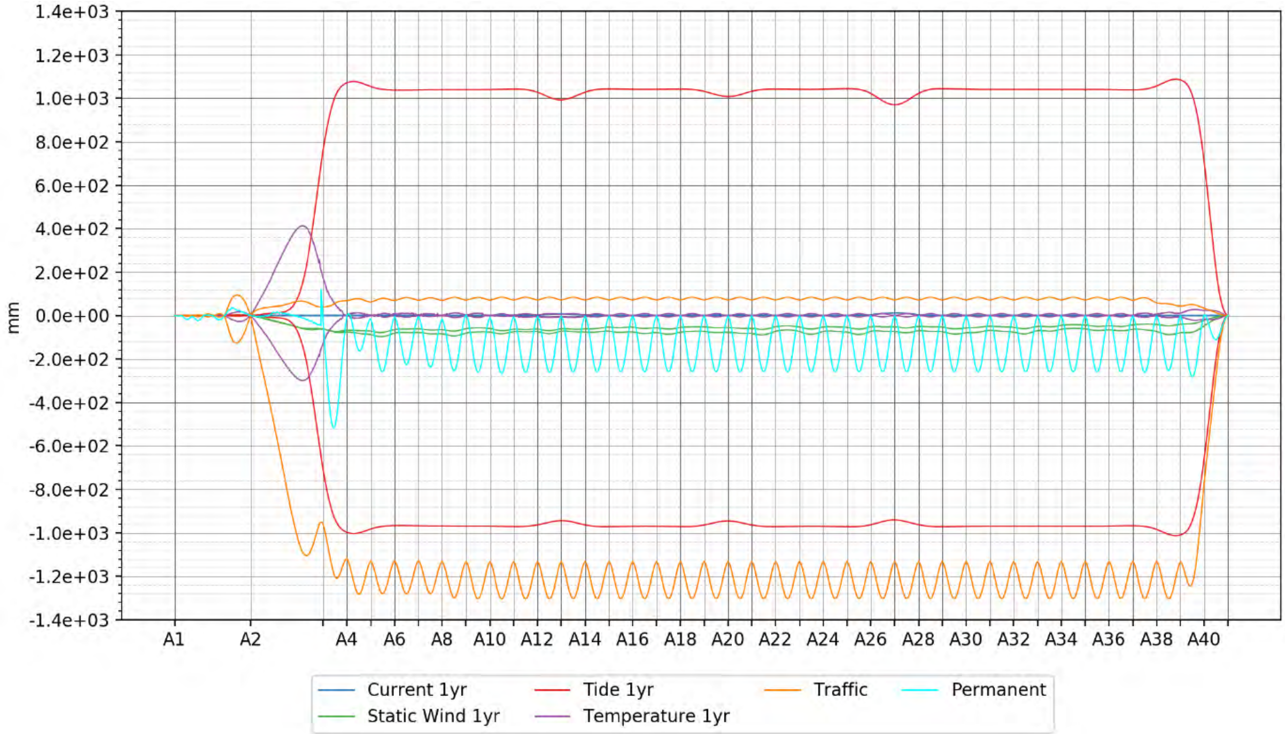

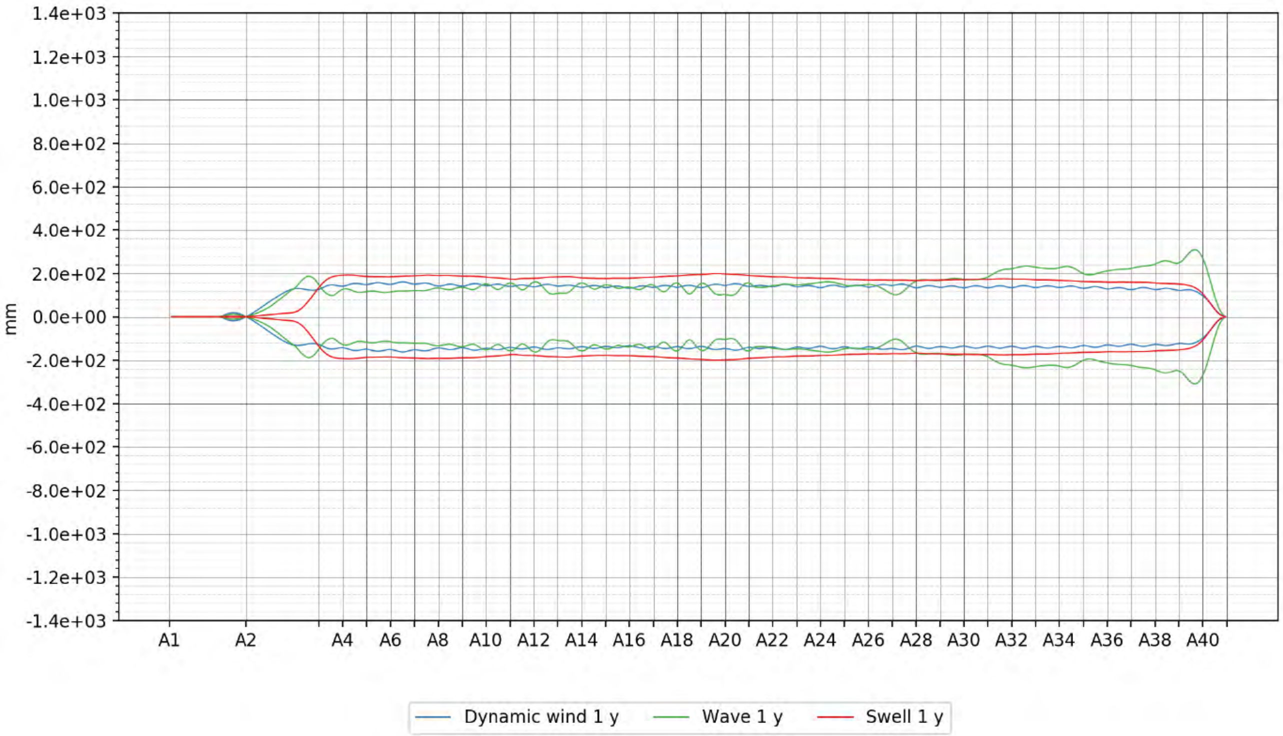

Figure 4-14 Overview of contributions to vertical displacements from slowly varying (top) and wave and wind (bottom) load components for the K12_07 concept, 1 year return period.

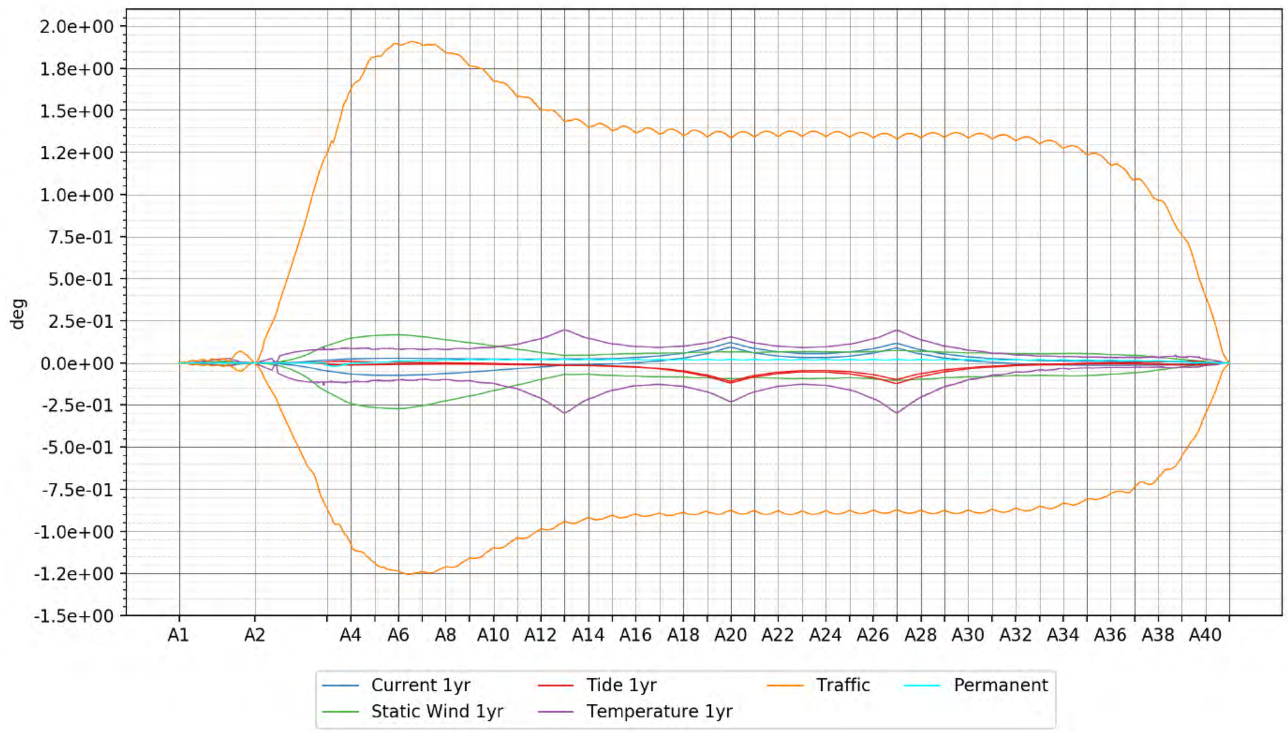

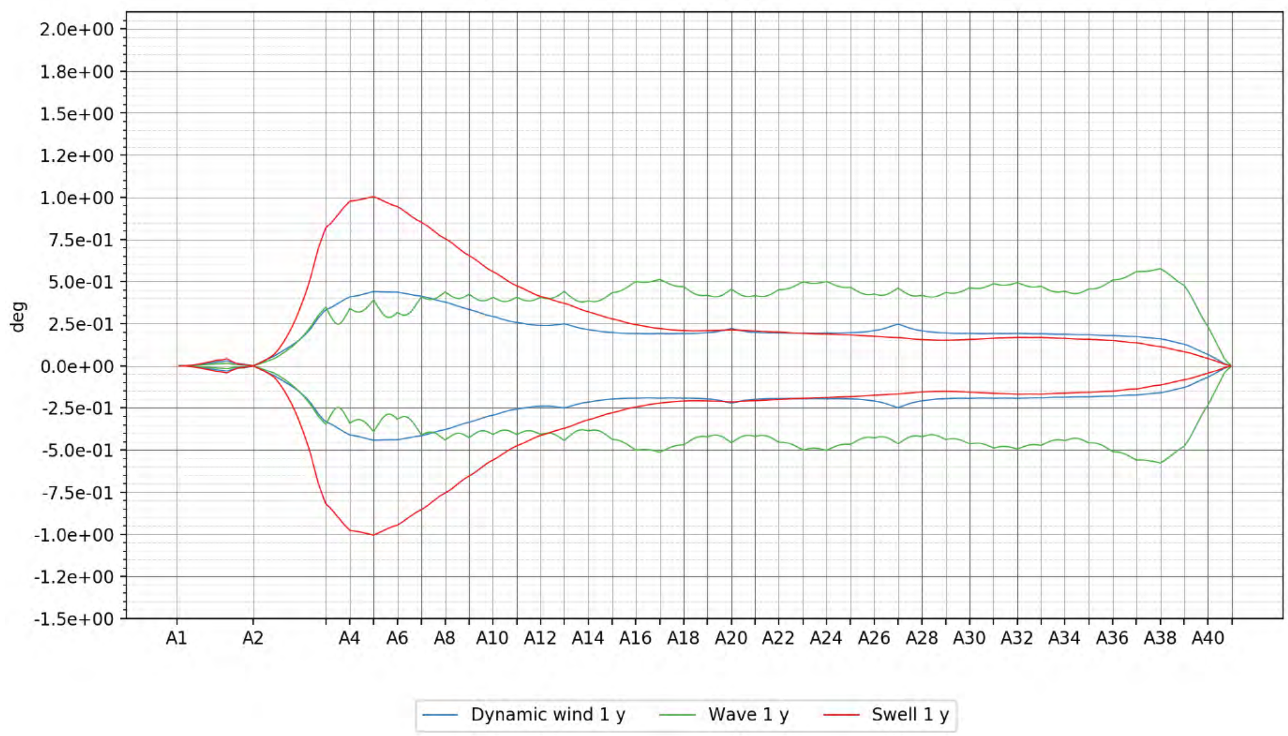

Figure 4-15 Overview of contributions to rotation about the longitudinal bridge axis from slowly varying (top) and wave and wind (bottom) load components for the K12_07 concept, 1 year return period.

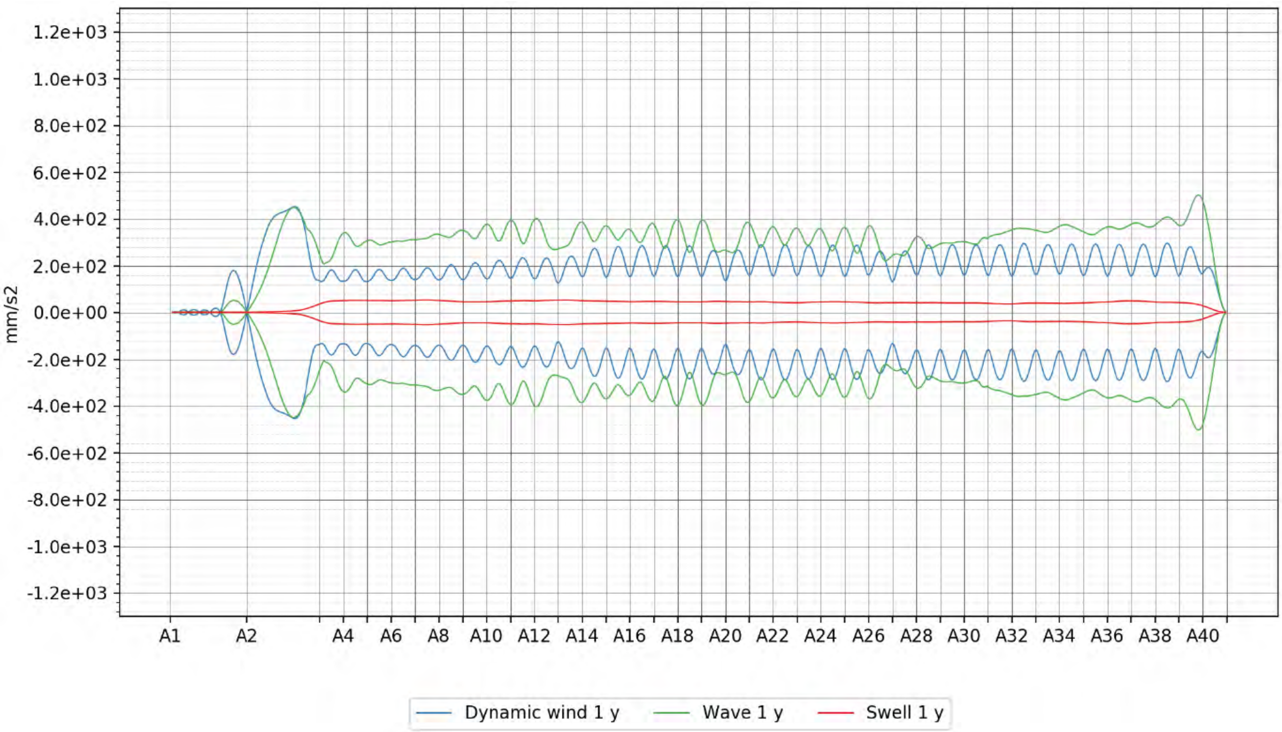

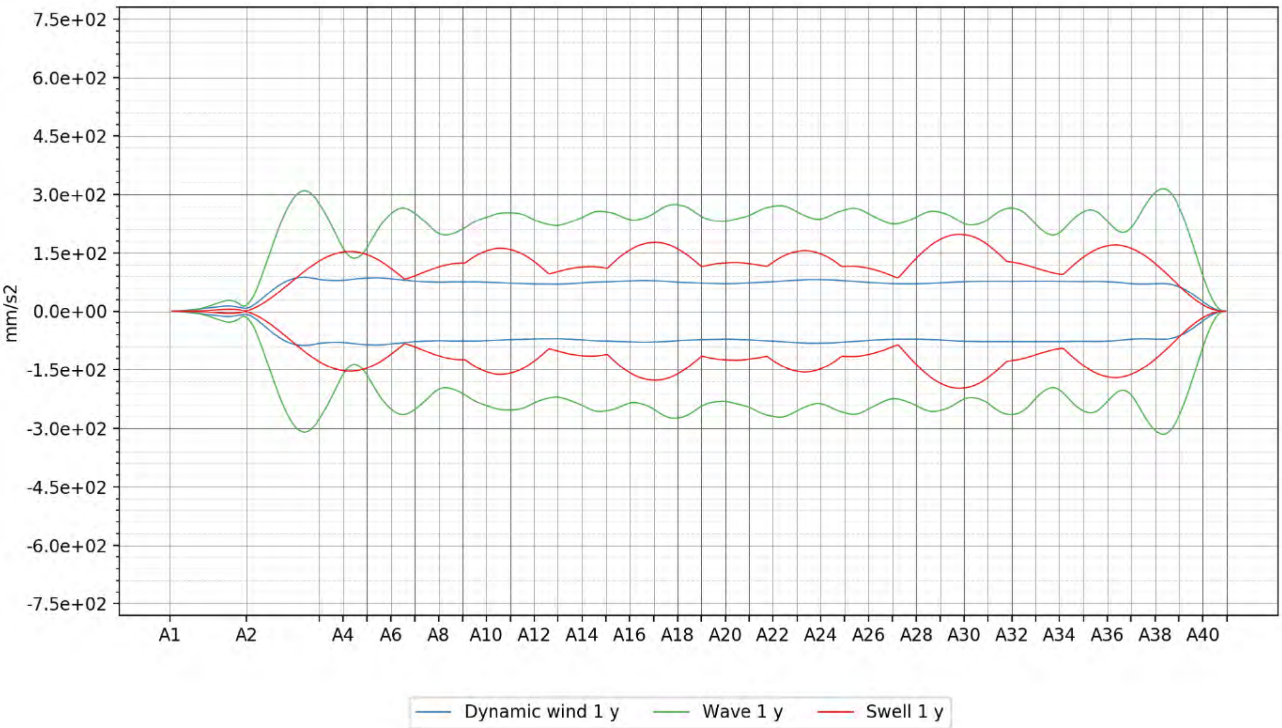

Figure 4-16 Overview of contributions to vertical (top) and transverse (bottom) acceleration from wave and wind load components for the K12_07 concept, 1 year return period.

4.3 RAO plot / wave elevation transfer functions

The RAOs of the bridge girder axial force response, weak axis moment response and strong axis moment response are given in Figure 4-17 to Figure 4-19 that maps the wave elevation process to the response, for more information see [8]. The RAOs are given for each individual wave direction, labelled in the figure. The RAOs are extracted for a point somewhat south of the Northern abutment. Axial RAOs are similar over the bridge, whereas bending RAOs have some variations.

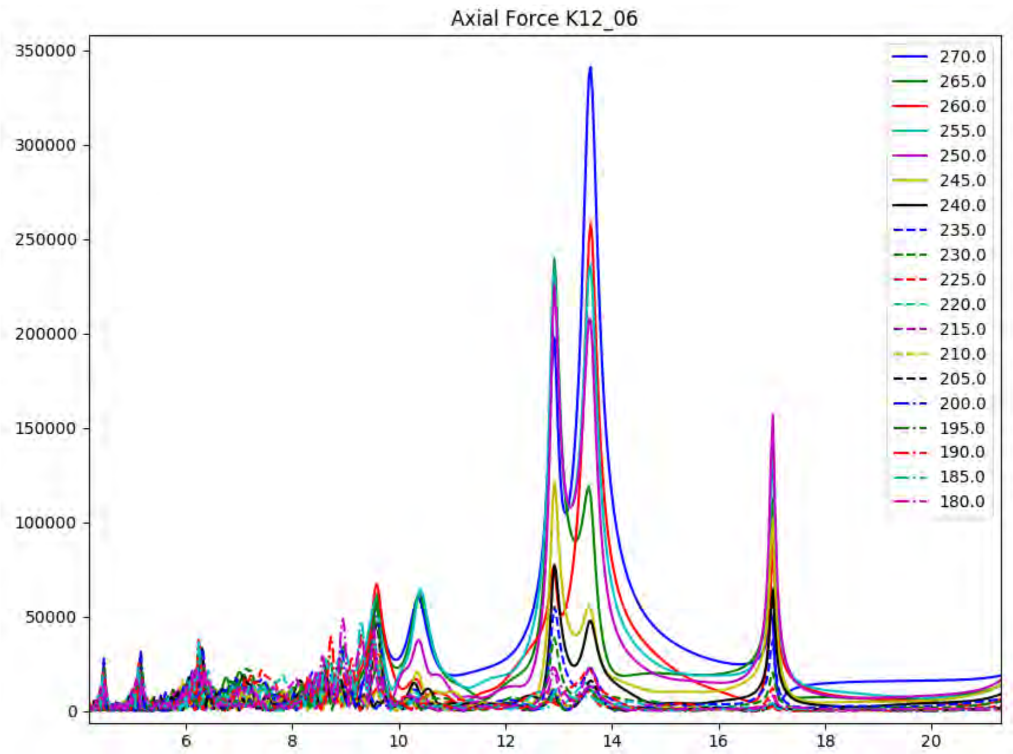

Figure 4-17 RAO of axial force vs. period for K12_06.

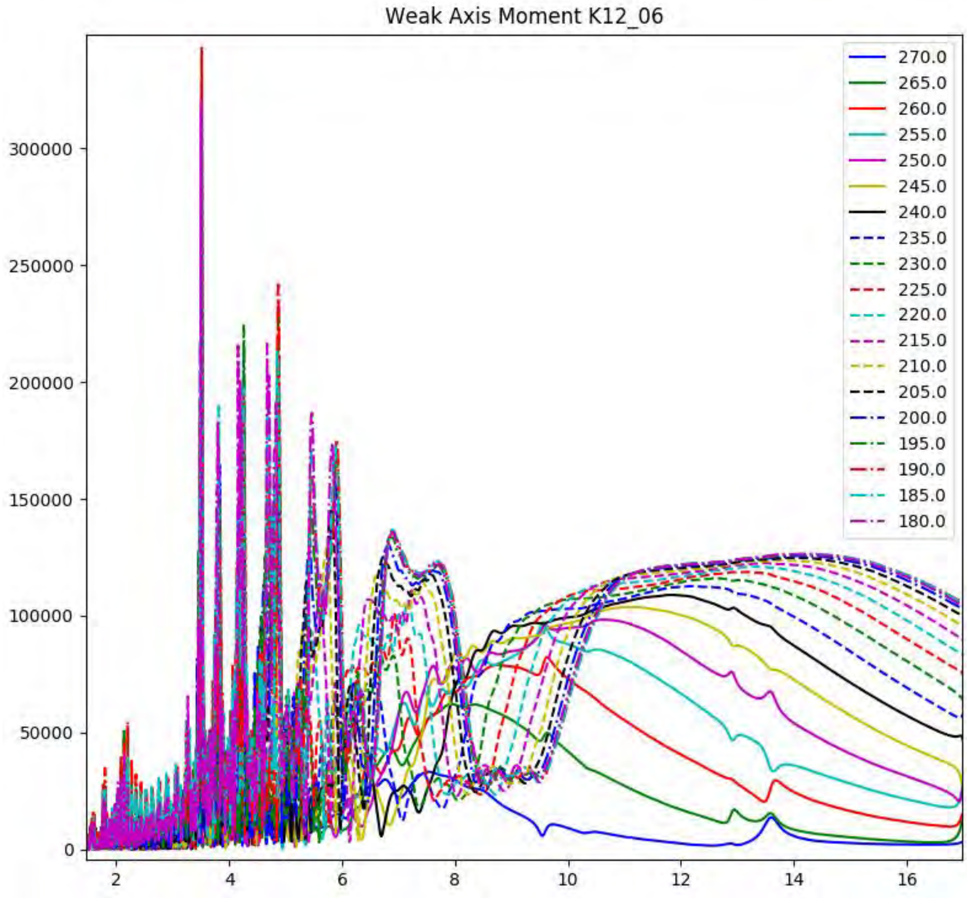

Figure 4-18 RAO of weak-axis moment vs. period for K12_06.

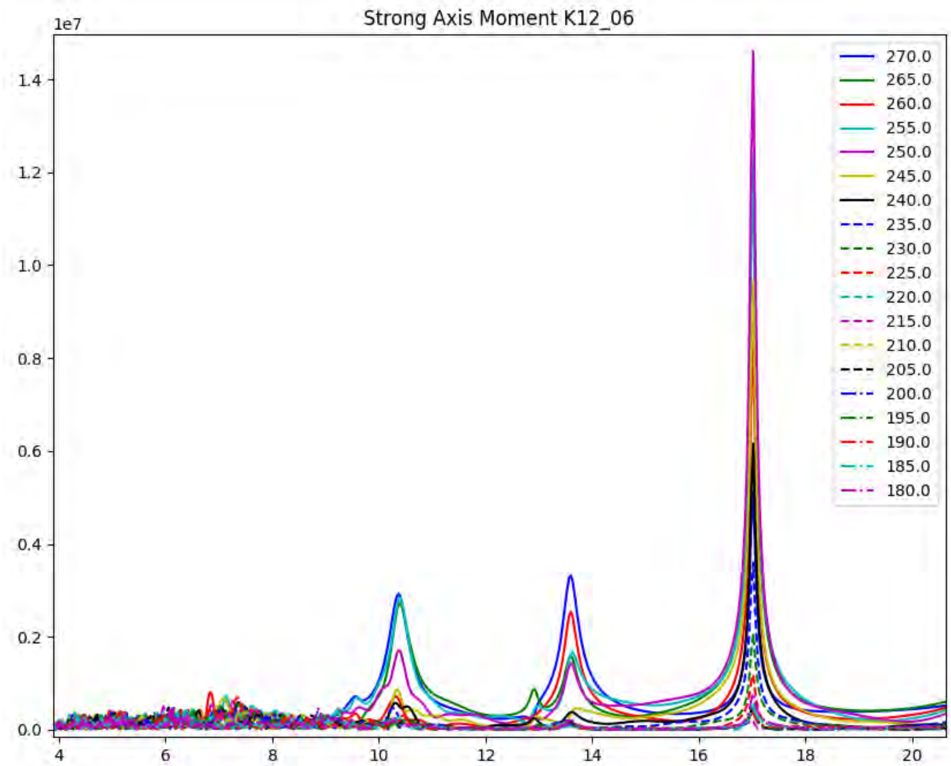

Figure 4-19 RAO of strong-axis moment vs. period for K12_06.

4.4 Dynamic response for individual load components

The dynamic response to various load components is compared in the following sections for K12_07.

All values given in the following are expected max for the given return period.

4.4.1 Static wind 1year

4.4.1.1 Axial force

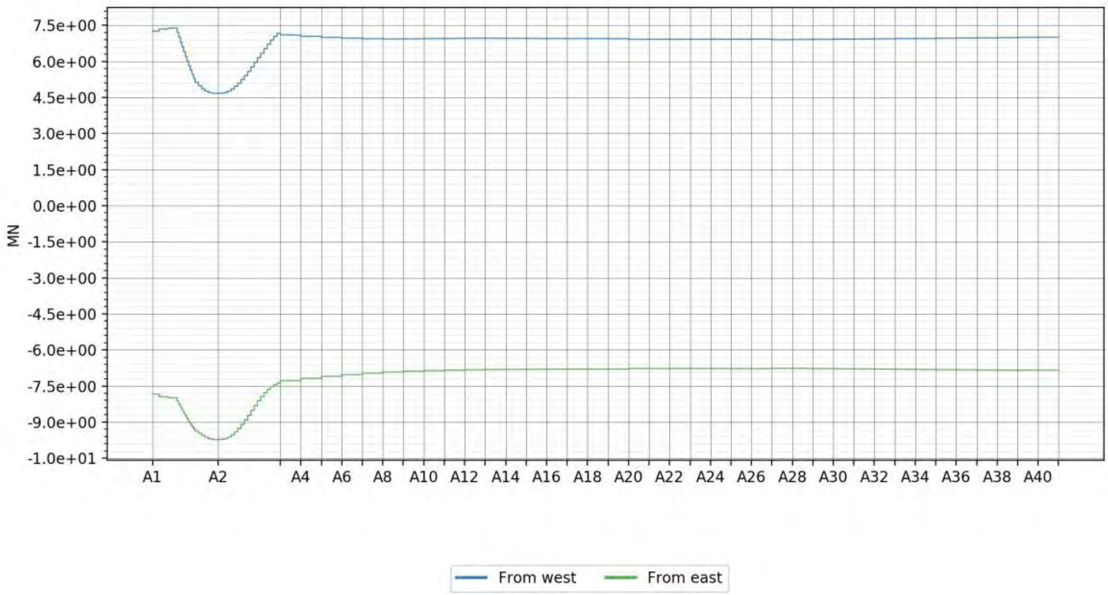

4.4.1.2 Bending moment strong axis

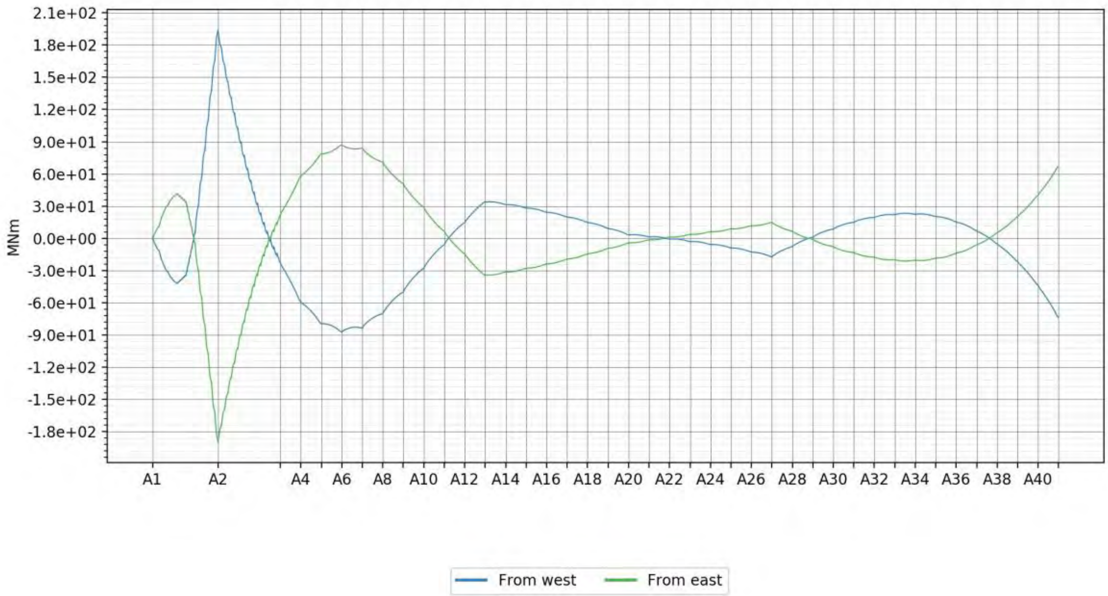

4.4.1.3 Bending moment weak axis

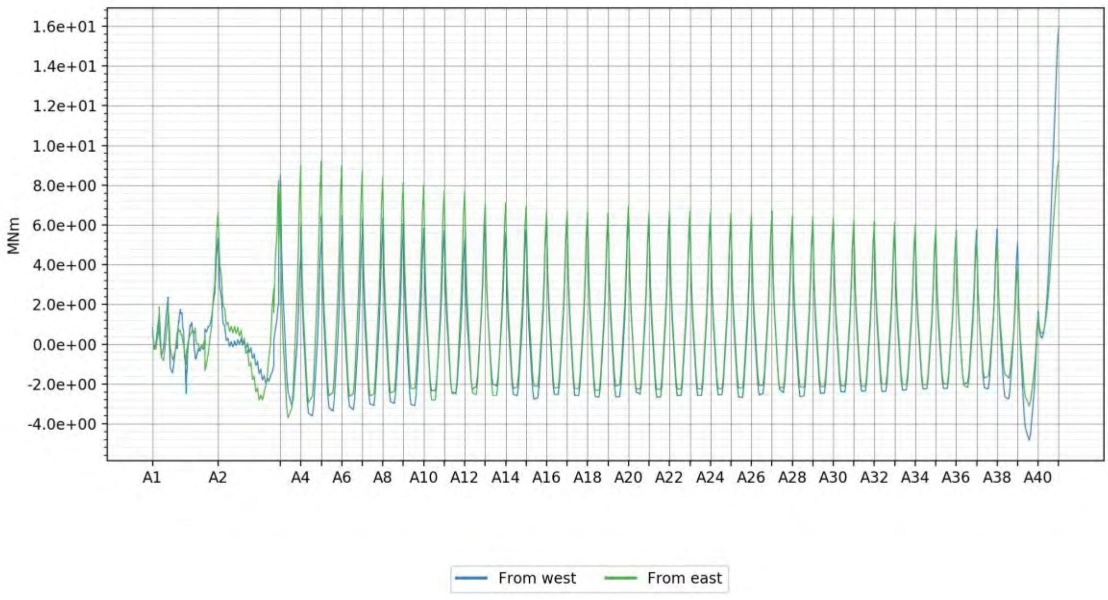

4.4.1.4 Torsional moment

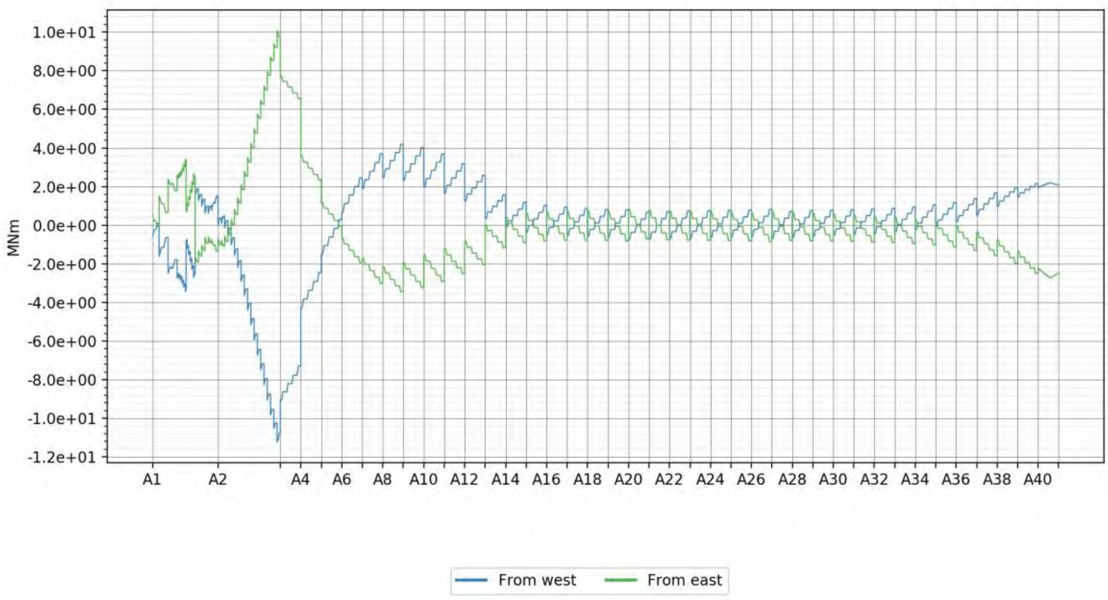

4.4.1.5 Vertical shear force

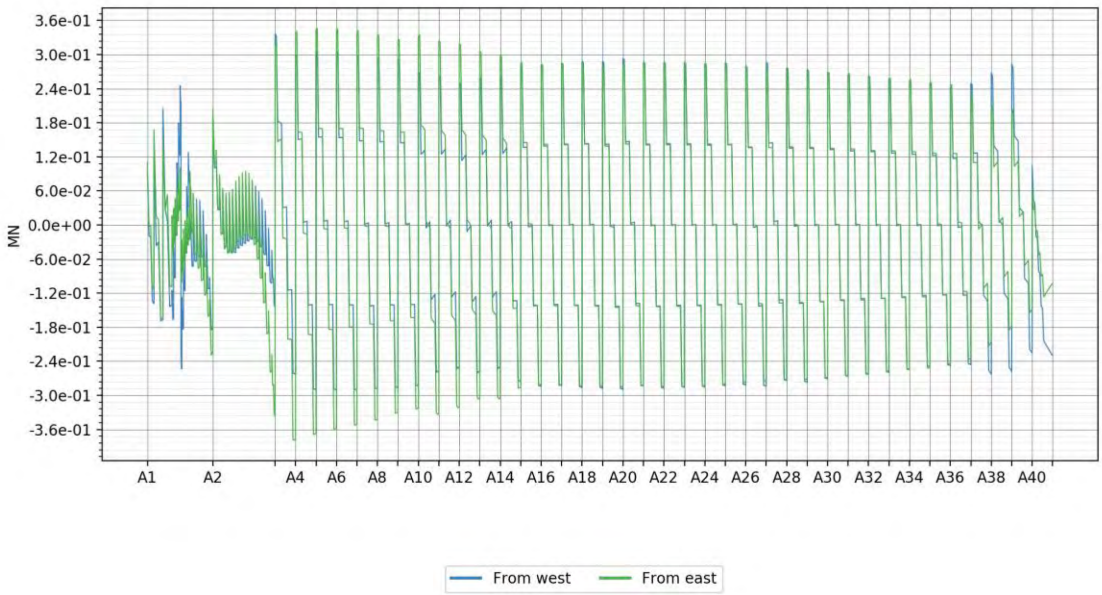

4.4.1.6 Transverse shear force

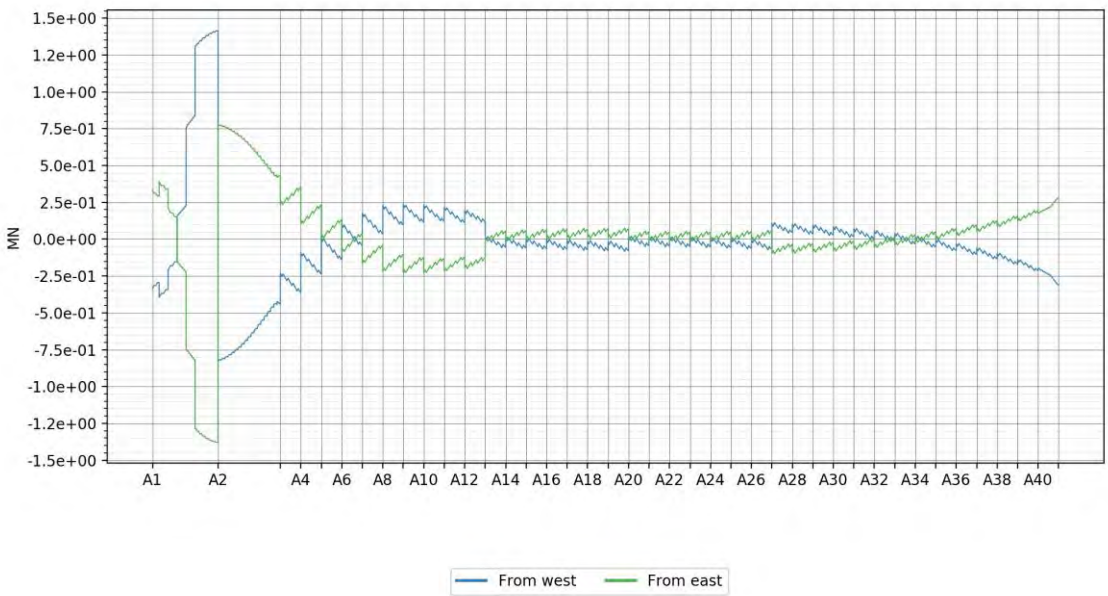

4.4.2 Dynamic wind 1 year

4.4.2.1 Axial force

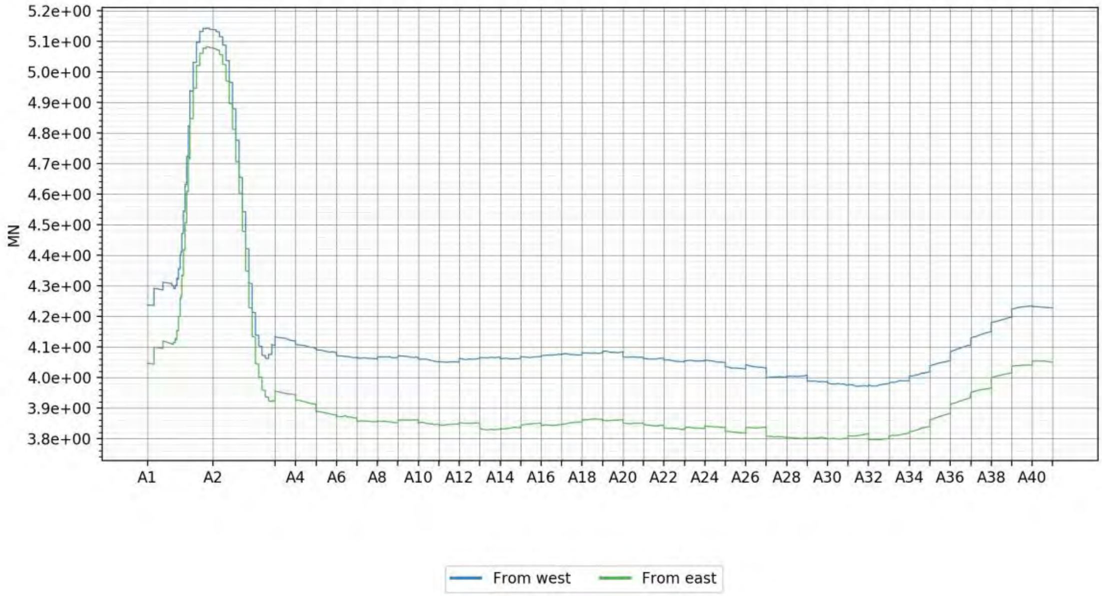

4.4.2.2 Bending moment strong axis

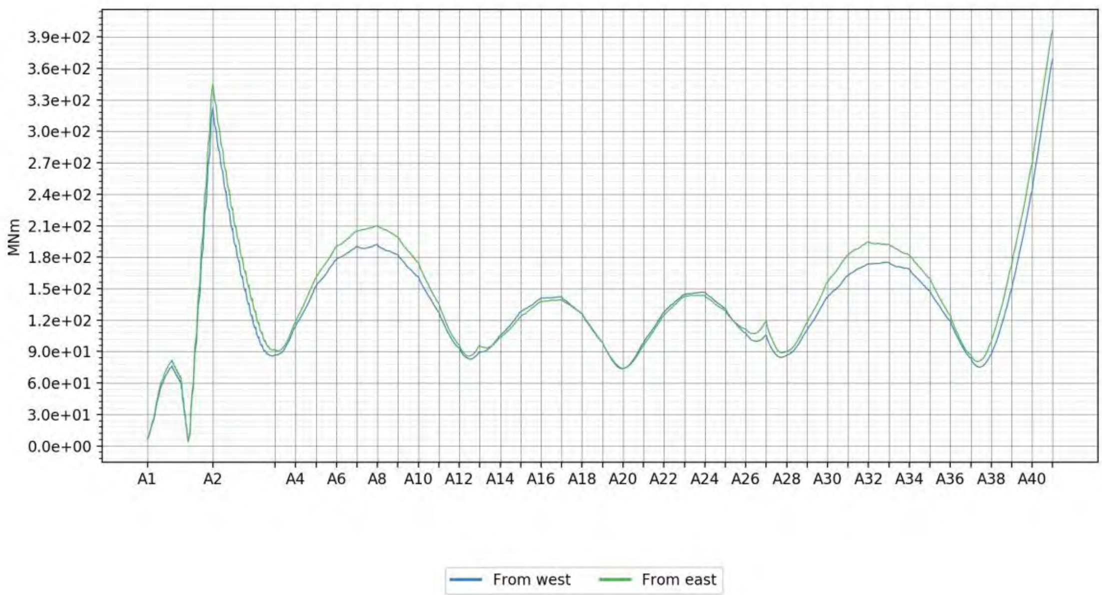

4.4.2.3 Bending moment weak axis

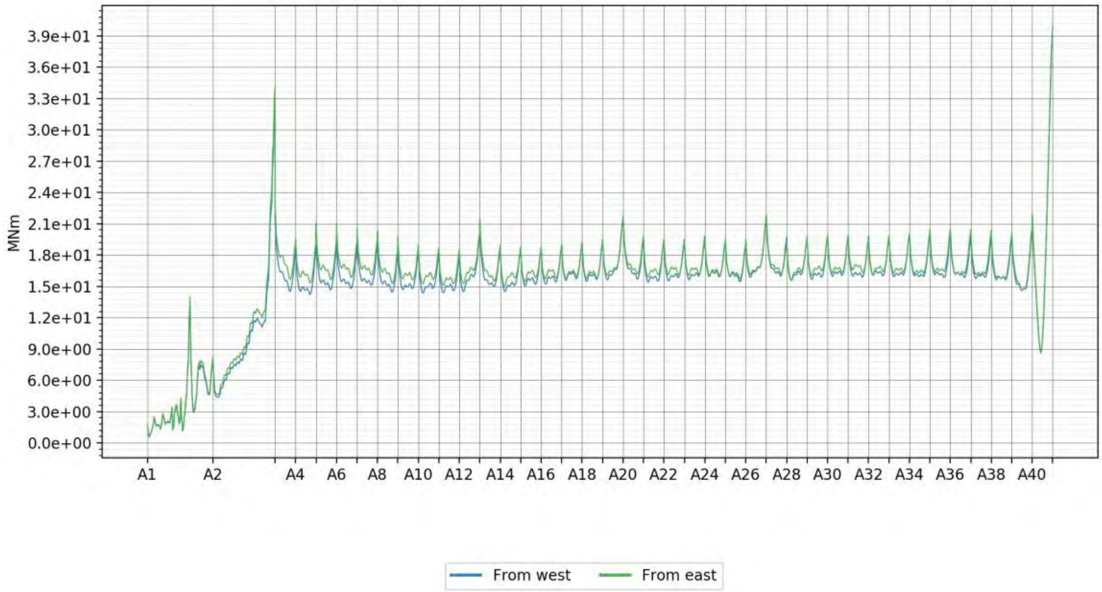

4.4.2.4 Torsional moment

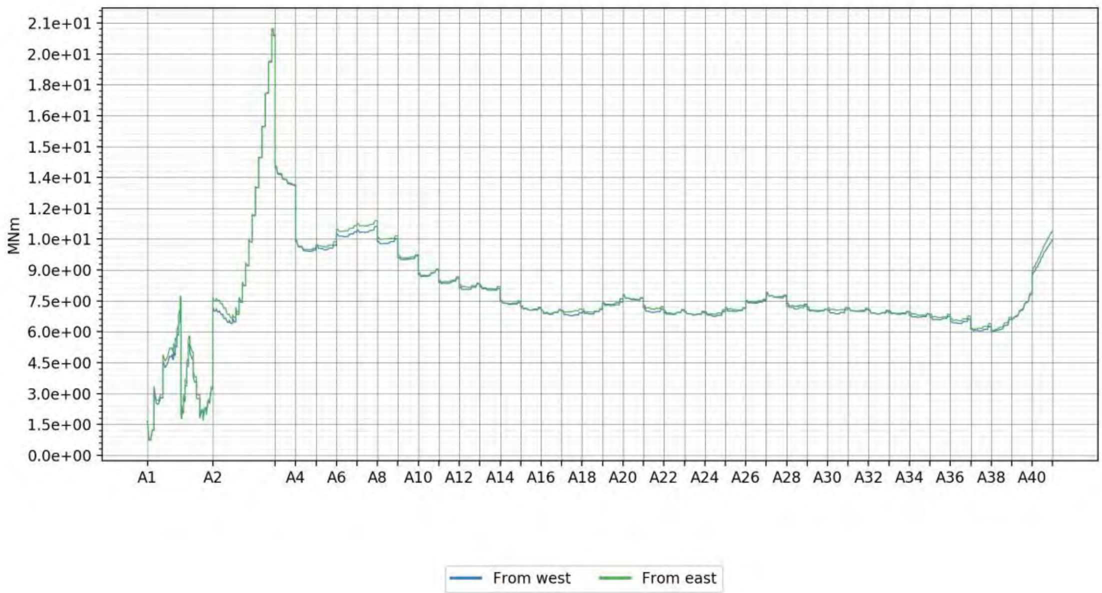

4.4.2.5 Vertical shear force

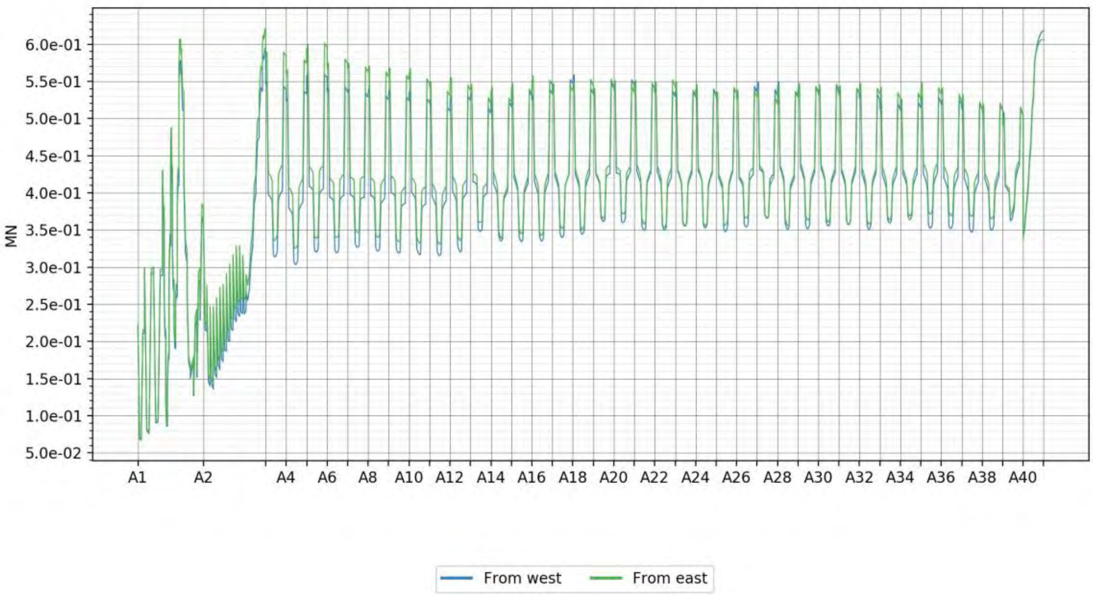

4.4.2.6 Transverse shear force

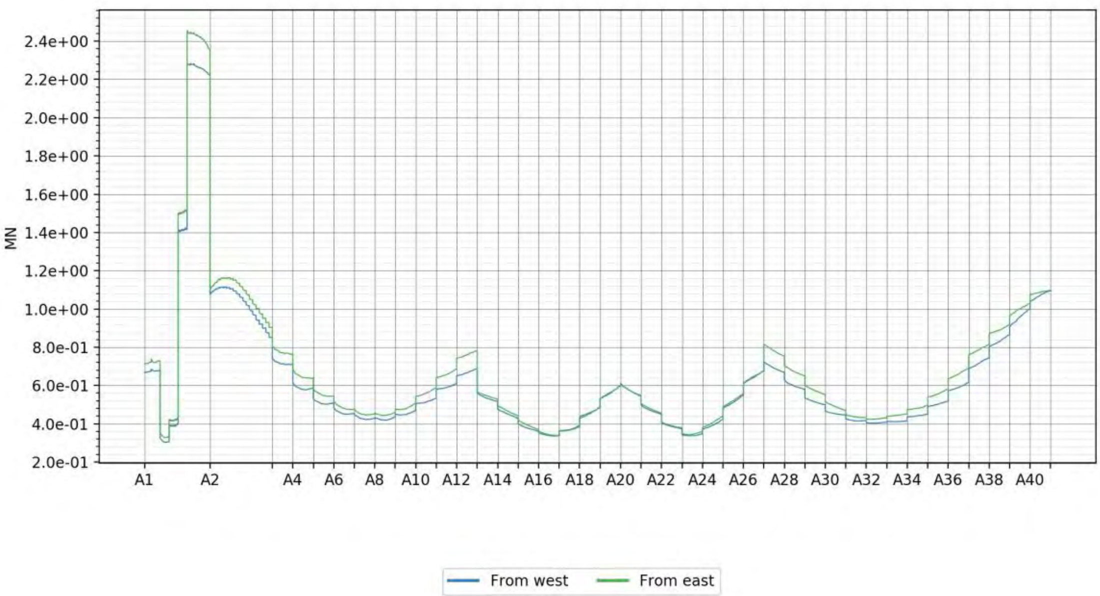

4.4.3 Wave 1 year

4.4.3.1 Axial force

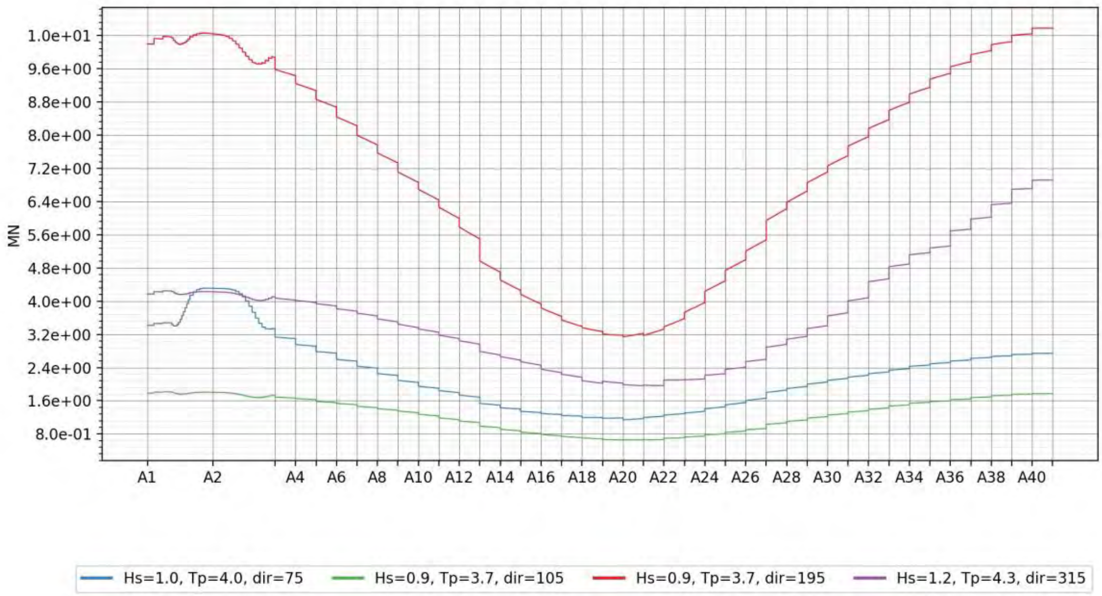

4.4.3.2 Bending moment strong axis

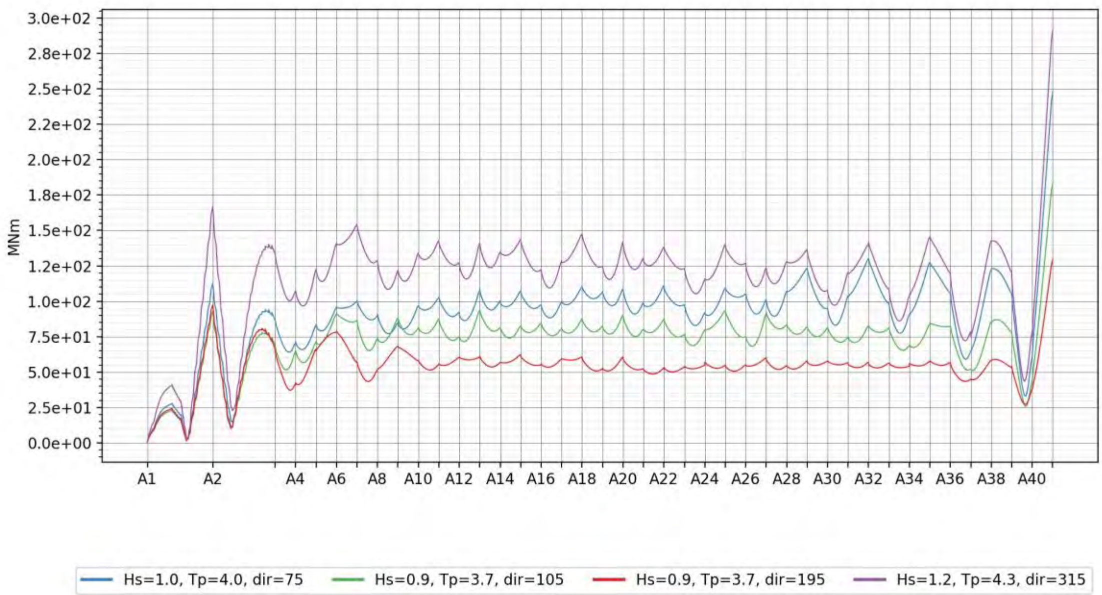

4.4.3.3 Bending moment weak axis

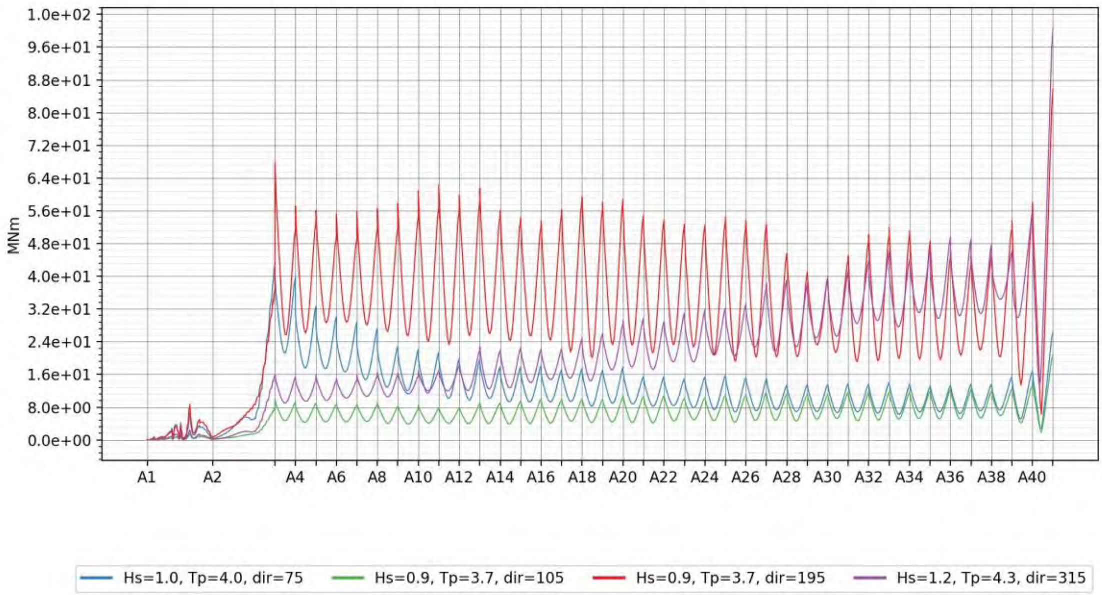

4.4.3.4 Torsional moment

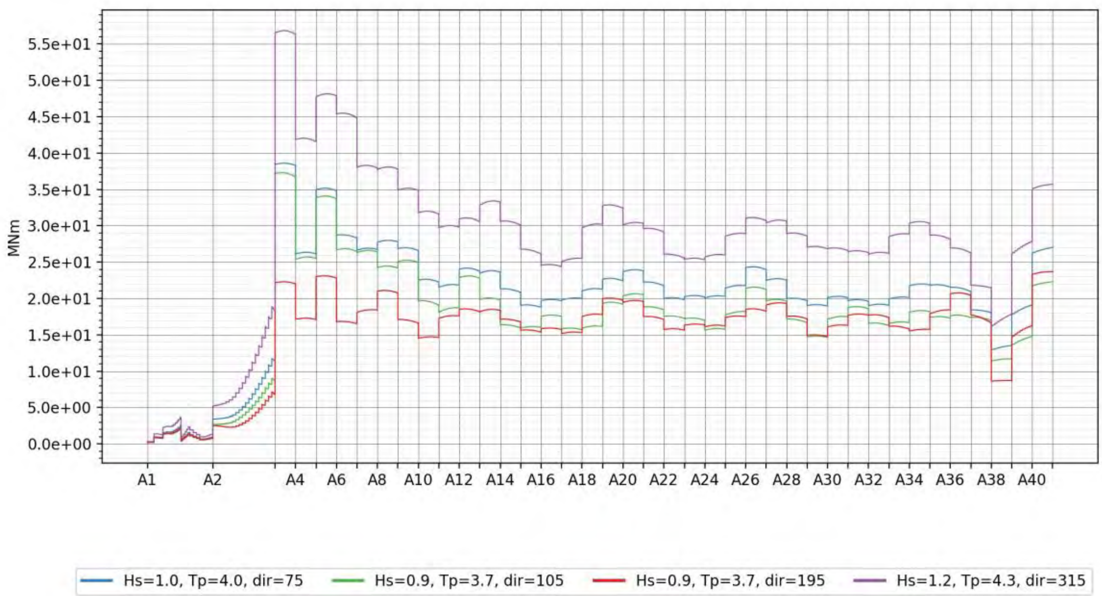

4.4.3.5 Vertical shear force

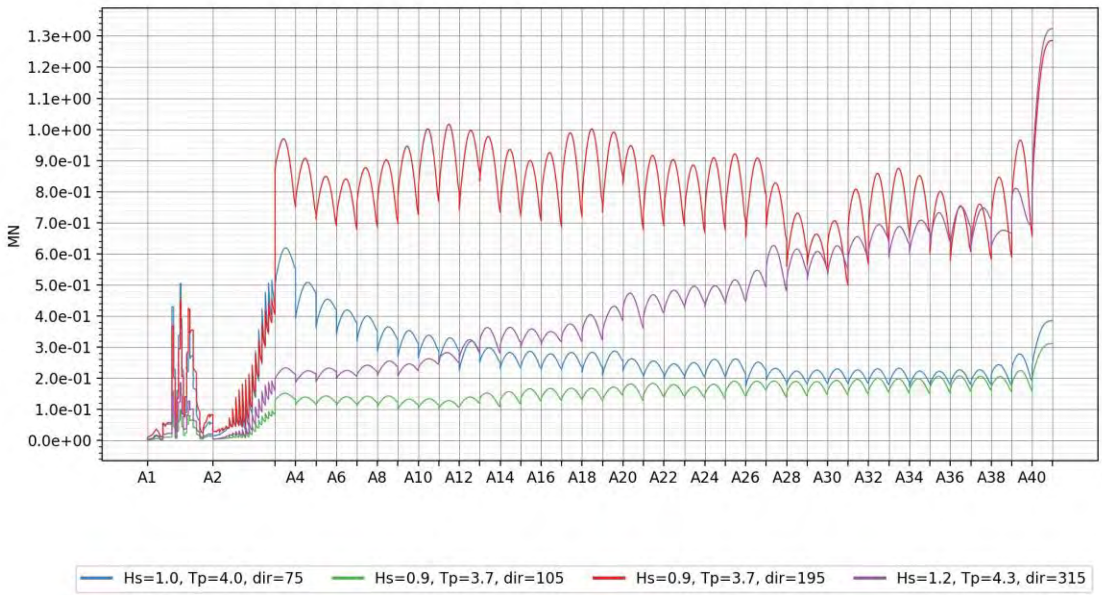

4.4.3.6 Transverse shear force

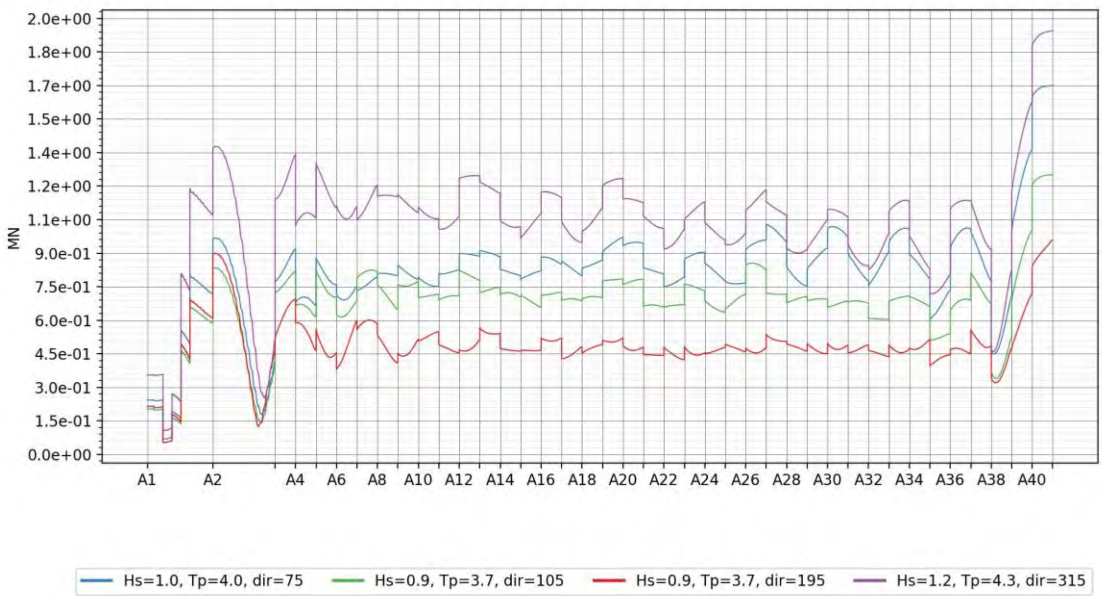

4.4.4 Swell 1 year

4.4.4.1 Axial force

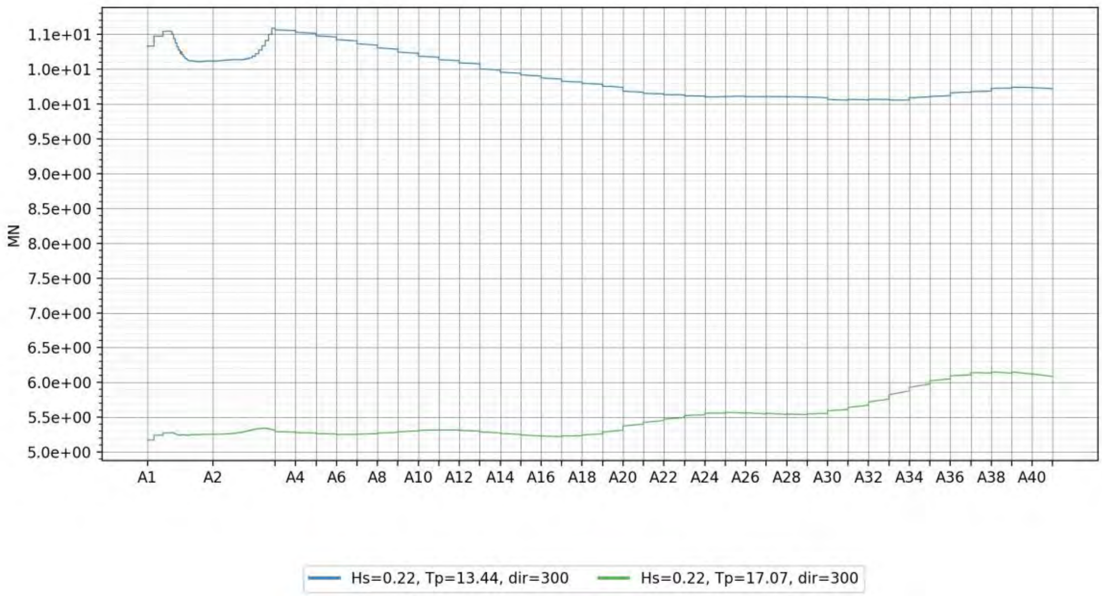

4.4.4.2 Bending moment strong axis

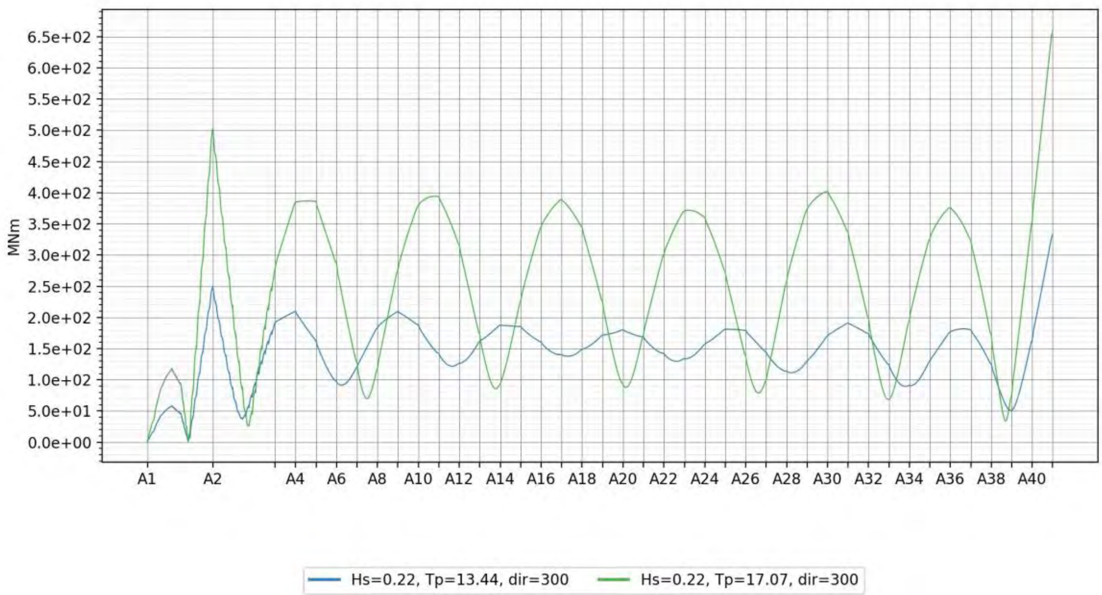

4.4.4.3 Bending moment weak axis

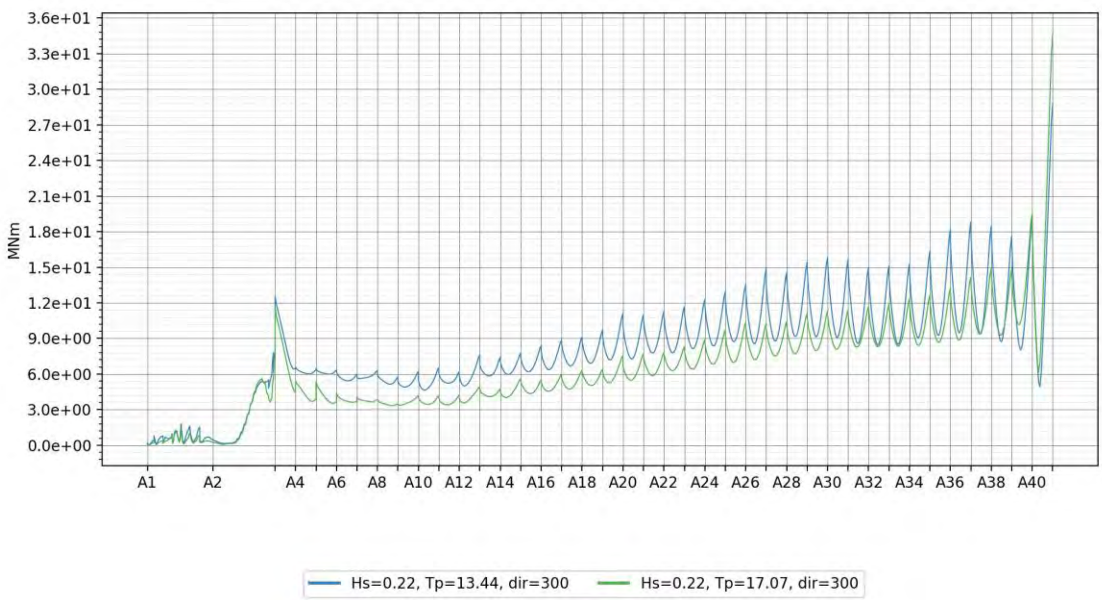

4.4.4.4 Torsional moment

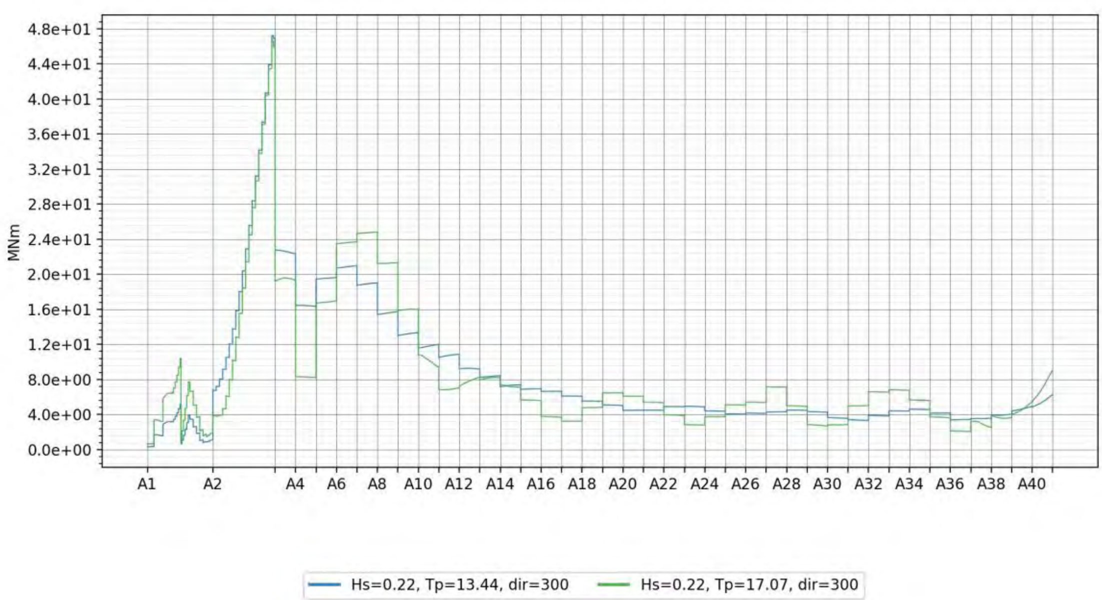

4.4.4.5 Vertical shear force

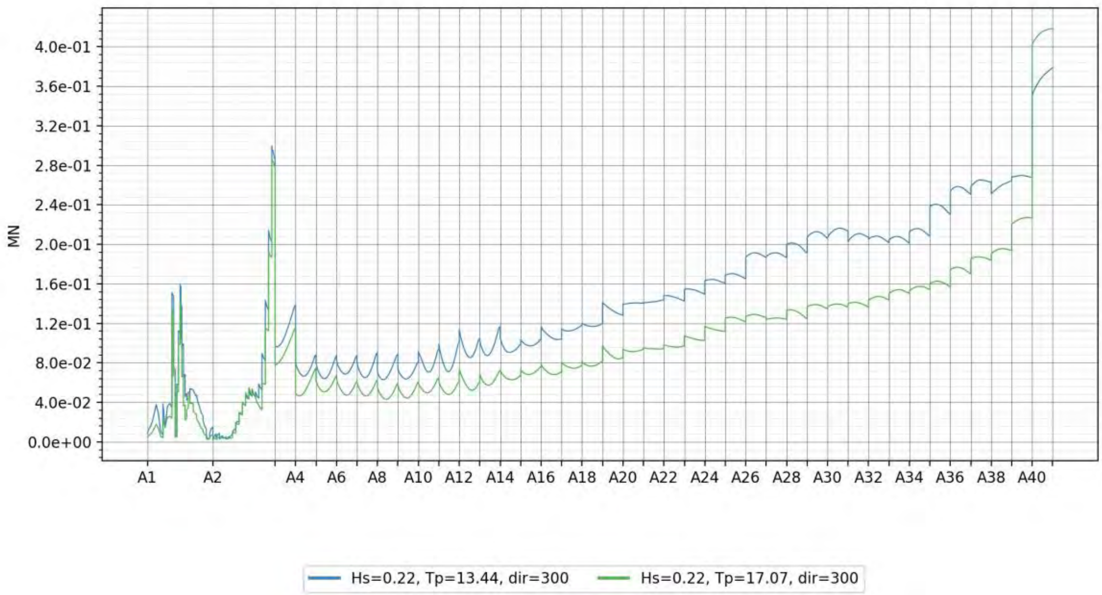

4.4.4.6 Transverse shear force

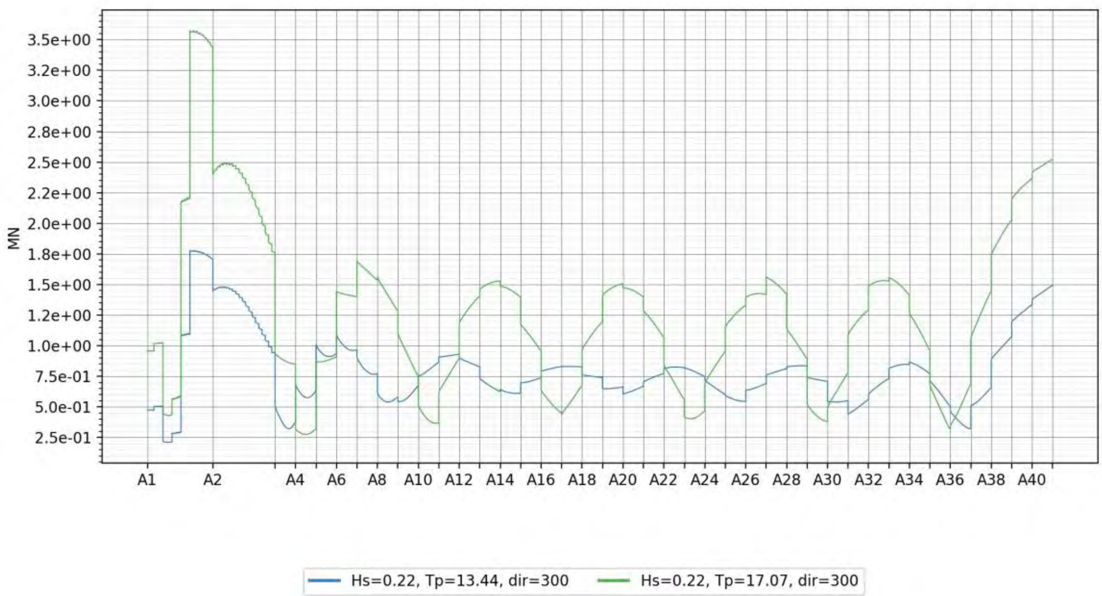

4.4.5 Static wind 100 year

4.4.5.1 Axial force

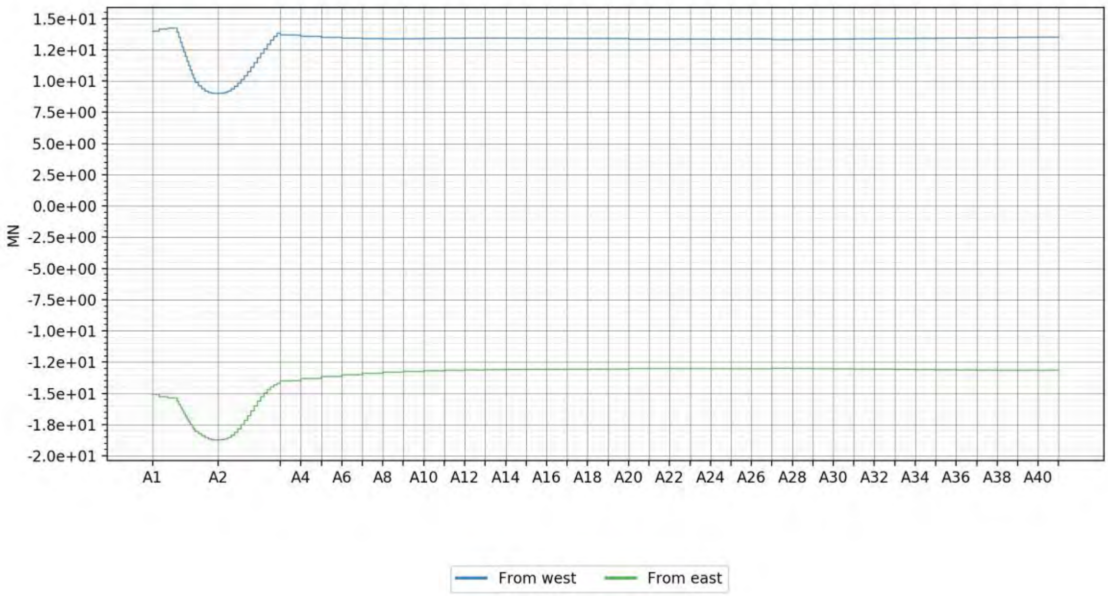

4.4.5.2 Bending moment strong axis

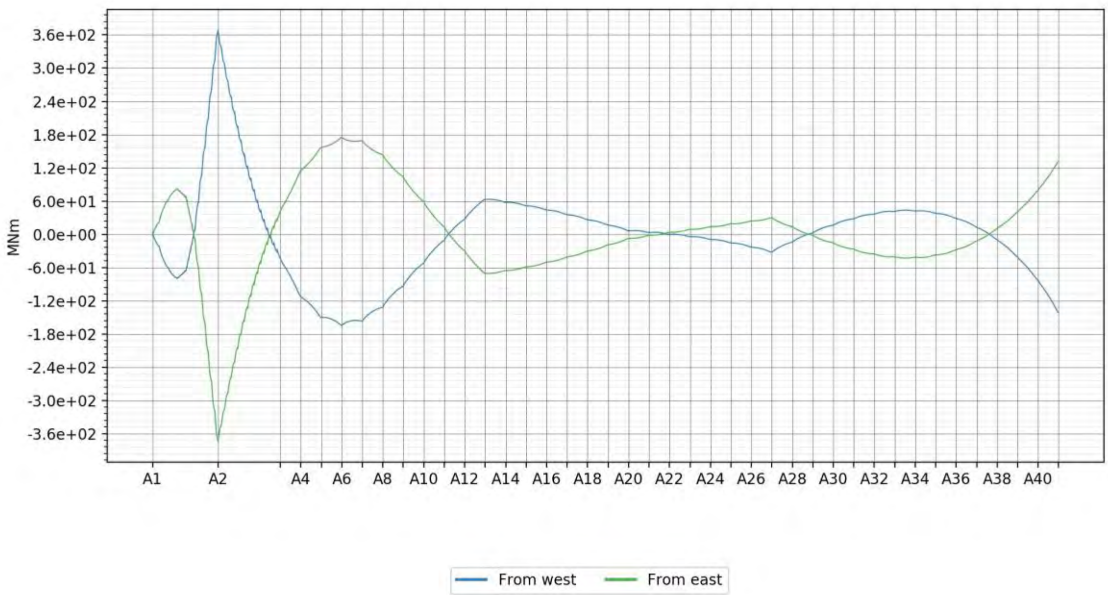

4.4.5.3 Bending moment weak axis

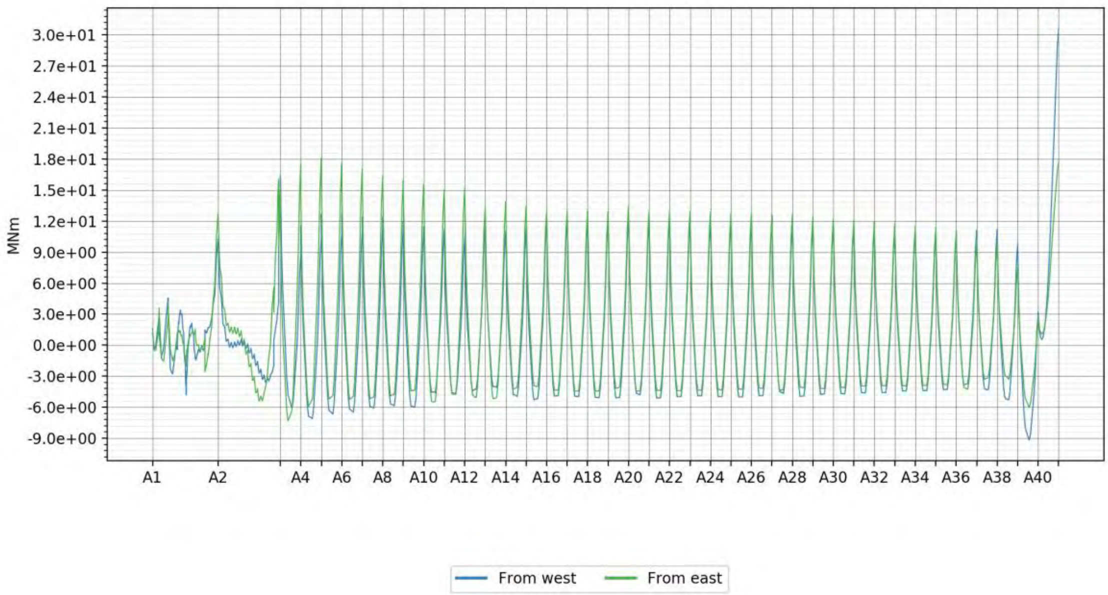

4.4.5.4 Torsional moment

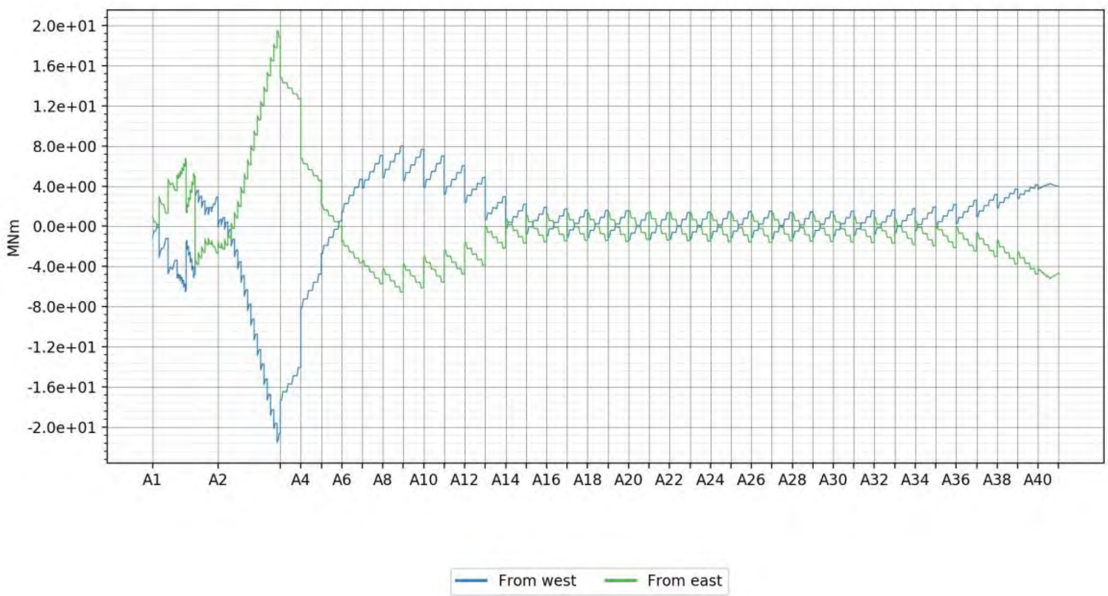

4.4.5.5 Vertical shear force

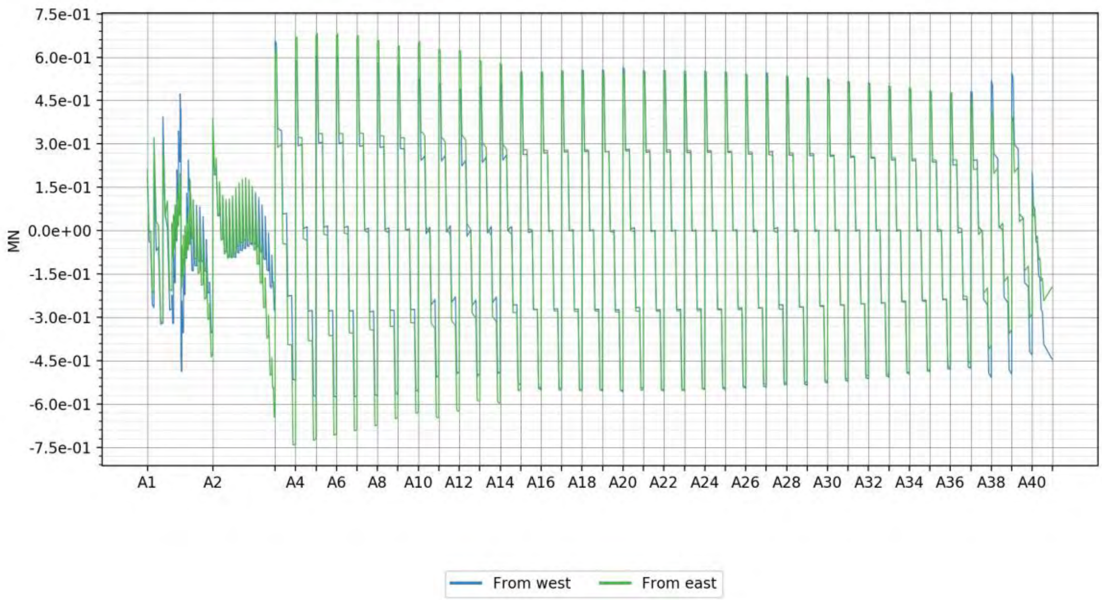

4.4.5.6 Transverse shear force

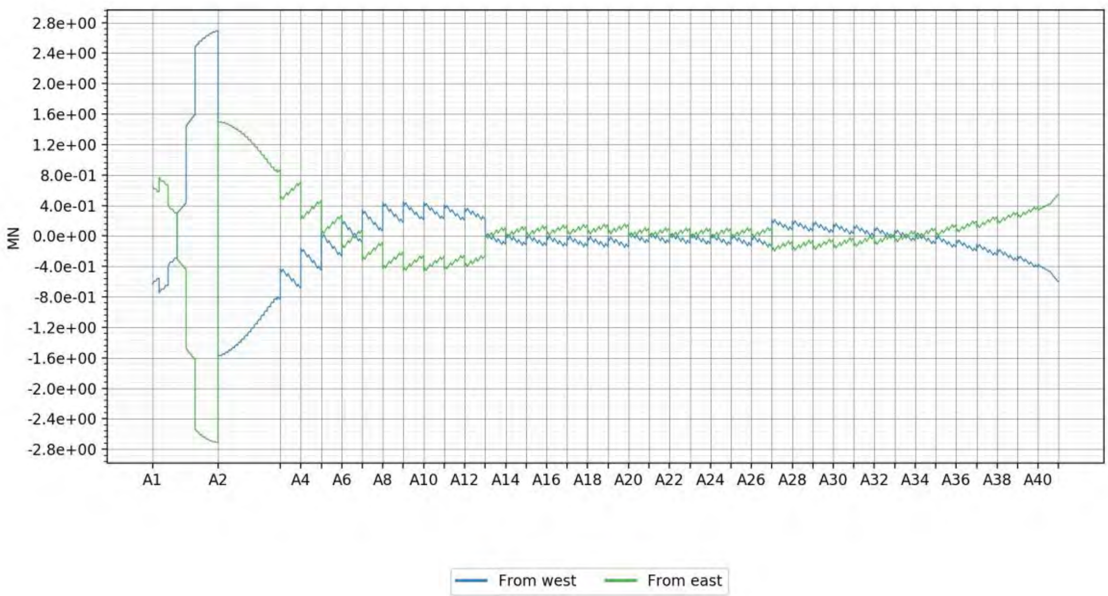

4.4.6 Dynamic wind 100 year

4.4.6.1 Axial force

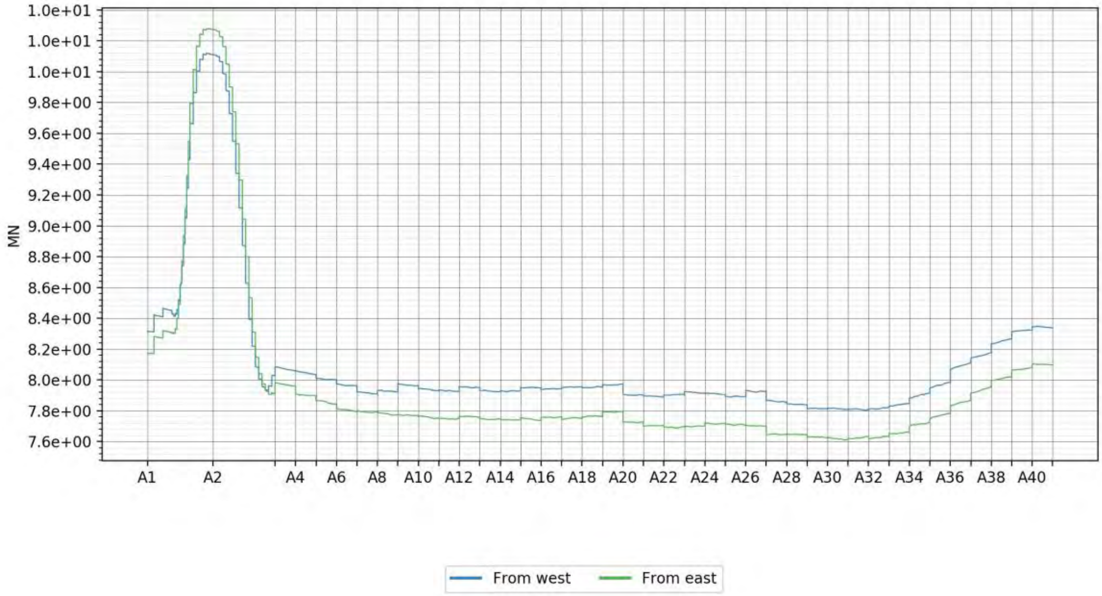

4.4.6.2 Bending moment strong axis

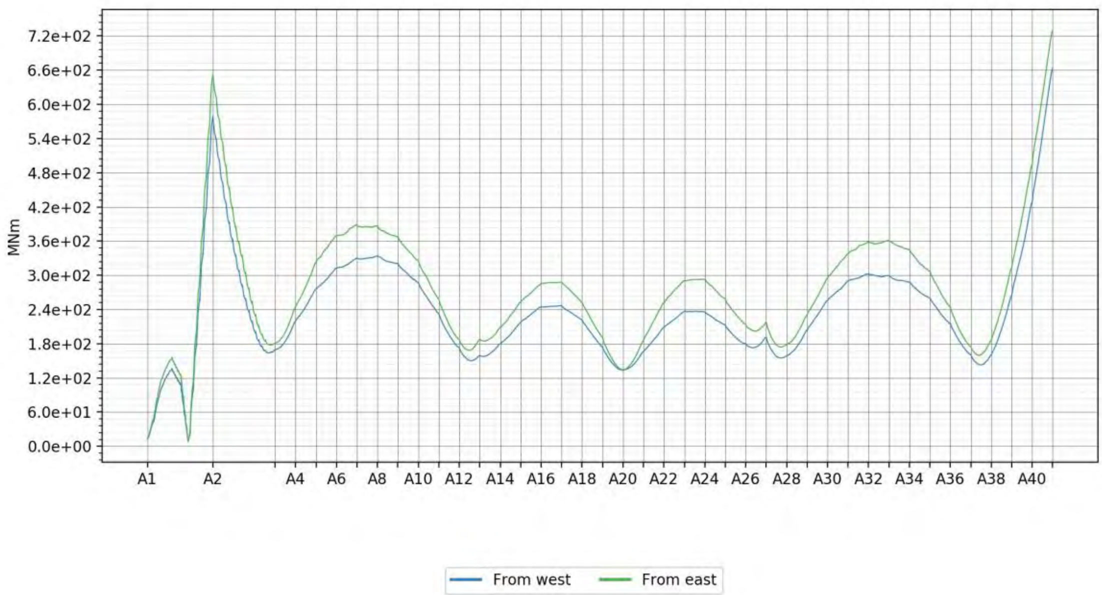

4.4.6.3 Bending moment weak axis

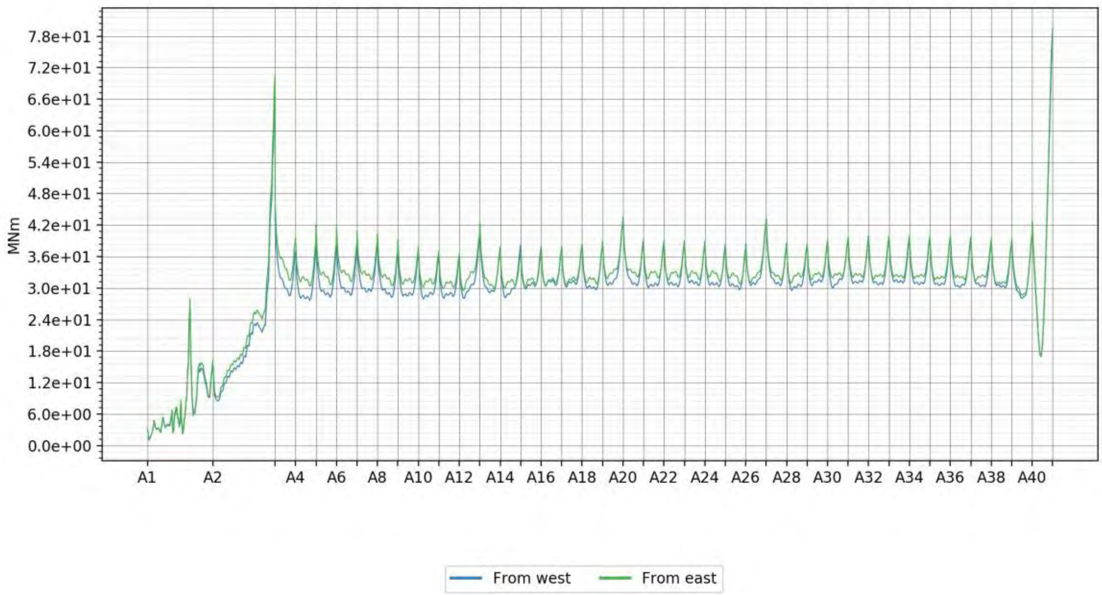

4.4.6.4 Torsional moment

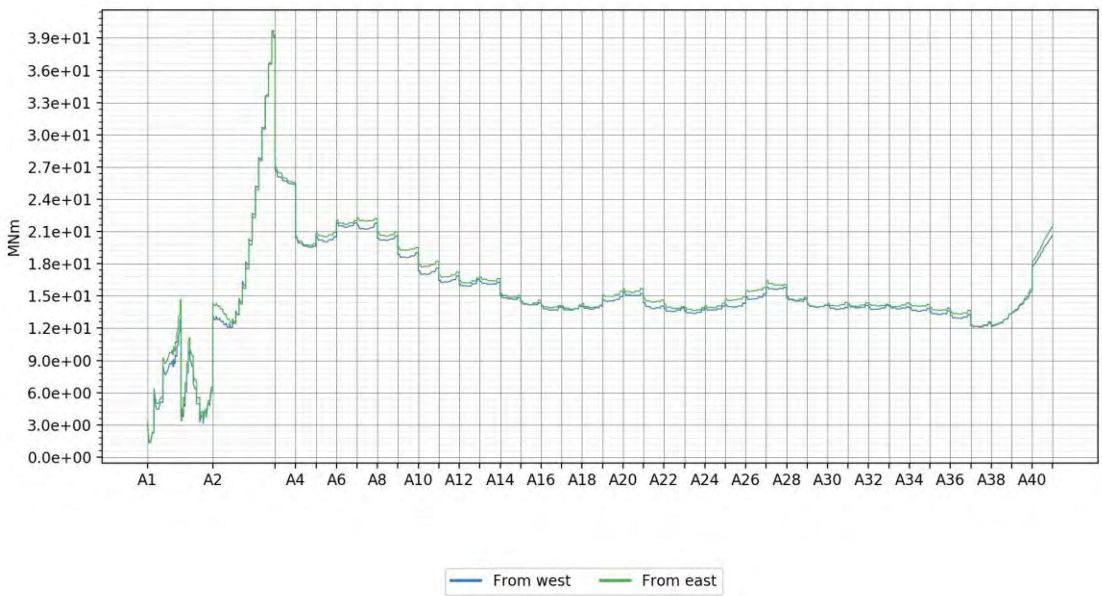

4.4.6.5 Vertical shear force

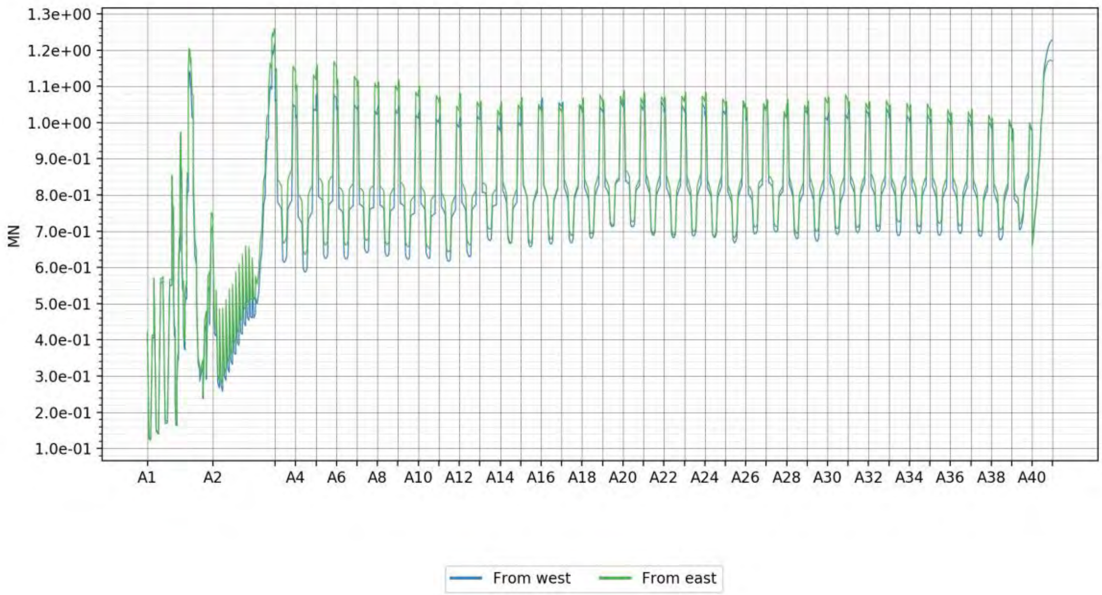

4.4.6.6 Transverse shear force

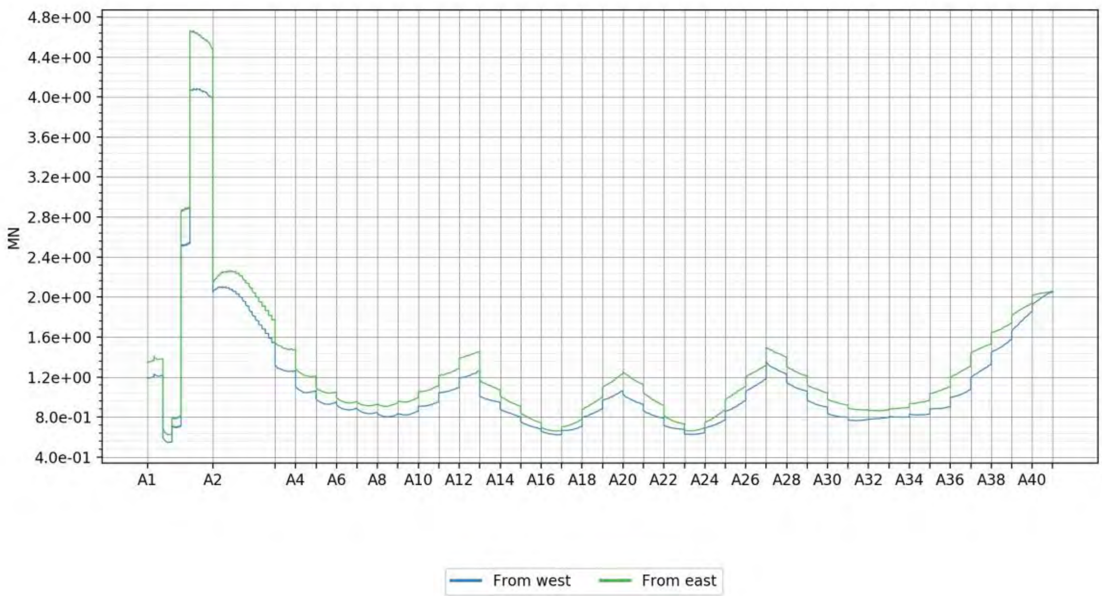

4.4.7 Wave 100 year

4.4.7.1 Axial force

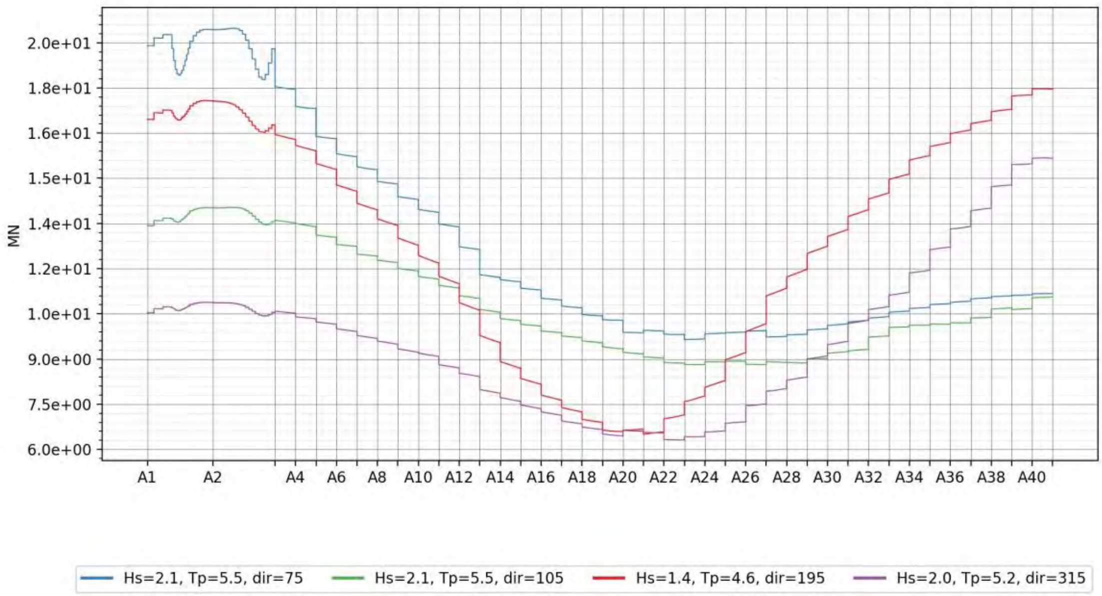

4.4.7.2 Bending moment strong axis

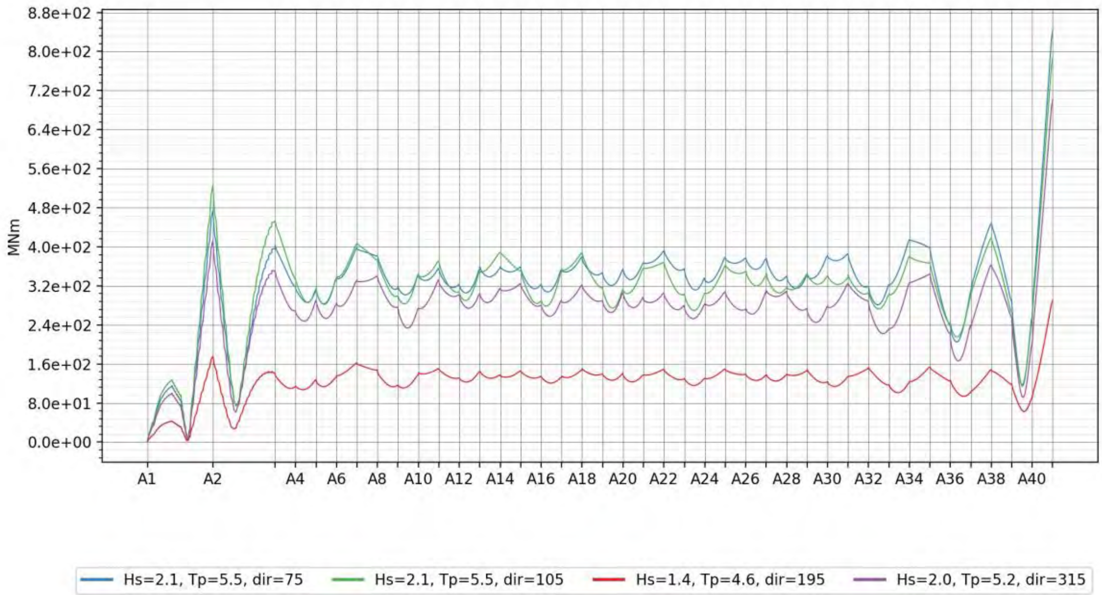

4.4.7.3 Bending moment weak axis

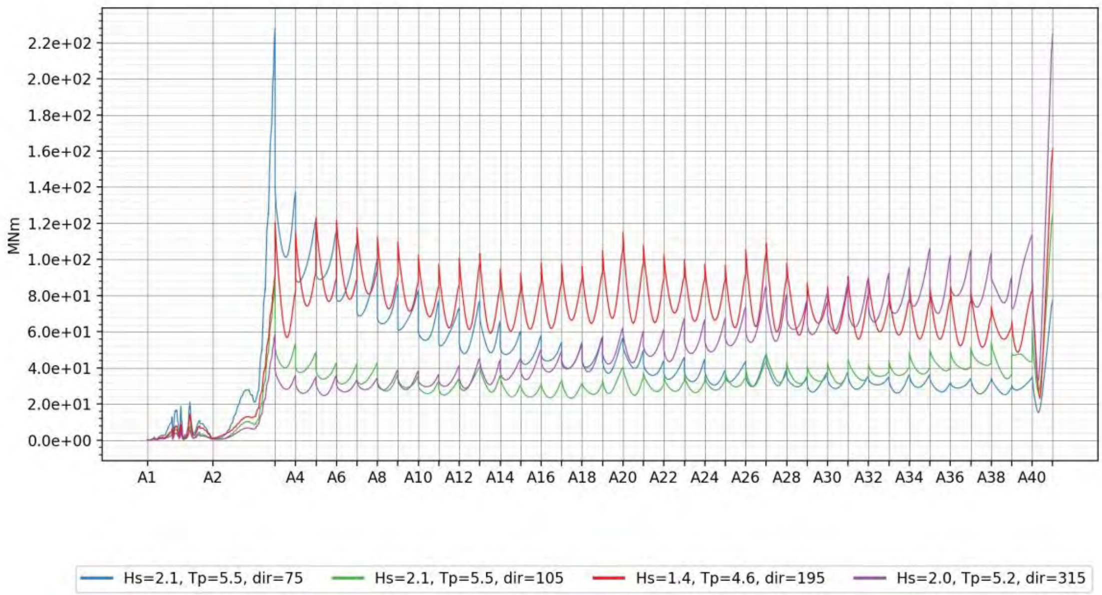

4.4.7.4 Torsional moment

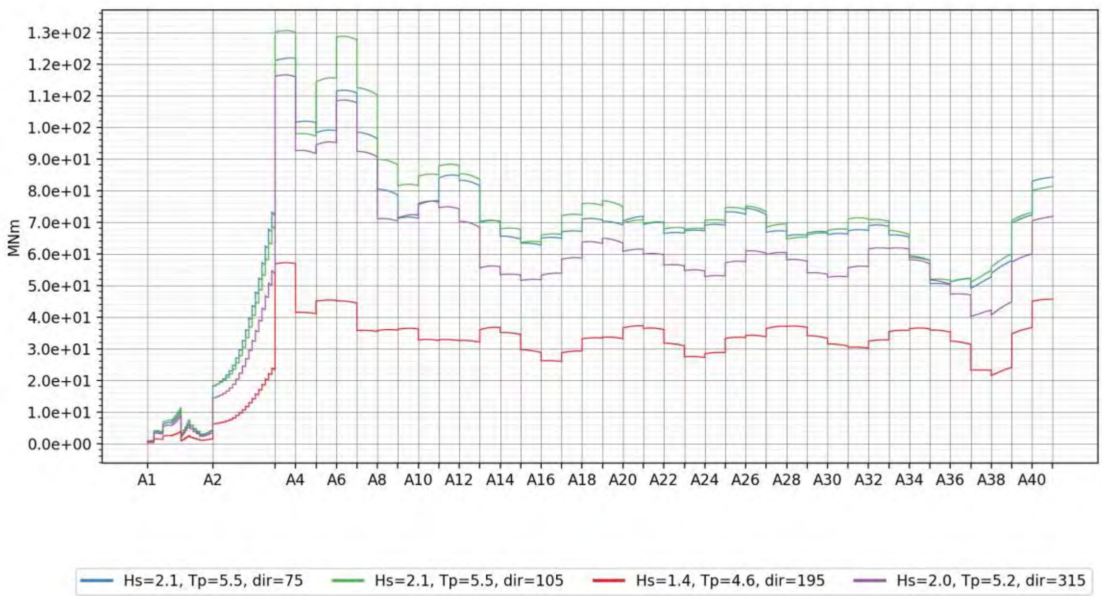

4.4.7.5 Vertical shear force

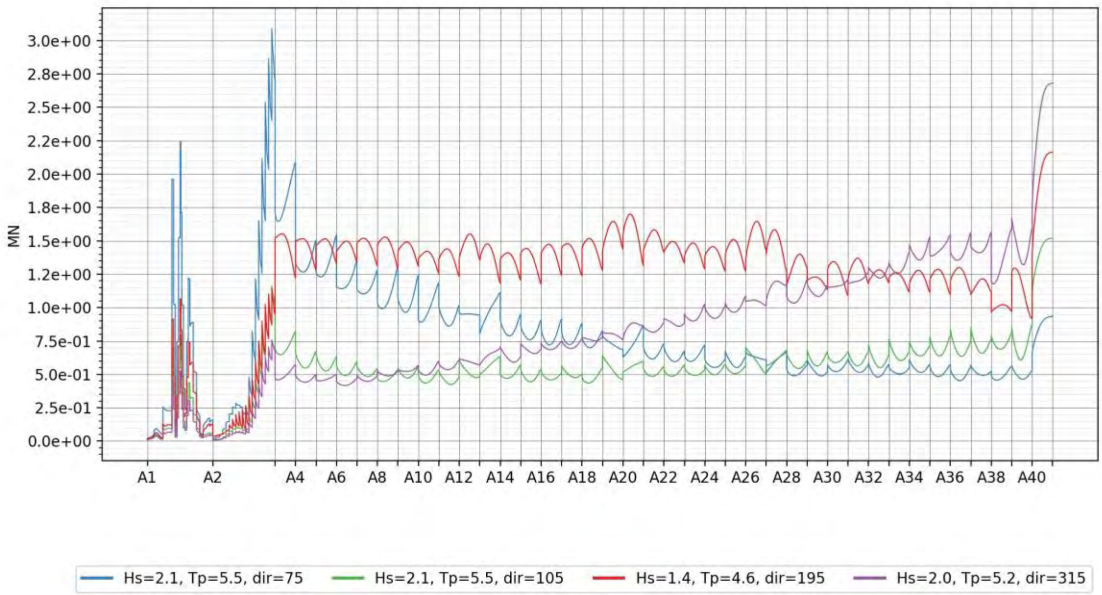

4.4.7.6 Transverse shear force

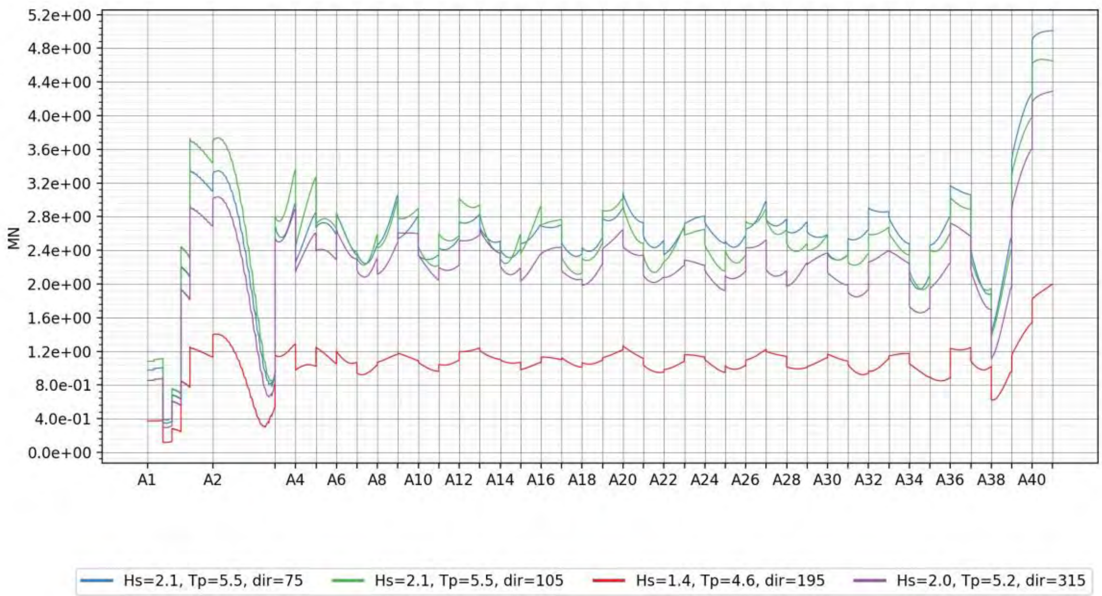

4.4.8 Swell 100 year

4.4.8.1 Axial force

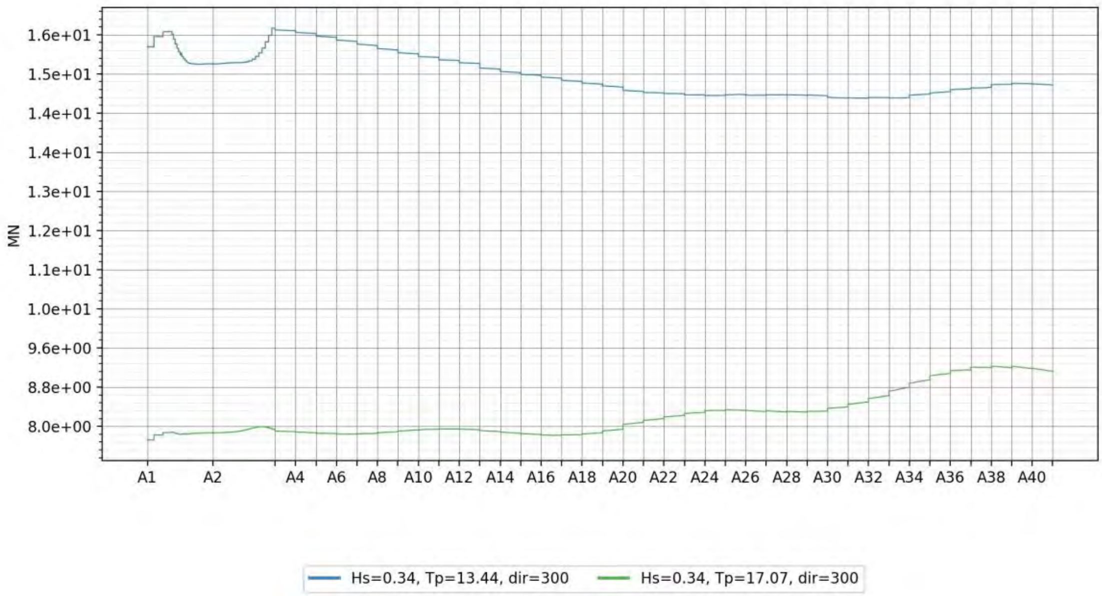

4.4.8.2 Bending moment strong axis

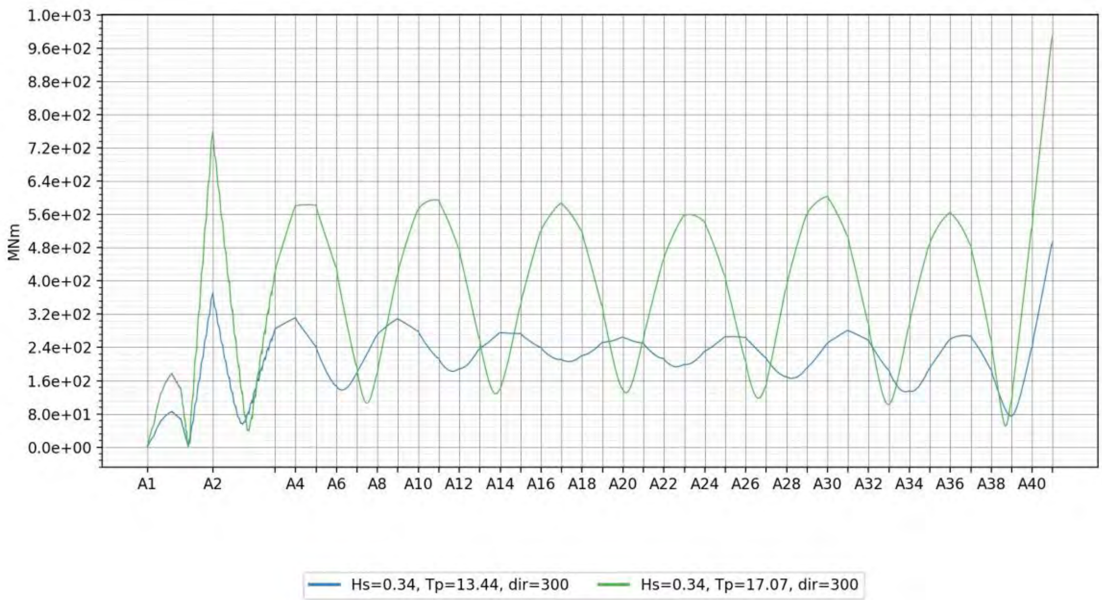

4.4.8.3 Bending moment weak axis

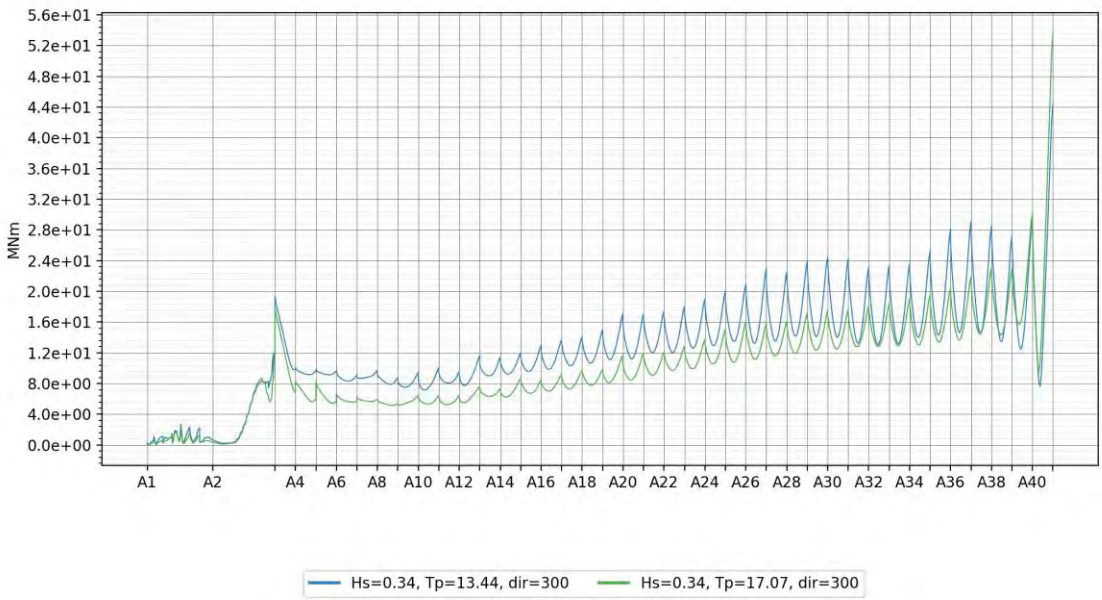

4.4.8.4 Torsional moment

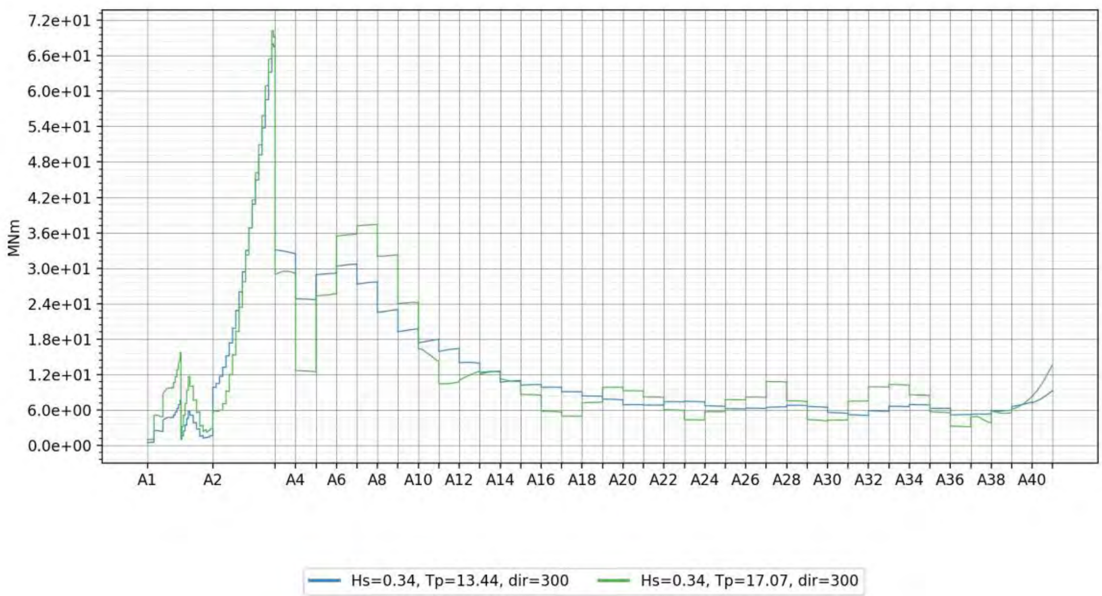

4.4.8.5 Vertical shear force

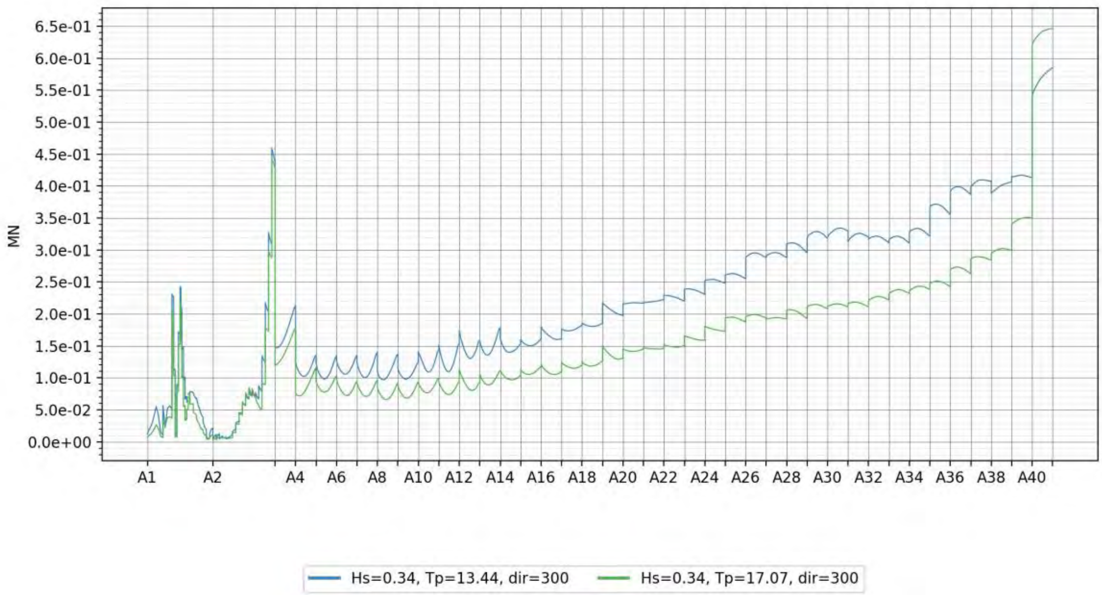

4.4.8.6 Transverse shear force

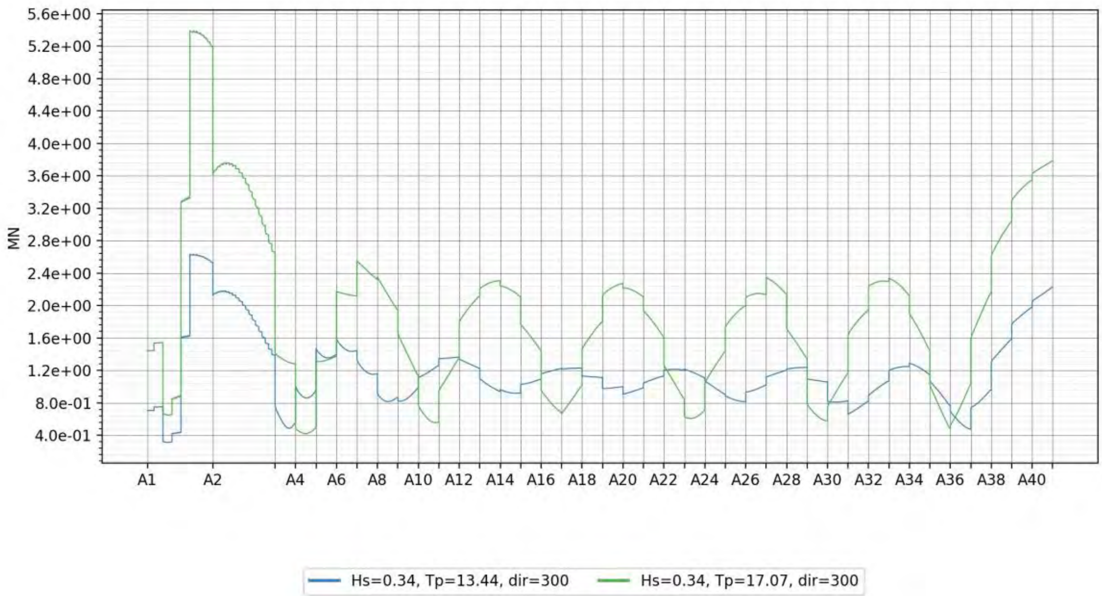

4.4.9 Current 100 year

The four different current cases are described in section 2.1.5. Note that in the plots all four cases are creating axial compressive forces in the bridge girder (only from east direction).

4.4.9.1 Axial force

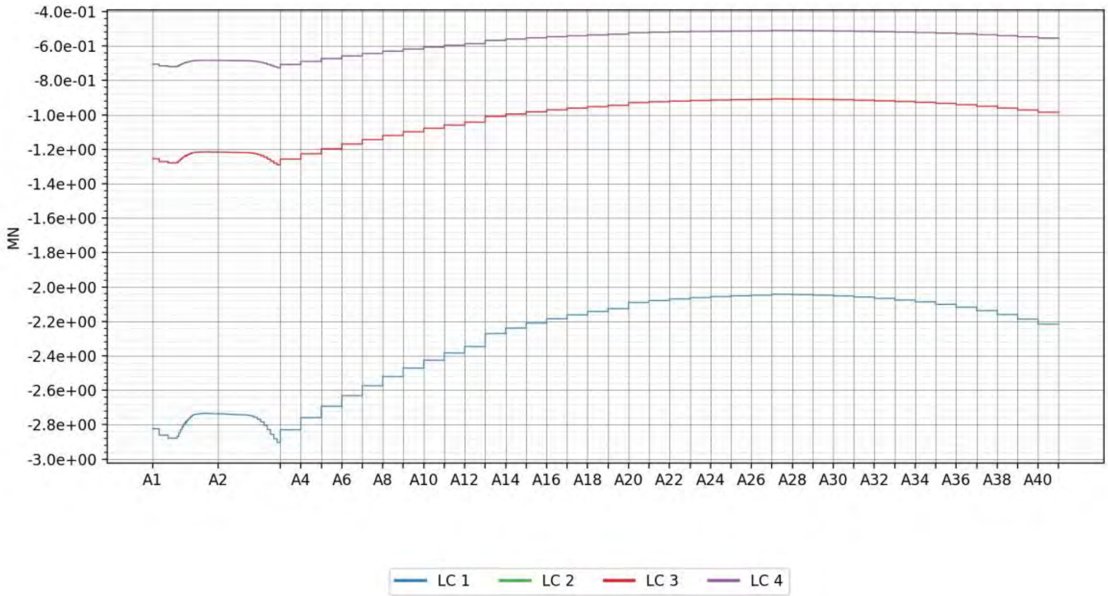

4.4.9.2 Bending moment strong axis